# Quantum Optics with Atomic Ensembles

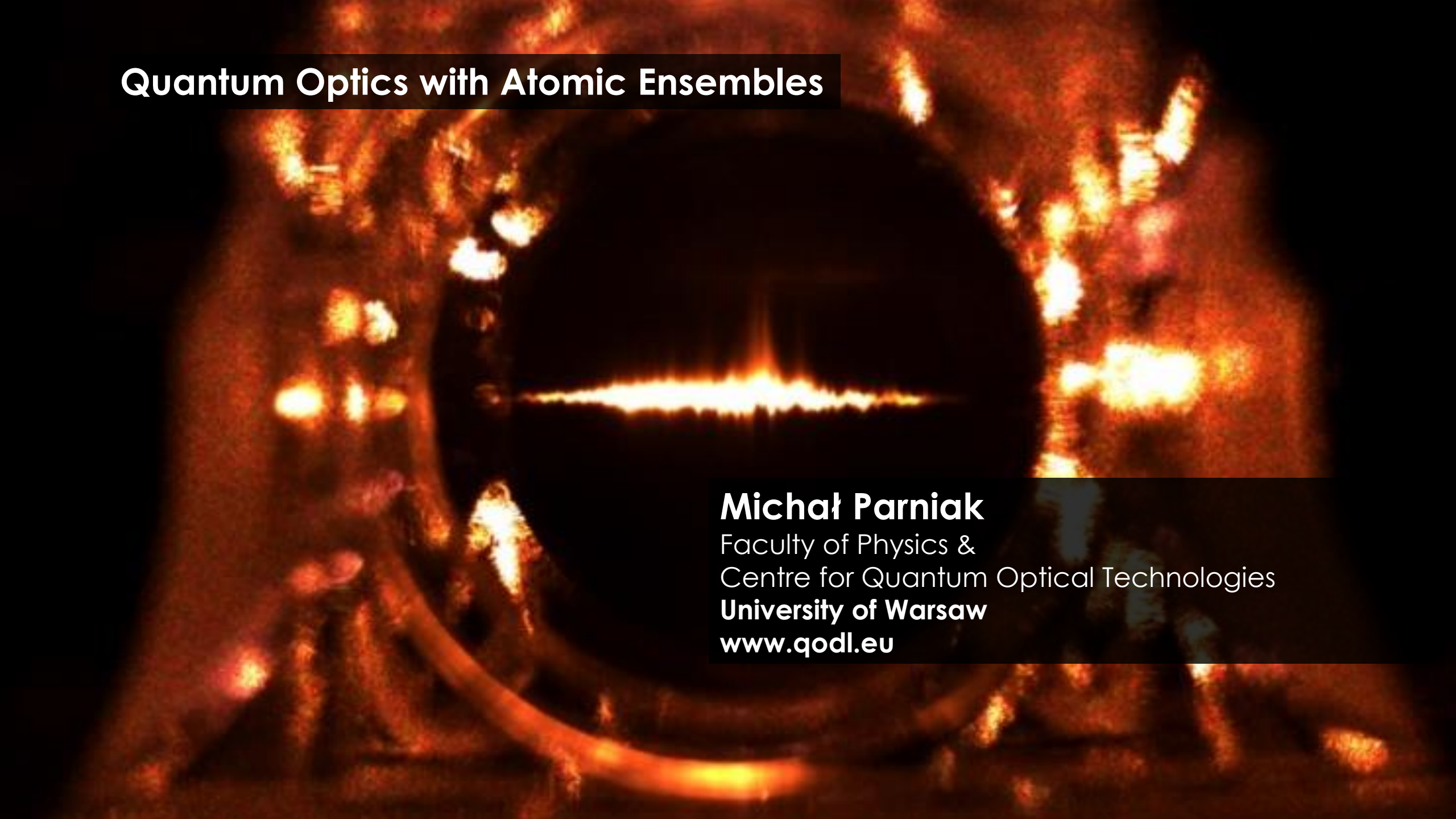

**Michał Parniak**
Faculty of Physics &
Centre for Quantum Optical Technologies
**University of Warsaw**
**www.qodl.eu**

C.NT QOD LAB QOT CENTRE FOR QUANTUM OPTICAL TECHNOLOGIES

WYDZIAŁ FIZYKI UNIWERSYTET WARSZAWSKI — UNIVERSITY OF WARSAW

**2012-2018** WYDZIAŁ FIZYKI UNIWERSYTET WARSZAWSKI

Cold atoms (MOT), Quantum memories,
Quantum information

**2018-2021** Niels Bohr Institutet

Cavity quantum optomechanics,
hot atoms

**2021-** QOT CENTRE FOR QUANTUM OPTICAL TECHNOLOGIES

Rydberg atoms (hot/cold), analog optical quantum signal processors (e.g. for superresolution spectroscopy)

**2023-** FACULTY OF PHYSICS UNIVERSITY OF WARSAW

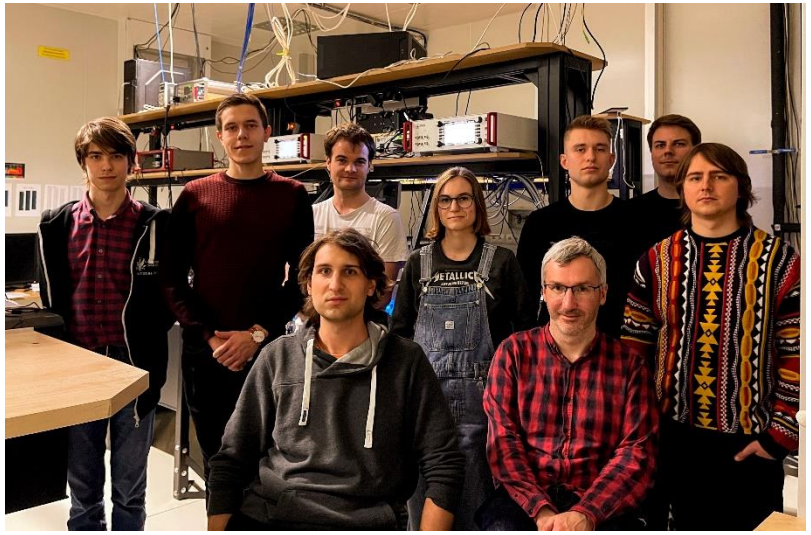

**www.qodl.eu – lab webpage**

European Funds for Smart Economy
Republic of Poland
Co-funded by the European Union

FENG.02.01-IP.05-0017/23

# Plan for today

- Photons, and photons in many modes
- Two-level atoms
- Three-level atoms, quantum memories
- Rydberg atom ensembles
- My research… ;)

# Quantization

$$\vec{D} = \sum_n -p_n(t)\vec{u}_n(\vec{x}) \qquad \vec{B} = \sum_n q_n(t)\vec{v}_n(\vec{x})$$

$$\vec{v}_n = \nabla \times \vec{u}_n$$

$$\dot{q}_n = p_n/\epsilon, \quad \dot{p}_n = -\epsilon\omega_n^2 q_n$$

$$|n_k, n_l, \ldots, n_m\rangle = \frac{\hat{a}_k^{\dagger n_k}\hat{a}_l^{\dagger n_l}\ldots\hat{a}_m^{\dagger n_m}}{\sqrt{n_k! n_l! \cdots n_m!}}|0\rangle$$

$$H = \int d^3r \left(\frac{D^2}{2\epsilon} + \frac{B^2}{2\mu}\right) \rightarrow \sum_k \left(\frac{p_k}{2\epsilon} + \frac{\epsilon\omega_k^2 q_k^2}{2}\right)$$

# Coherent states

$$\hat{a}|\alpha\rangle = \alpha|\alpha\rangle$$

$$|\alpha\rangle = e^{-|\alpha|^2/2} e^{\alpha \hat{a}^\dagger} |0\rangle$$

$$\langle q|\alpha\rangle \propto \exp\left( i\frac{\langle\hat{p}\rangle\hat{q}}{\hbar} - \frac{\epsilon\omega}{\hbar}\frac{(\hat{q}-\langle\hat{q}\rangle)^2}{2} \right)$$

$$\frac{\hat{p}}{\sqrt{\hbar\epsilon\omega}} = \frac{\hat{a}-\hat{a}^\dagger}{i\sqrt{2}}$$

$$\frac{\langle\alpha|\hat{p}|\alpha\rangle}{\sqrt{\hbar\epsilon\omega}} = \frac{\alpha-\alpha^*}{i\sqrt{2}}$$

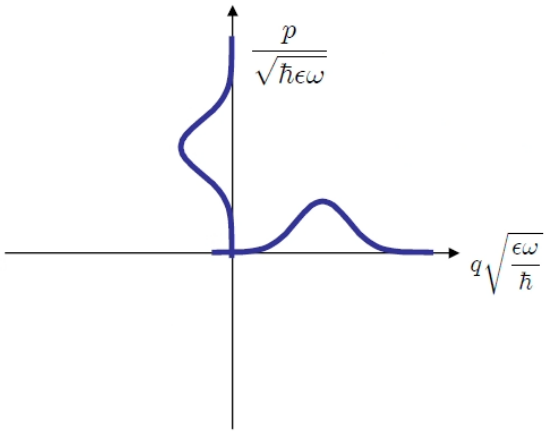


$$H = \hbar\omega(a^\dagger a + 1/2)$$

$$q(t) = q(0)\cos(\omega t) + \frac{p(0)}{\epsilon\omega}\sin(\omega t)$$
$$p(t) = p(0)\cos(\omega t) - q(0)\epsilon\omega\sin(\omega t)$$

$$\hat{a}(t) = \hat{a}(0)e^{-i\omega t}$$

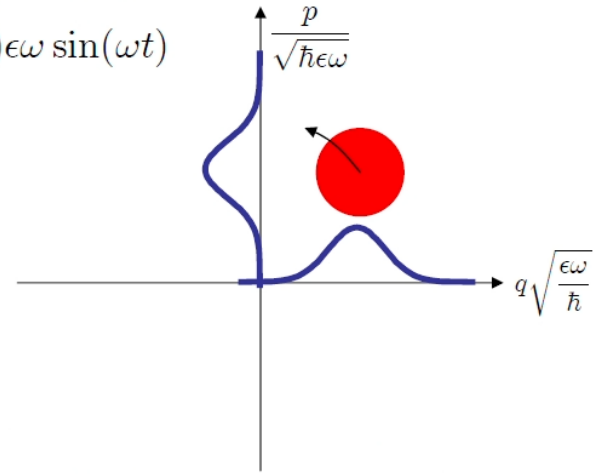

# Fields in space and time

$$u_{\vec{k},\lambda} = \frac{1}{\sqrt{V}} \vec{e}_{\vec{k},\lambda} \exp(i\vec{k} \cdot \vec{x})$$

$$\hat{\vec{E}}(\vec{x},t) = i \sum_{\vec{k},\lambda} \sqrt{\frac{\hbar\omega_k}{2\epsilon V}} \hat{a}_{\vec{k},\lambda} \vec{e}_{\vec{k},\lambda} \exp(i\vec{k} \cdot \vec{x}) + H.c.$$

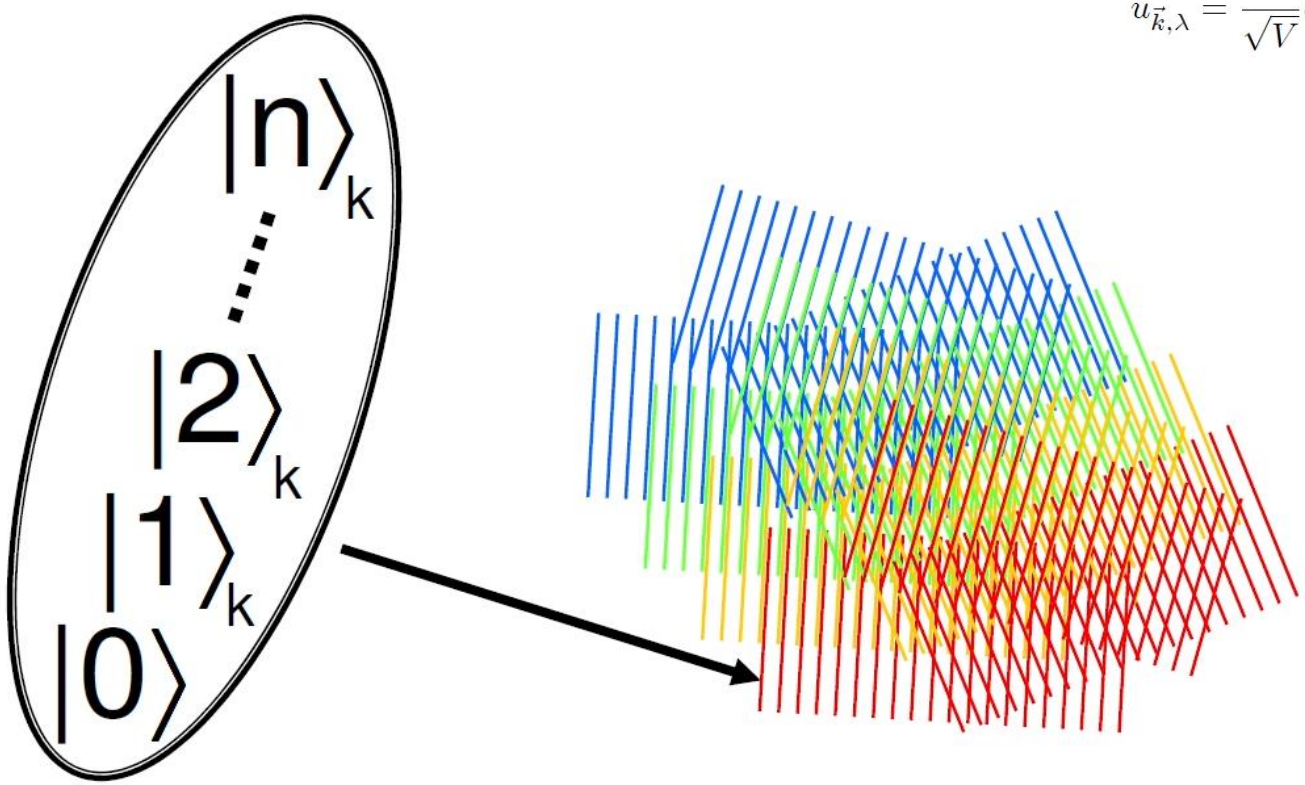

# Observing fields: homodyne detection

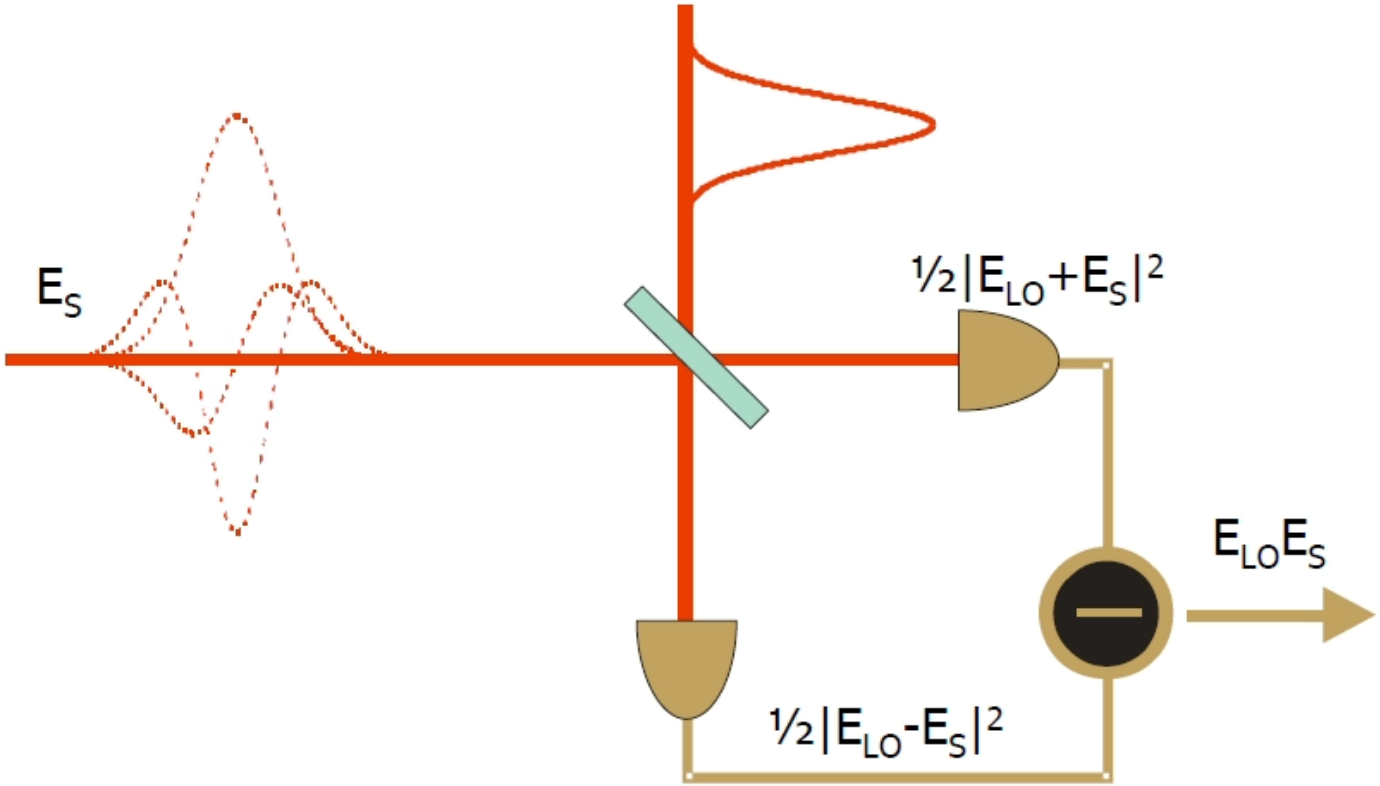

# Observing fields: homodyne detection

$$\hat{E} = -\int d^3k \frac{\hat{p}_k(t)}{\epsilon_0} e^{ikr}$$

$$\hat{p} = \sqrt{\hbar\epsilon\omega}\frac{\hat{a} - \hat{a}^\dagger}{i\sqrt{2}}$$

$$\hat{a} = \sqrt{\frac{\epsilon\omega}{2\hbar}}\left(\hat{q} + i\frac{\hat{p}}{\epsilon\omega}\right)$$

$$\langle p|1\rangle = \sqrt{2}\sqrt[4]{\epsilon\omega\pi\hbar}\exp\left(-\frac{\epsilon\omega p^2}{2\hbar}\right)\sqrt{\frac{\epsilon\omega}{\hbar}}p$$

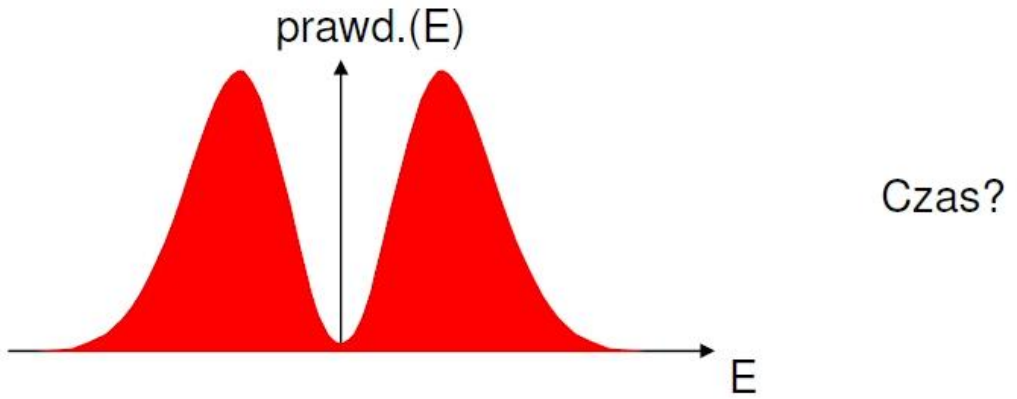


Czas?

# Observing fields: homodyne detection

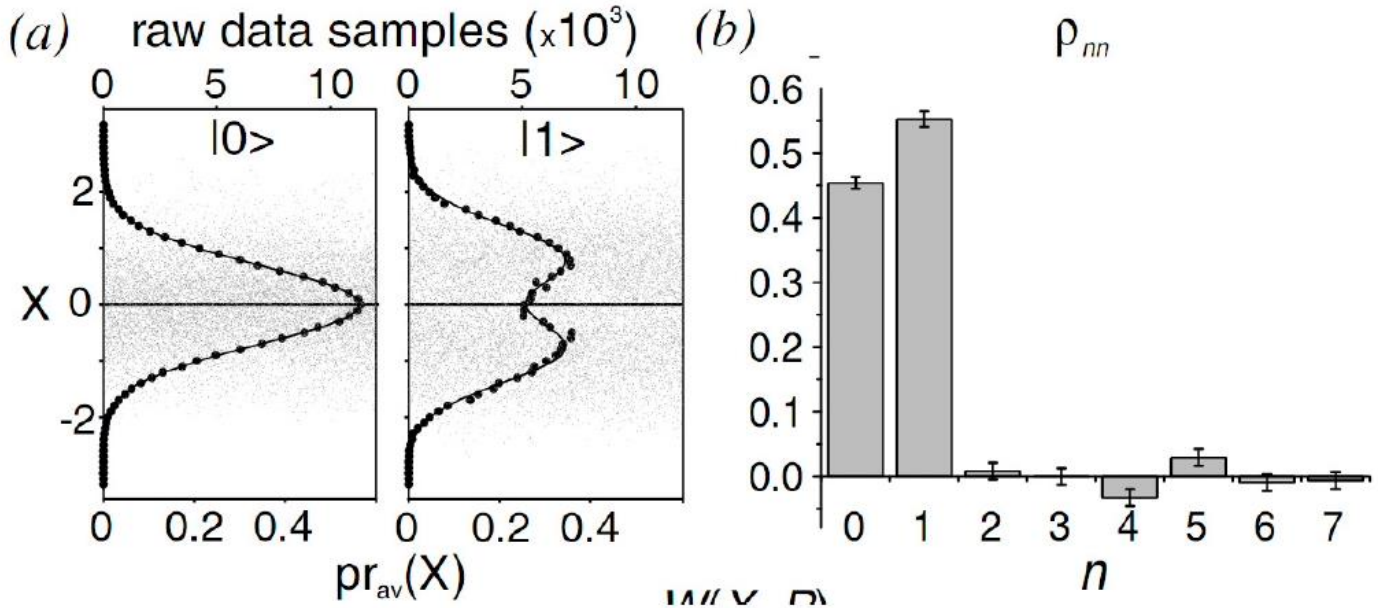


**Lvovsky et al., Phys. Rev. Lett. 87, 050402 (2001)**

# Observing fields: photon counting

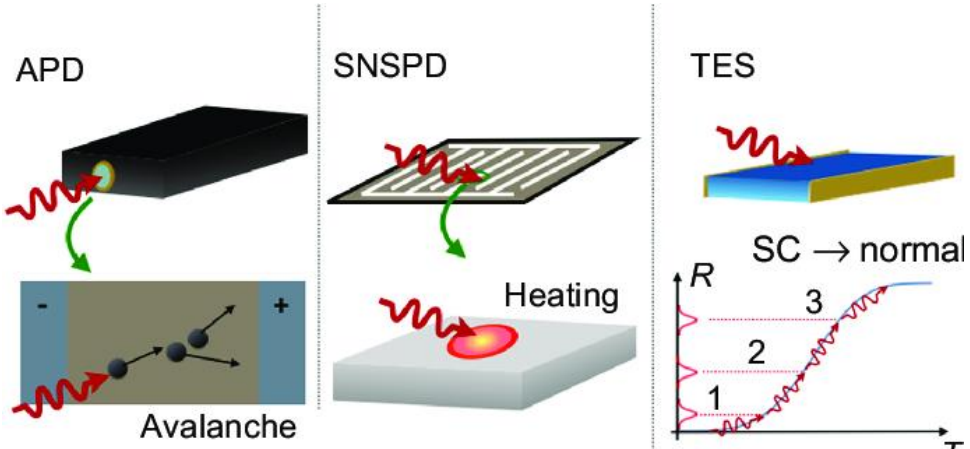


$$\Pi_0 = |0\rangle\langle 0|$$

$$\Pi_1 = \mathbb{I} - |0\rangle\langle 0|$$

$$\Pi_n = |n\rangle\langle n|$$

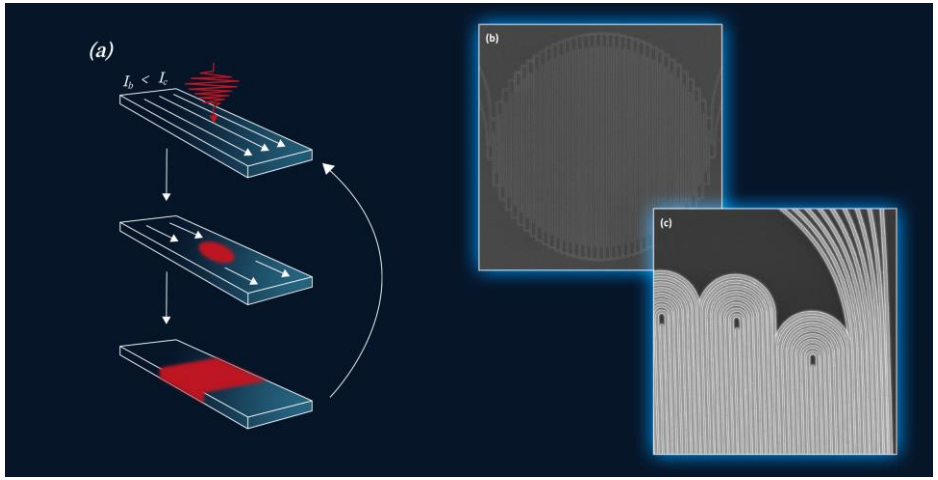



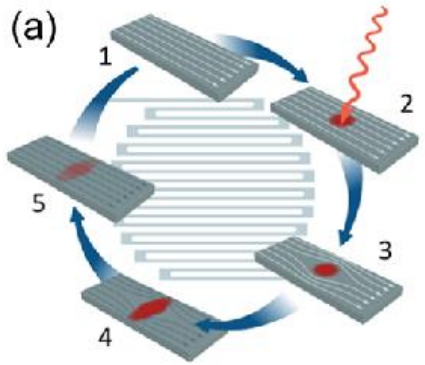


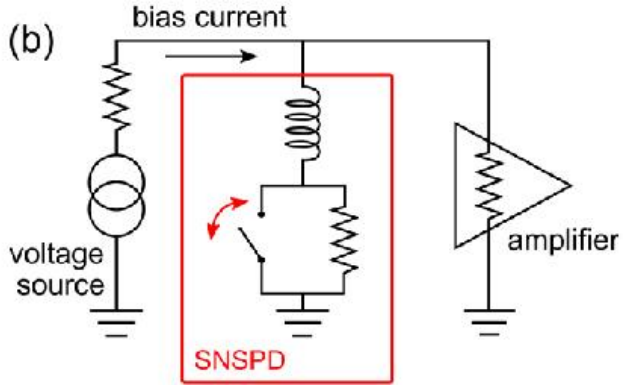

# Interference: Hong-Ou-Mandel

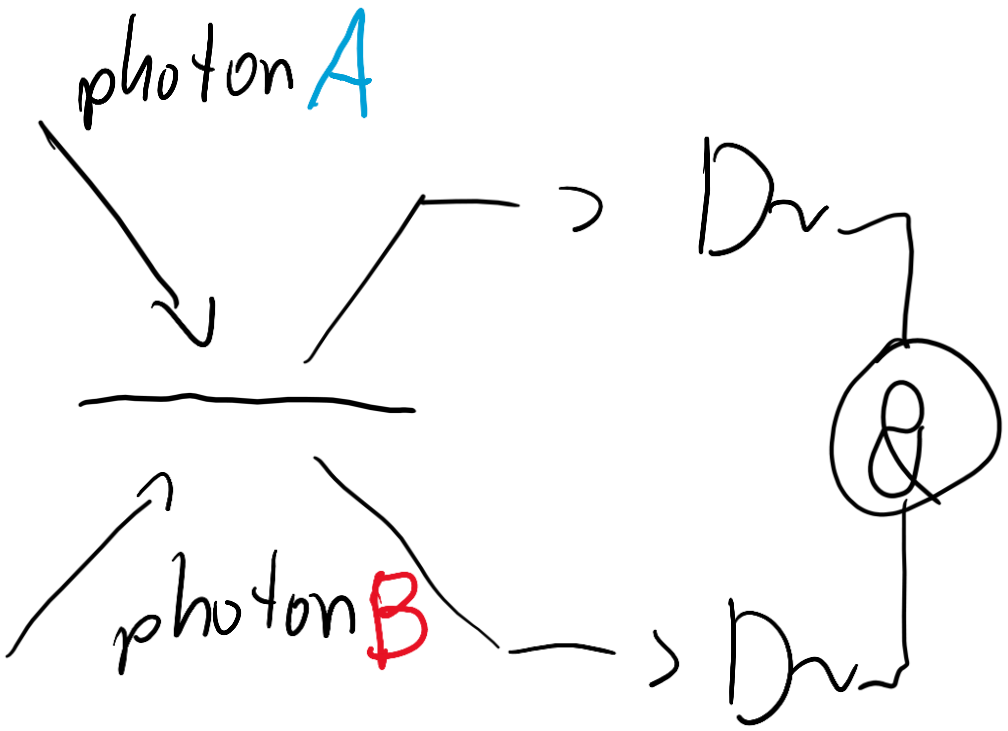


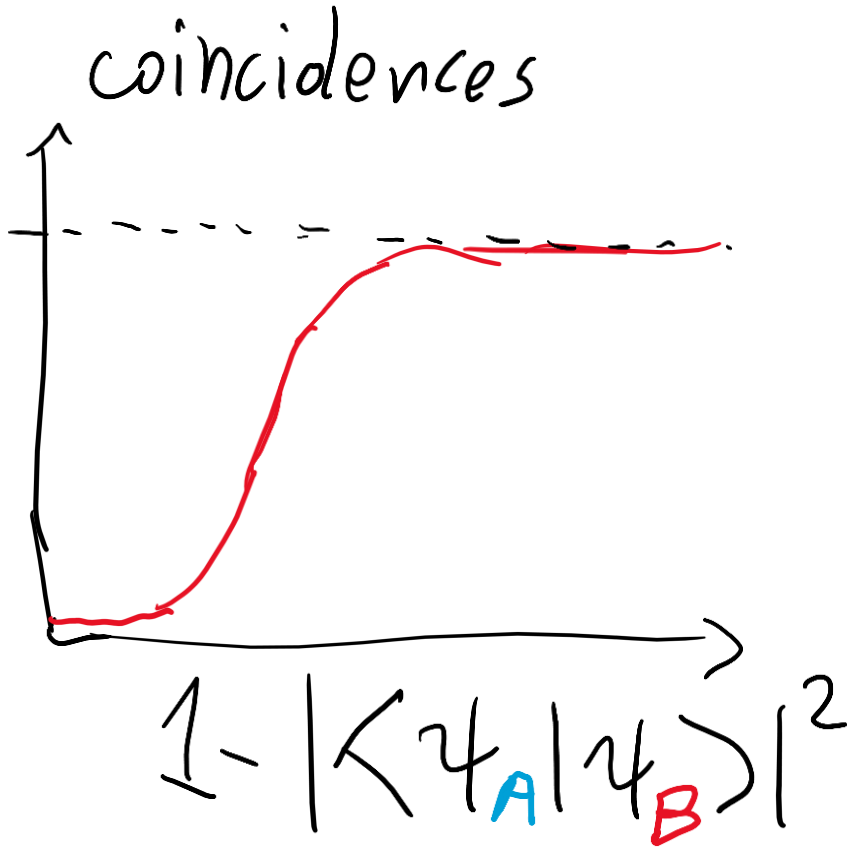


BS matrix $= \frac{1}{\sqrt{2}}\begin{pmatrix} 1 & -1 \\ 1 & 1 \end{pmatrix}$

# Propagation through medium

$$\triangle_\perp \mathcal{E} + 2ik_0 \frac{\partial}{\partial z}\mathcal{E} + 2i\frac{(1+\chi)\omega_0}{c^2}\frac{\partial}{\partial t}\mathcal{E} = -\frac{\omega_0^2}{\epsilon_0 c^2}\mathcal{P}^{NL}$$

$$\triangle \mathbf{E} - \frac{1}{c^2}\frac{\partial^2 \mathbf{E}}{\partial t^2} = \frac{1}{\epsilon_0 c^2}\frac{\partial^2 \mathbf{P}}{\partial t^2}$$

$$\triangle_\perp \mathcal{E} + 2ik_0 \frac{\partial}{\partial z}\mathcal{E} = -\frac{\omega_0^2}{\epsilon_0 c^2}\mathcal{P}^{NL}$$

$$\left|\frac{\partial^2 \boldsymbol{\mathcal{P}}^{NL}}{\partial t^2}\right| \ll \omega_0 \left|\frac{\partial \boldsymbol{\mathcal{P}}^{NL}}{\partial t}\right| \ll \omega_0^2 \left|\boldsymbol{\mathcal{P}}^{NL}\right|$$

$$\left|\frac{\partial^2 \boldsymbol{\mathcal{E}}}{\partial t^2}\right| \ll \omega_0 \left|\frac{\partial \boldsymbol{\mathcal{E}}}{\partial t}\right| \ll \omega_0^2 \left|\boldsymbol{\mathcal{E}}\right|$$

$$\left|\frac{\partial^2 \boldsymbol{\mathcal{E}}}{\partial z^2}\right| \ll k_0 \left|\frac{\partial \boldsymbol{\mathcal{E}}}{\partial z}\right| \ll k_0^2 \left|\boldsymbol{\mathcal{E}}\right|$$

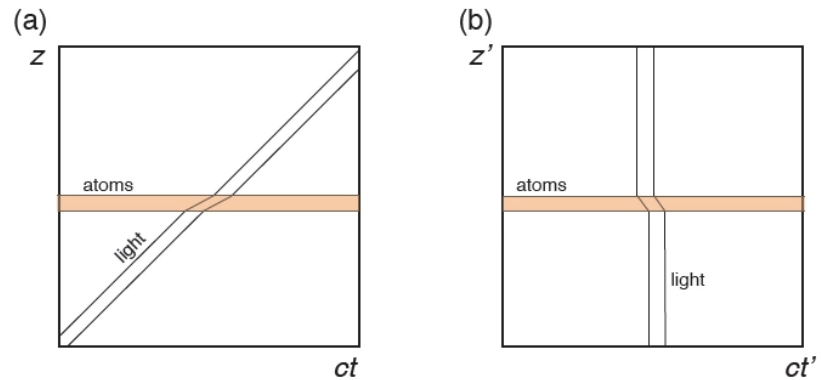


$$\mathbf{E}(\mathbf{r},t) = \bar{\mathbf{E}}(\mathbf{r},t) + c.c. = \frac{1}{2}\boldsymbol{\mathcal{E}}(\mathbf{r},t)e^{i(k_0 z - \omega_0 t)} + c.c.$$

$$\mathbf{P}^{NL}(\mathbf{r},t) = \bar{\mathbf{P}}^{NL}(\mathbf{r},t) + c.c. = \frac{1}{2}\boldsymbol{\mathcal{P}}^{NL}(\mathbf{r},t)e^{i(k_0 z - \omega_0 t)} + c.c.$$

$$\mathbf{P} = \frac{1}{V}\mathrm{Tr}(\bigotimes_i^N \hat{\rho}_i \sum_j^N \hat{\mathbf{d}}^{(j)}) = \frac{1}{V}\sum_j^N \prod_i^N \mathrm{Tr}(\hat{\rho}_i \hat{\mathbf{d}}^{(j)}) = \frac{N}{V}\mathrm{Tr}(\hat{\rho}\hat{\mathbf{d}}),$$

$$\boxed{\mathbf{P}(\mathbf{r},t) = n(\mathbf{r})\mathrm{Tr}(\hat{\rho}(\mathbf{r},t)\hat{\mathbf{d}}),}$$

# Atoms: 2 levels, Rabi oscillations

$$\hat{H} = \hat{H}_B + \hat{V}.$$

$$\hat{H}_B = \hbar\omega_{ge}|e\rangle\langle e|.$$

$$\hat{V} = -\mathbf{E}\cdot\hat{\mathbf{d}},$$

$$\hat{H}_I = \exp(i\hat{H}_0 t/\hbar)(\hat{H} - \hat{H}_0)\exp(-i\hat{H}_0 t/\hbar) =$$
$$= -\hbar\Delta\hat{\sigma}_{ee} - \frac{1}{2}\mathbf{d}_{ge}\cdot(\mathbf{A}e^{-2i\omega t} + \mathbf{A}^*)\hat{\sigma}_{ge} - \frac{1}{2}\mathbf{d}_{eg}\cdot(\mathbf{A}^* e^{2i\omega t} + \mathbf{A})\hat{\sigma}_{eg},$$

$$\hat{H}_I' = -\hbar\Delta|1\rangle\langle 1| - \hbar\frac{\Omega^*}{2}|0\rangle\langle 1| - \hbar\frac{\Omega}{2}|1\rangle\langle 0|.$$

$$\Omega = \frac{\mathbf{A}\cdot\mathbf{d_{eg}}}{\hbar}$$

$$\hat{V} = -\frac{1}{2}(\mathbf{A}\cdot\mathbf{d}_{ge}e^{-i\omega t} + \mathbf{A}^*\cdot\mathbf{d}_{ge}e^{i\omega t})\hat{\sigma}_{ge} - \frac{1}{2}(\mathbf{A}\cdot\mathbf{d}_{eg}e^{-i\omega t} + \mathbf{A}^*\cdot\mathbf{d}_{eg}e^{i\omega t})\hat{\sigma}_{eg},$$

# Steady state: atomic polarization, absorption, dipsersion

$$\dot{\hat{\rho}} = \mathcal{L}(\hat{\rho}), \qquad \hat{\Lambda} = \Gamma\hat{\sigma}_{gg}\rho_{ee}. \qquad \hat{\Gamma} = \Gamma\hat{\sigma}_{ee}.$$

$$\dot{\hat{\rho}} = -\frac{i}{\hbar}[\hat{H}'_I, \hat{\rho}] - \frac{1}{2}\{\hat{\Gamma}, \hat{\rho}\} + \hat{\Lambda},$$

$$\dot{\hat{\rho}}_S = -\frac{i}{\hbar}[\hat{H}_S, \hat{\rho}_S] + \sum_i \gamma_i(\hat{R}_i\hat{\rho}_S\hat{R}_i^\dagger - \frac{1}{2}\{\hat{R}_i^\dagger\hat{R}_i, \hat{\rho}_S\}),$$

$$\dot{\hat{\rho}} = -\frac{i}{\hbar}[\hat{H}_I, \hat{\rho}] + \gamma_1(\hat{\sigma}_{ge}\hat{\rho}\hat{\sigma}_{eg} - \frac{1}{2}\{\hat{\sigma}_{eg}\hat{\sigma}_{ge}, \hat{\rho}\}) + \gamma_2(\hat{\sigma}_{he}\hat{\rho}\hat{\sigma}_{eh} - \frac{1}{2}\{\hat{\sigma}_{eh}\hat{\sigma}_{he}, \hat{\rho}\}) +$$
$$+\gamma_3(|g\rangle\langle g|\hat{\rho}|g\rangle\langle g| - \frac{1}{2}\{|g\rangle\langle g|, \hat{\rho}\}) + \gamma_4(|h\rangle\langle h|\hat{\rho}|h\rangle\langle h| - \frac{1}{2}\{|h\rangle\langle h|, \hat{\rho}\}). \qquad (1.12)$$

$$\rho_{ee} = \frac{|\Omega|^2}{\Gamma^2 + 2|\Omega|^2 + 4\Delta^2},$$

$$\rho_{eg} = -\frac{2(\Delta - i\Gamma/2)\Omega}{\Gamma^2 + 2|\Omega|^2 + 4\Delta^2}. \qquad \rho_{eg} = \approx -\frac{\Omega}{2(\Delta + i\Gamma/2)}.$$

$$\boxed{\mathbf{P}(\mathbf{r}, t) = n(\mathbf{r})\mathrm{Tr}(\hat{\rho}(\mathbf{r}, t)\hat{\mathbf{d}}),}$$

# Lightshift (AC Stark shift)

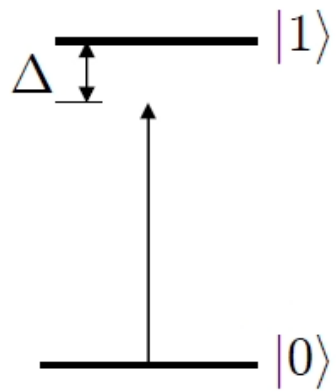


$$H = \hbar \begin{pmatrix} \omega_0 & \Omega e^{i\omega t}/2 \\ \Omega^* e^{-i\omega t}/2 & 0 \end{pmatrix}$$

$$H_{int} = \frac{\hbar}{2} \begin{pmatrix} 2\Delta & \Omega \\ \Omega^* & 0 \end{pmatrix}$$

Potraktujmy to jako $\underbrace{\hbar \begin{pmatrix} \Delta & 0 \\ 0 & 0 \end{pmatrix}}_{H_0} + \underbrace{\frac{\hbar}{2} \begin{pmatrix} 0 & \Omega \\ \Omega^* & 0 \end{pmatrix}}_{V}$

$$E_0 = E_0^{(0)} + \langle 0|V|0\rangle + \frac{|\langle 0|V|1\rangle|^2}{\Delta}$$

=0

$$\sum_{m\neq 0} \frac{1}{4\hbar} \frac{|Ed_{m0}|^2}{\omega - \omega_{m0}}$$

# Three levels: EIT

$$\hat{H}_I = -\frac{\hbar}{2}\begin{pmatrix} 0 & 0 & \Omega_1^* \\ 0 & 2\delta & \Omega_2^* \\ \Omega_1 & \Omega_2 & -2\Delta \end{pmatrix},$$

$$\rho_{gr} = -\frac{\Omega_c^* \Omega_p}{(\gamma - i\delta)(\Gamma/4 - i\Delta) + |\Omega_c|^2}$$

$$\chi_\Xi = i\frac{n d_{ge}^2}{\varepsilon_0 \hbar}\frac{\gamma - i\delta}{(\gamma - i\delta)(\Gamma/4 - i\Delta) + |\Omega_c|^2}$$

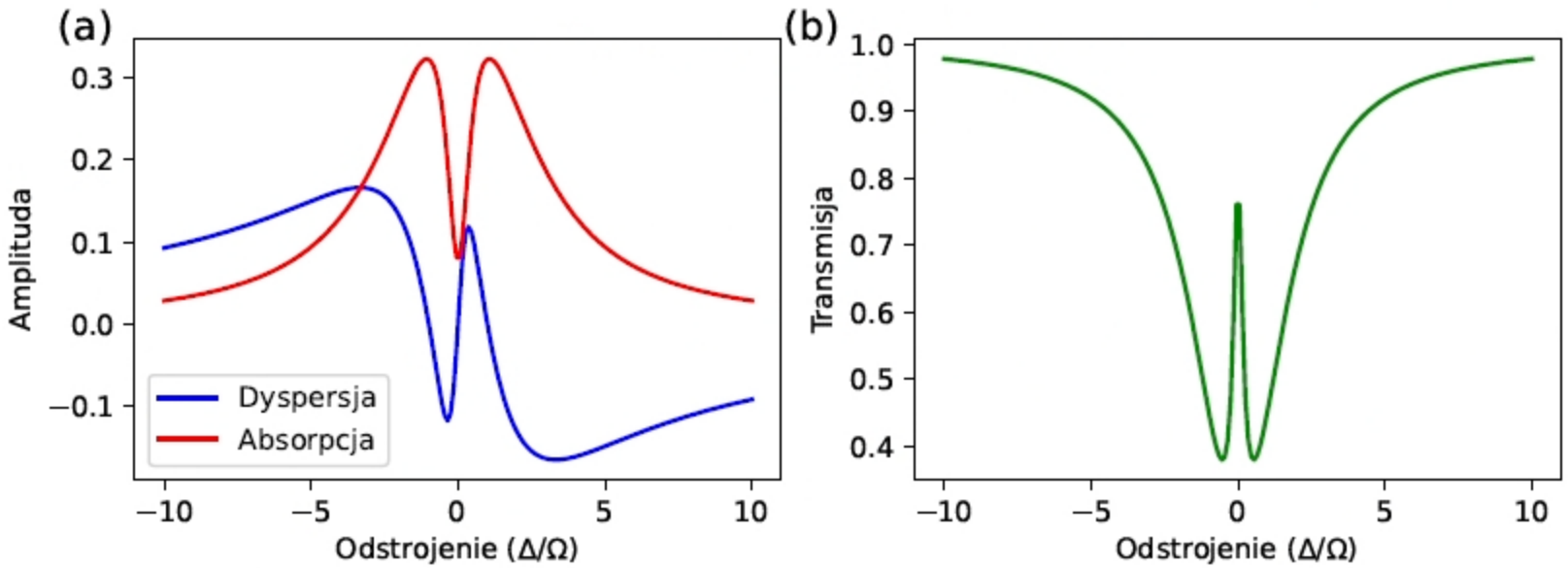

# Three levels: two-Photon Rabi oscillation

$$\hat{H}_I = -\frac{\hbar}{2}\begin{pmatrix} 0 & 0 & \Omega_1^* \\ 0 & 2\delta & \Omega_2^* \\ \Omega_1 & \Omega_2 & -2\Delta \end{pmatrix},$$

$$\dot{\rho}_{hg} = -\underbrace{\frac{\Omega_1\Omega_2^*}{2\Gamma + 4i\Delta}}_{\text{Raman}} + i\left(\underbrace{\frac{\Delta|\Omega_2|^2}{\Gamma^2+4\Delta^2}}_{\text{ac-Stark shift}} + \delta\right)\rho_{hg} - \left(\frac{1}{2}\gamma + \underbrace{\frac{\Gamma|\Omega_2|^2}{2\Gamma^2+8\Delta^2}}_{\text{power broadening}}\right)\rho_{hg}. \quad (2.68)$$

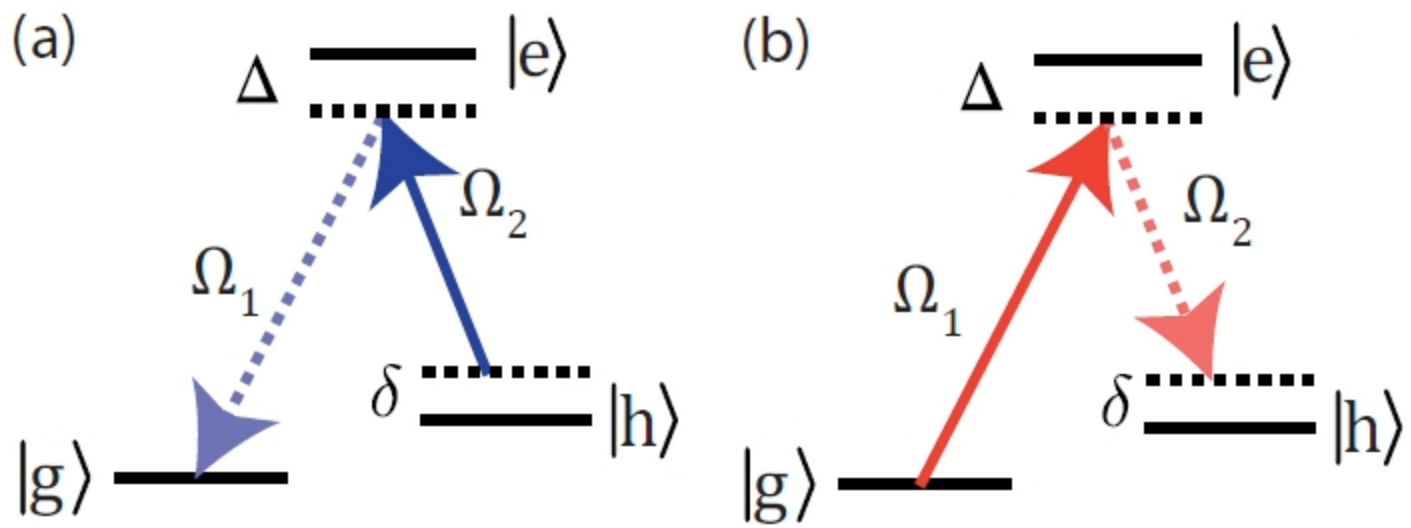

# Rydberg atoms

- large principal quantum numbers n ≈ 15-100+
- long state lifetimes τ ≈ 15-200 μs
- long interaction radii ~μm
- microwave (and mm-wave) energy levels transitions Δf ≈ 1000-2 GHz

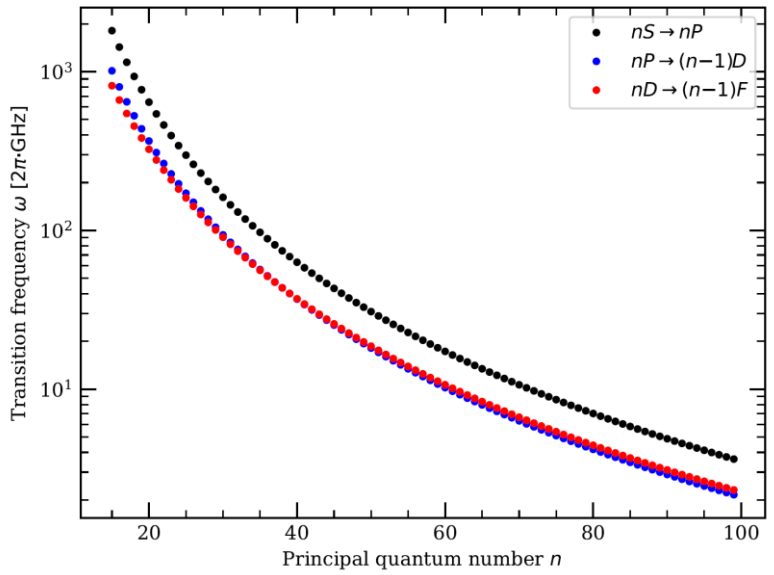


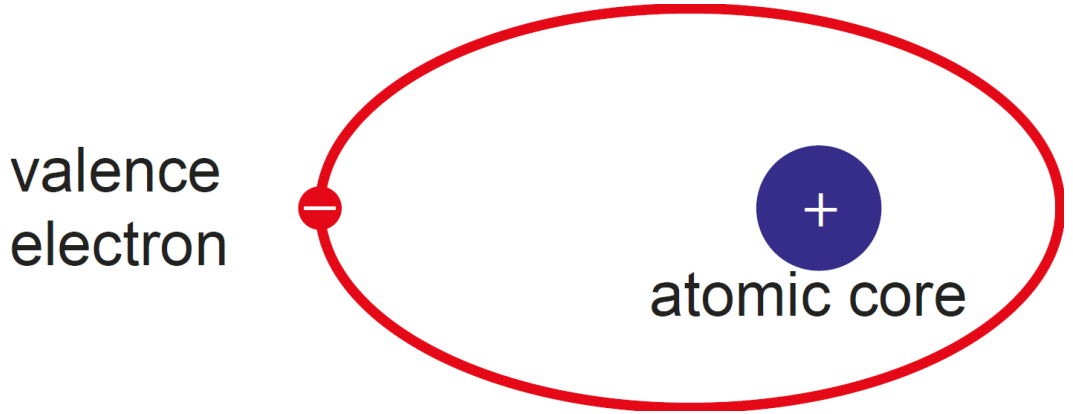

# Interacting atoms

$$V(R)_{dd} = \frac{1}{4\pi\varepsilon_0 R^3}\left(\vec{d}_1 \cdot \vec{d}_2 - 3(\vec{d}_1 \cdot \hat{R})(\vec{d}_2 \cdot \hat{R})\right)$$

$$\hat{H} = \begin{pmatrix} 0 & V(R) \\ V(R)^* & \Delta_{r'r''} \end{pmatrix}$$

$$\delta E = \frac{\Delta_{r'r''}}{2} - \sqrt{\frac{\Delta_{r'r''}^2}{4} + V(R)^2}$$

$$\delta E = -\frac{V^2}{\Delta_{r'r''}} \propto -\frac{1}{R^6} \qquad , V(R) \ll \Delta_{r'r''}$$

$$\delta E = -V(R) \propto \frac{1}{R^3} \qquad V(R) \gg \Delta_{r'r''}$$

# Rydberg blockade

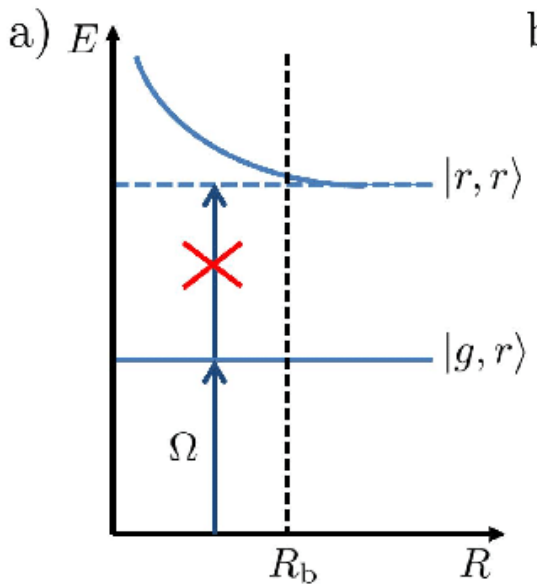


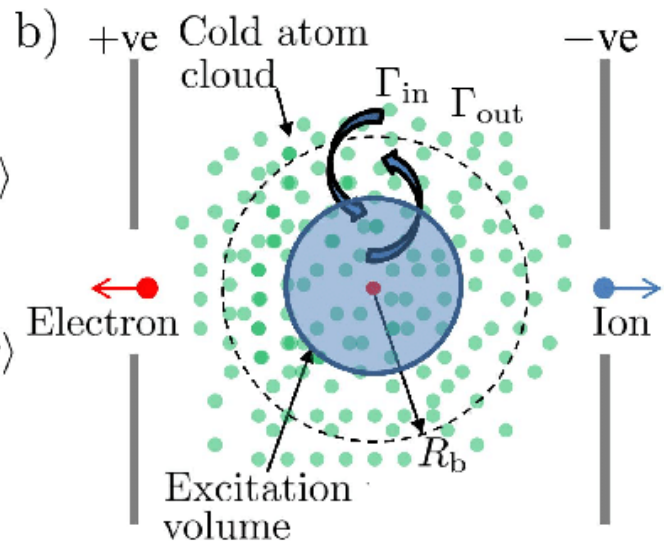


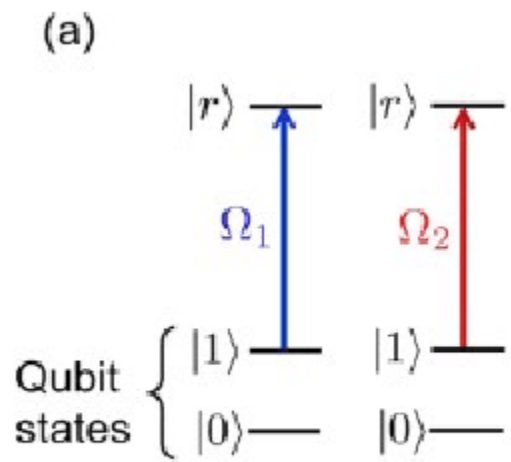


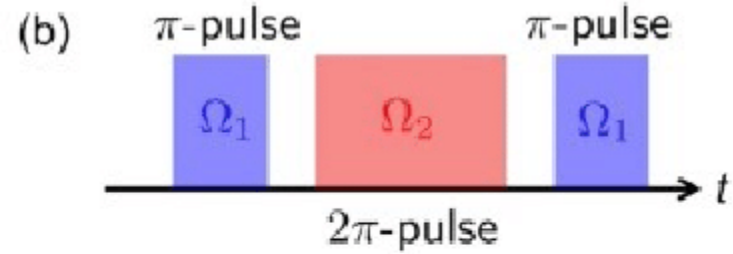


(c)

$$
\begin{aligned}
|00\rangle &\rightarrow |00\rangle \\
|01\rangle &\rightarrow -|01\rangle \\
|10\rangle &\rightarrow -|10\rangle \\
|11\rangle &\rightarrow -|11\rangle
\end{aligned}
$$

# Multifunctional quantum memories

Photon spin-wave storage

Photon generation

Spin-wave interference

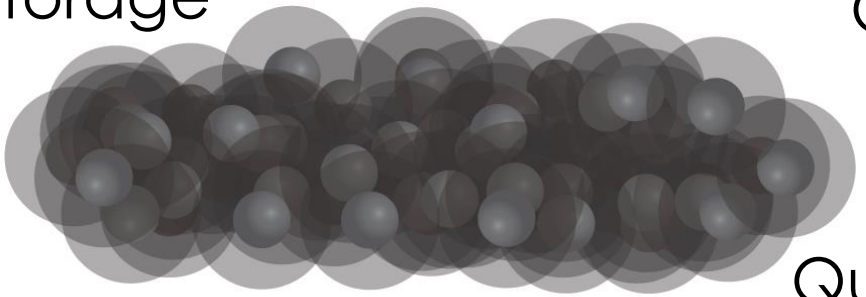

Quantum repeater

Error correction

Quantum gates: linear, nonlinear

Qu**d**it storage: spatial, temporal

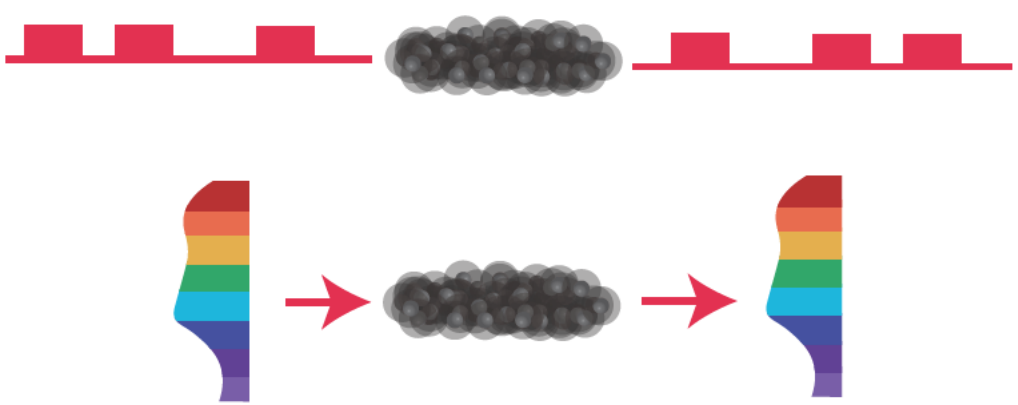

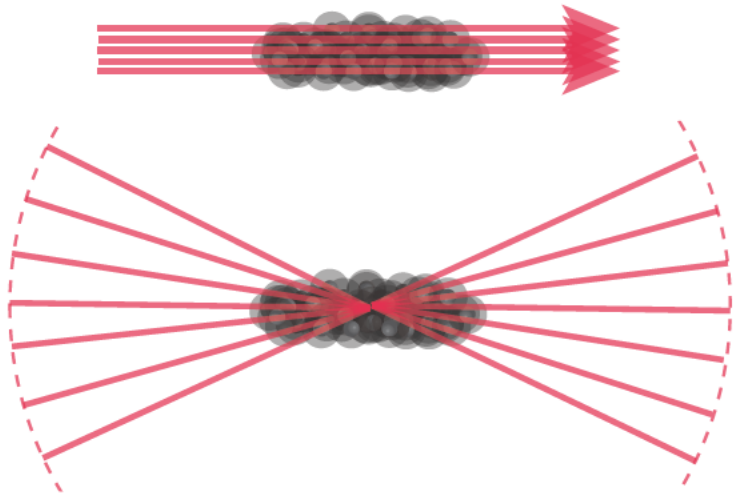

# Raman interface

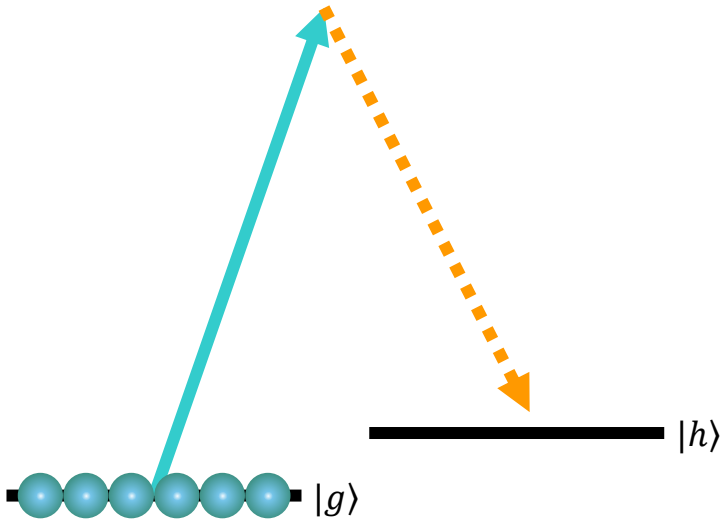


**two-mode squeezed state**
creation via off-resonant
**Raman scattering**

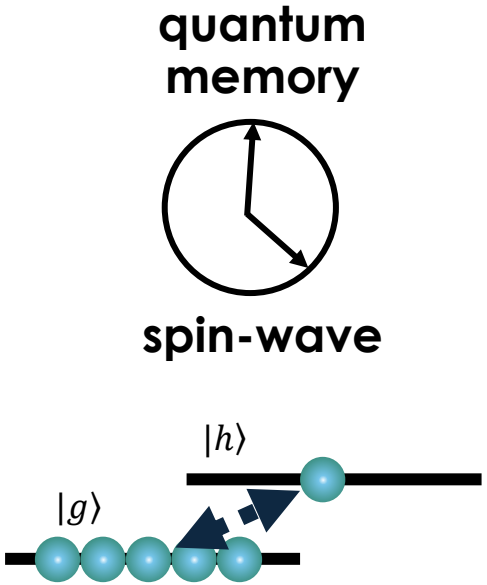


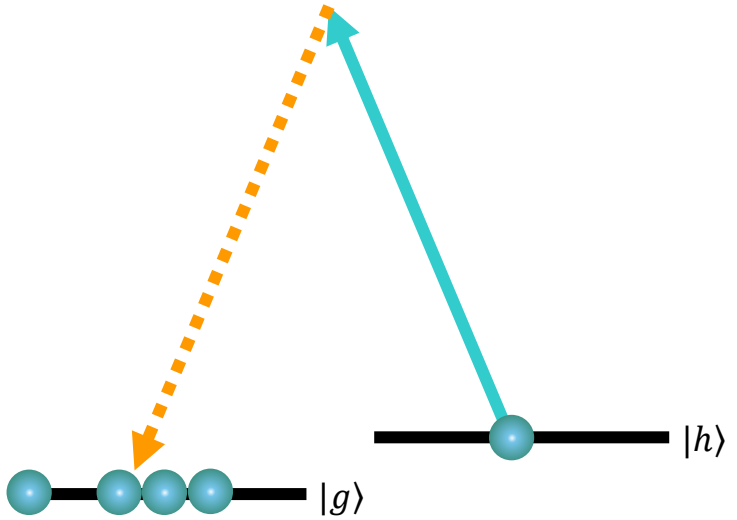


**readout stage** after storage time
results in **anihilation of spin-wave**

$$\frac{1}{\sqrt{N}}\left(e^{i\mathbf{K}\cdot\mathbf{r}_1}\left|\;\right\rangle + e^{i\mathbf{K}\cdot\mathbf{r}_2}\left|\;\right\rangle + e^{i\mathbf{K}\cdot\mathbf{r}_3}\left|\;\right\rangle + \ldots\right)$$

$|g\rangle$
$|h\rangle$

# Wavevector Multiplexing

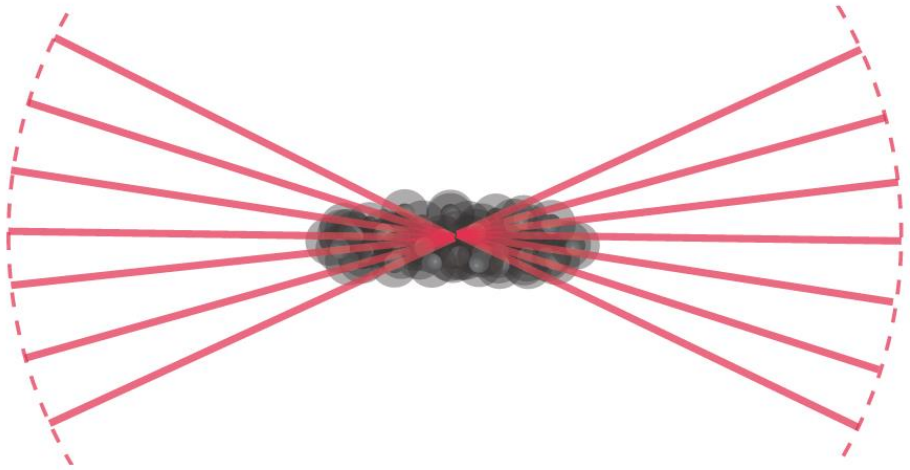

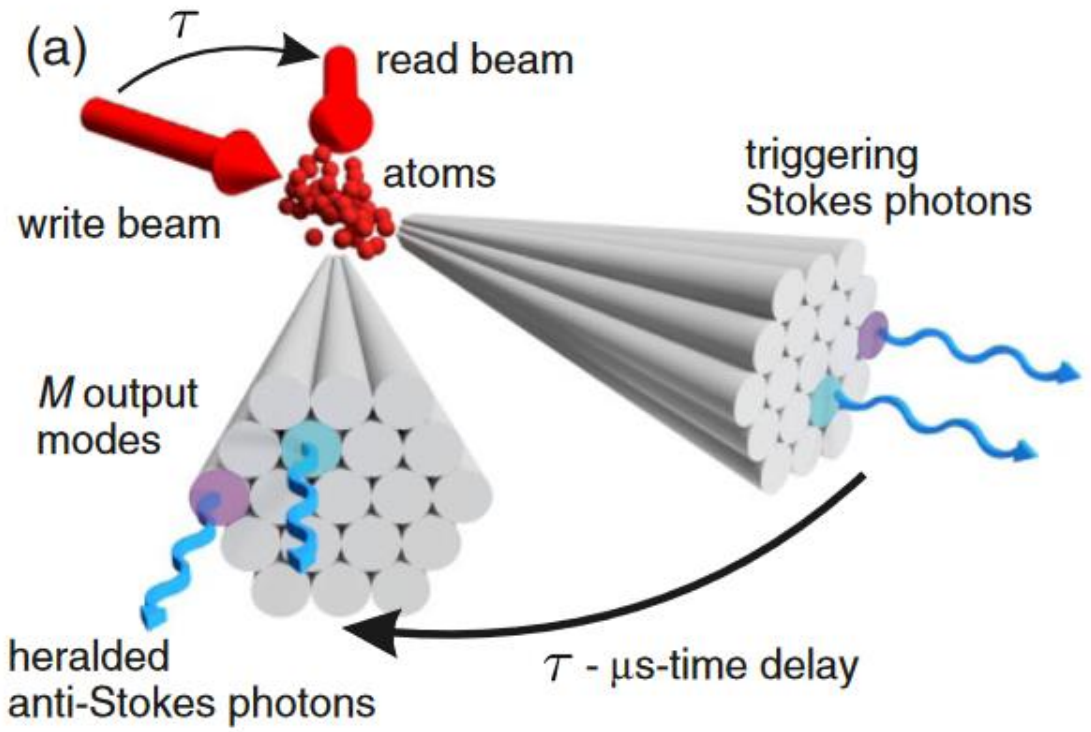


Radosław Chrapkiewicz, Michał Dąbrowski, and Wojciech Wasilewsk
Phys. Rev. Lett. 118, 063603

# Deterministic single and multi-photons

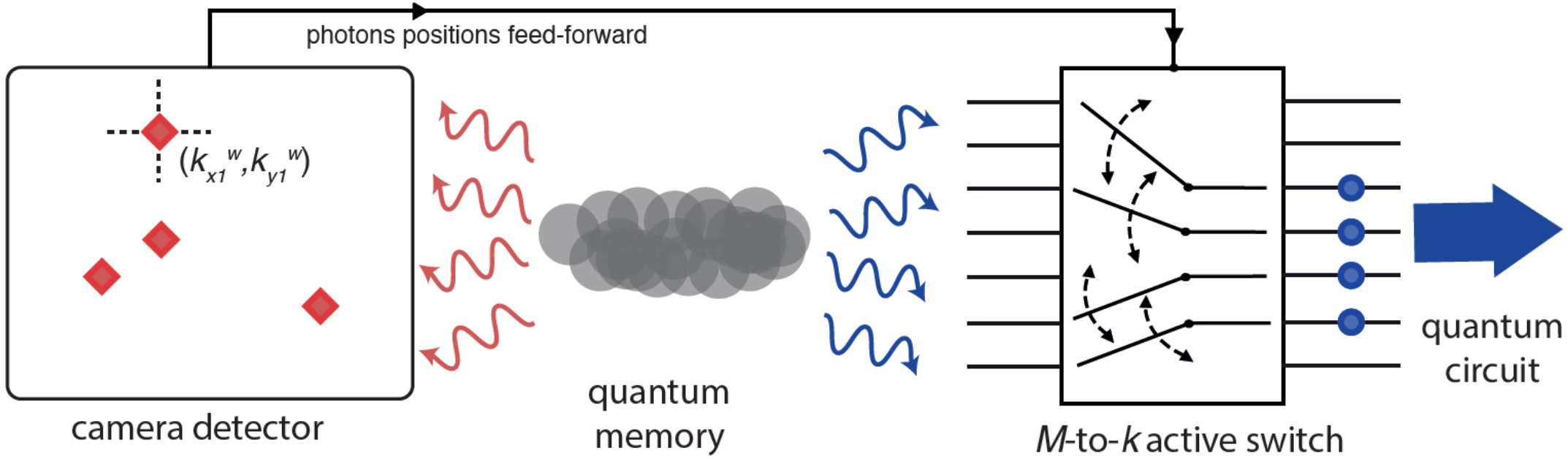


**MP**, M. Dąbrowski, M. Mazelanik, A. Leszczyński, M. Lipka, W. Wasilewski, Nat. Commun **8**, 2140 (2017)

# I-sCMOS camera

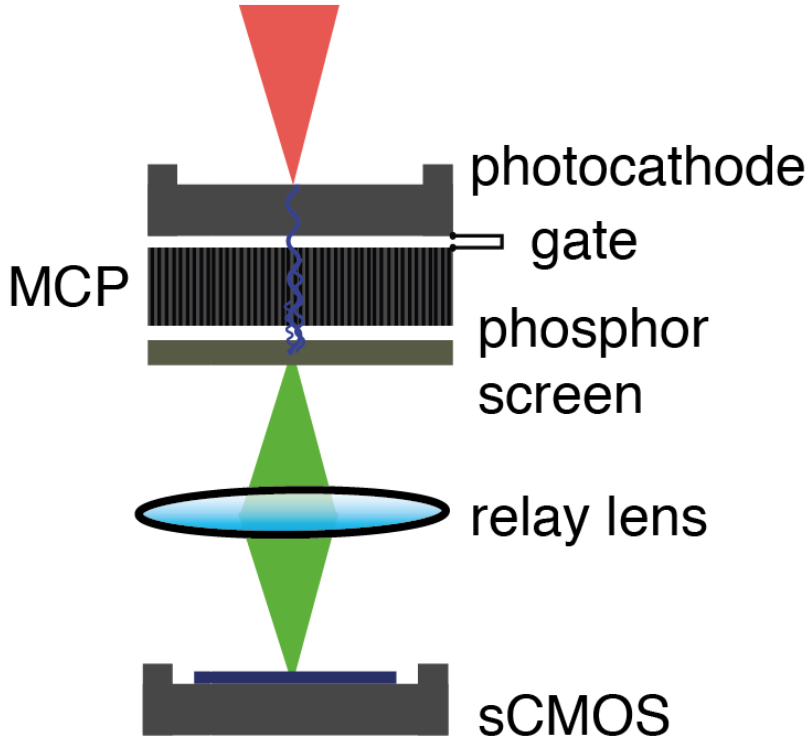


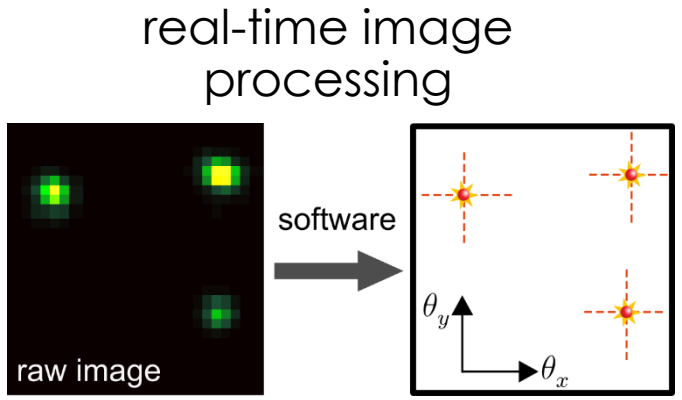


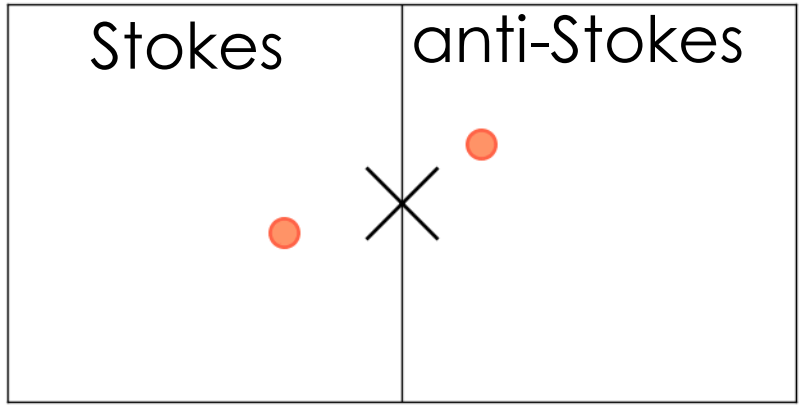


R. Chrapkiewicz, M. Jachura, K. Banaszek, W. Wasilewski, Nat. Photonics **10**, 576 (2016)
M. Jachura, R. Chrapkiewicz, W. Wasilewski, R. Demkowicz-Dobrzański, K. Banaszek, Nat. Commun. **7**, 11411(2016)
**MP**, M. Dąbrowski, M. Mazelanik, A. Leszczyński, M. Lipka, W. Wasilewski, Nat. Commun. **8**, 2140 (2017)

# Photon number correlations

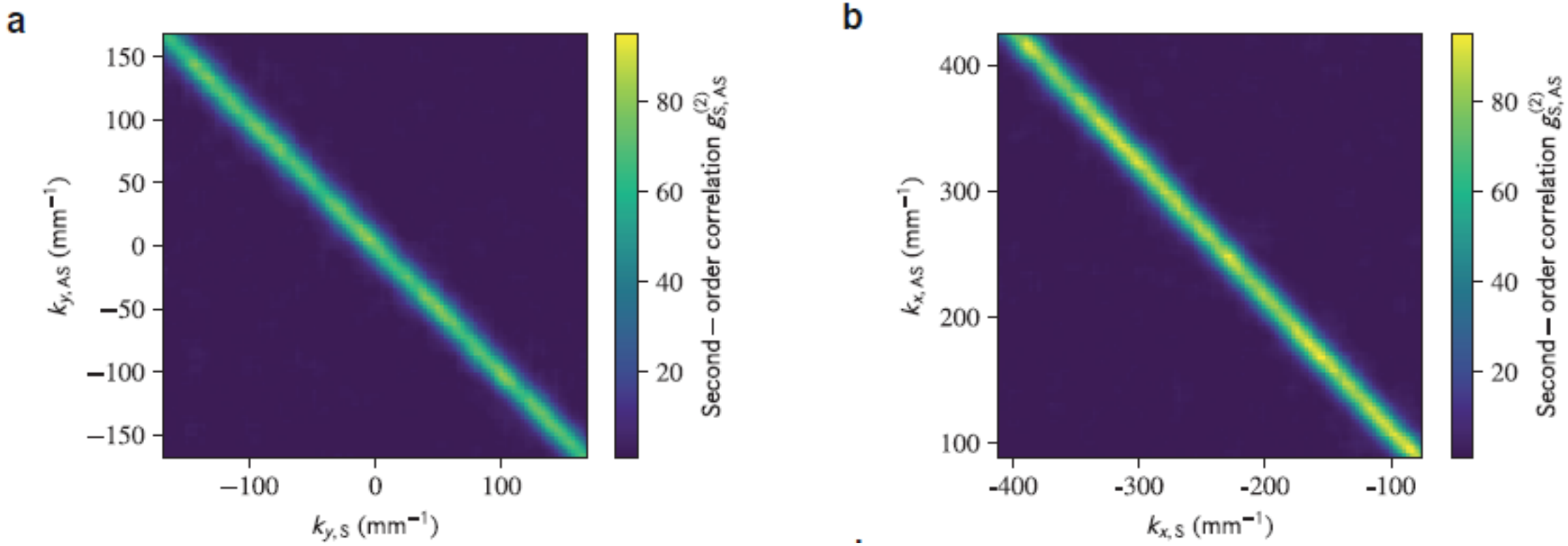


**non-classical** correlations

$$g^{(2)} = \frac{\langle n_S n_{AS} \rangle}{\langle n_S \rangle \langle n_{AS} \rangle} = 72 \pm 5 \gg 2$$

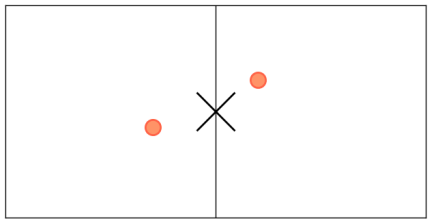

- **>500 modes**
- **>50 μs storage**

Nat. Commun **8**, 2140 (2017)

# New system

Custom FPGA data processing

New custom high-voltage gating module

Now 100.000 frames per second, **~10 microseconds from detection to information**

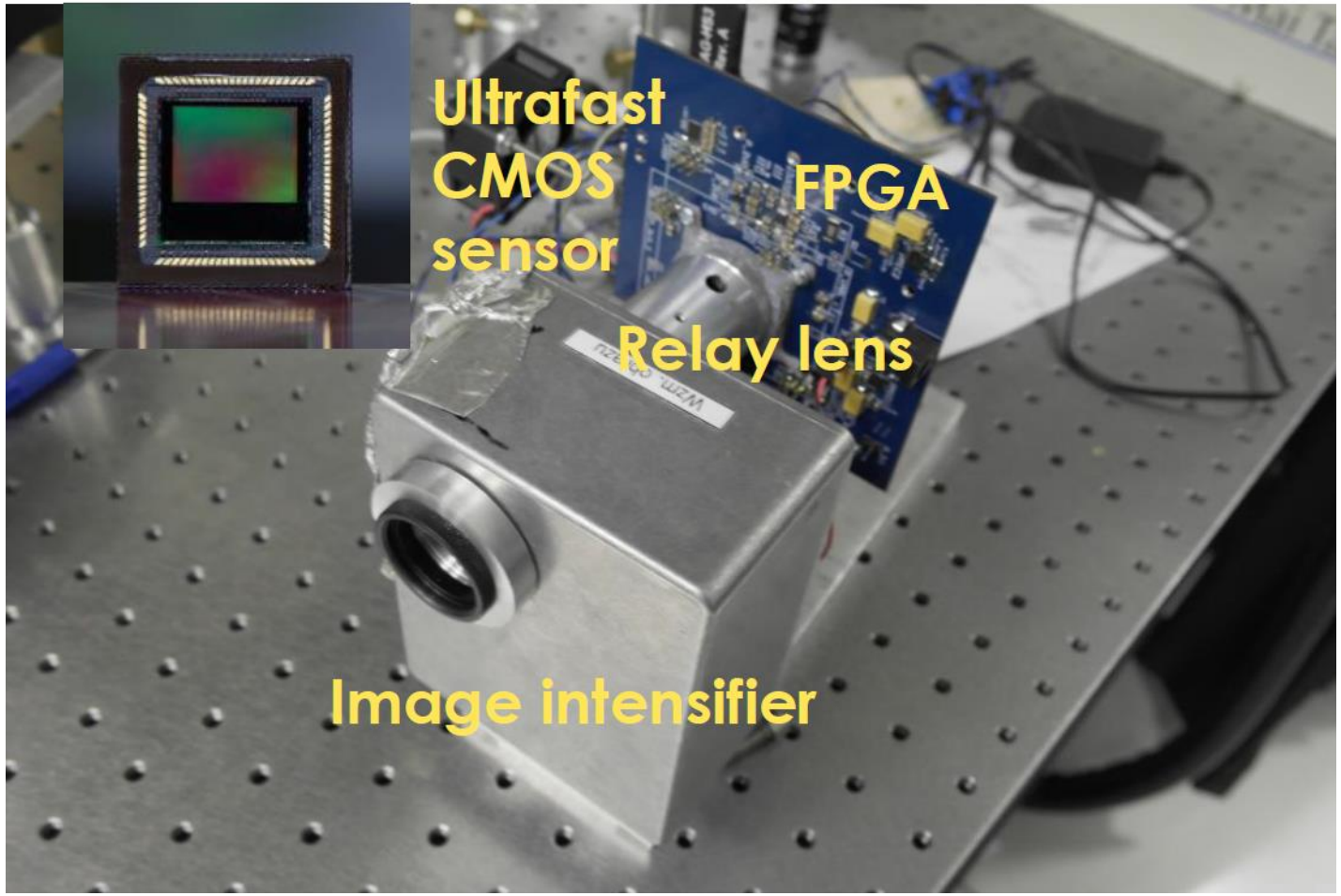


Optics Letters 46, 3009-3012 (2021)

# Photon rate gains

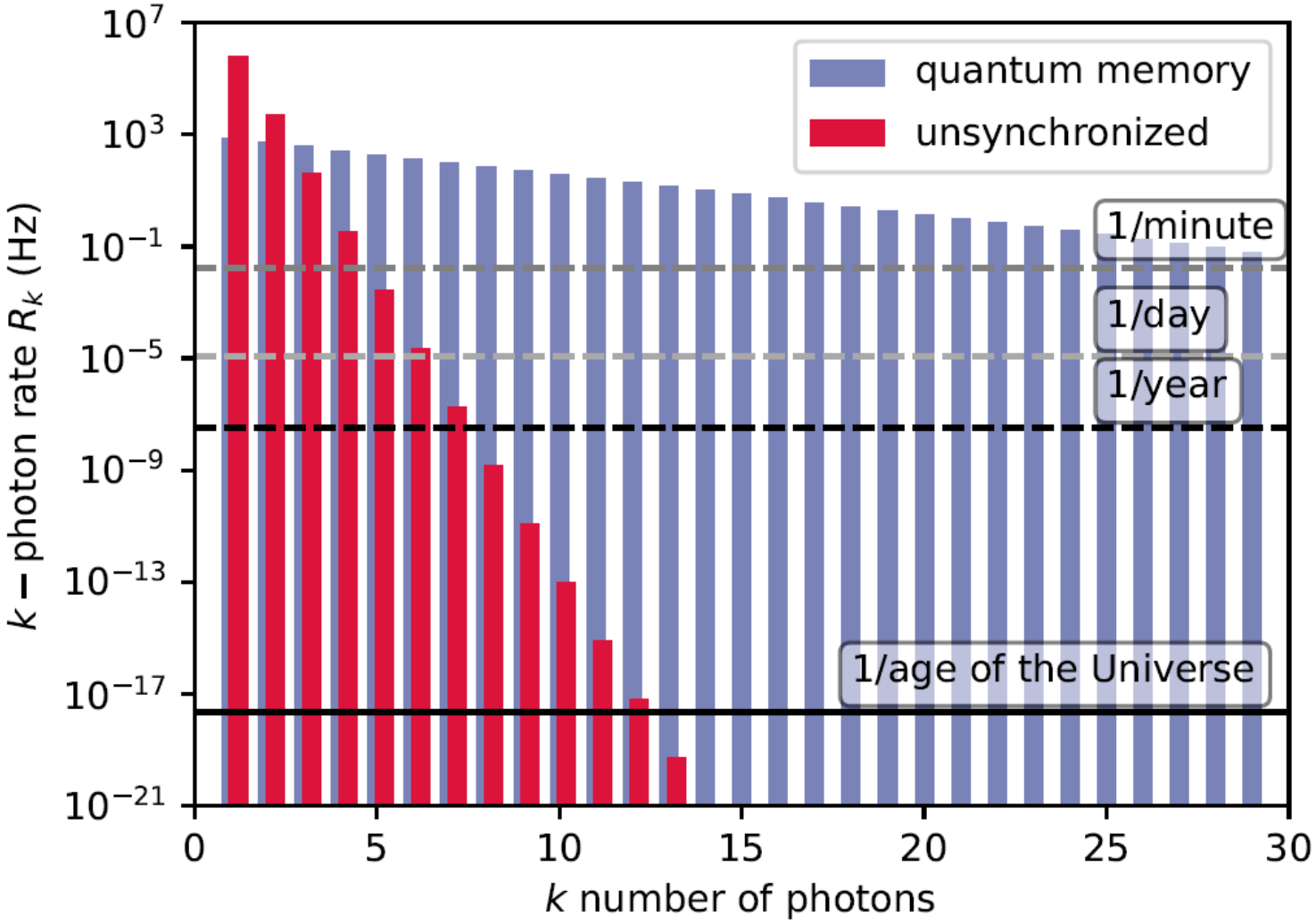


**1 kHz rep. rate quantum memory**

vs

**80 MHz rep. rate SPDC**

# Temporal multiplexing

# Gradient echo memory (GEM)

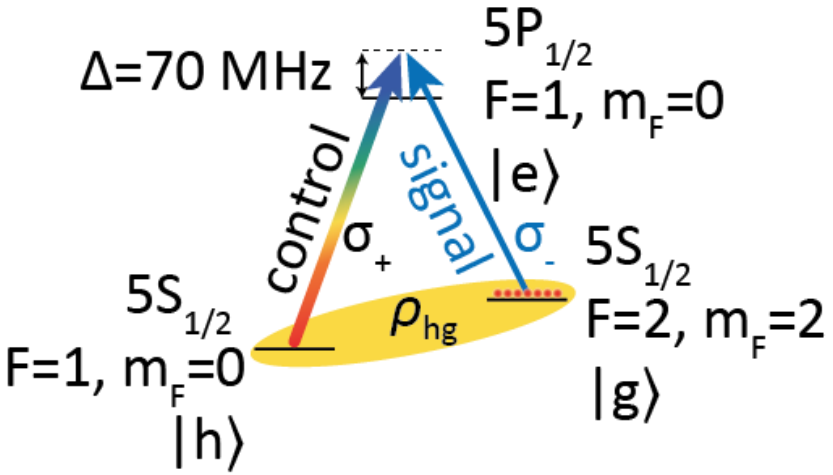


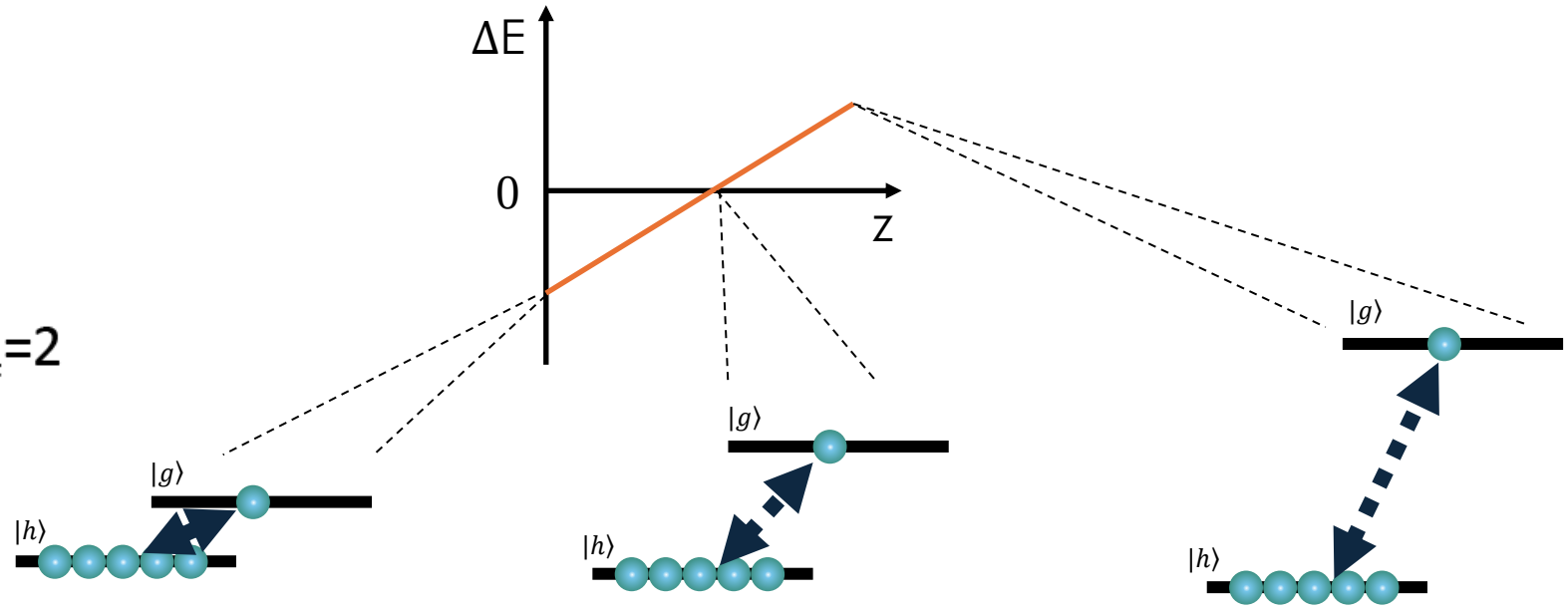


$$\frac{\partial \check{\rho}_{hg}(z,t)}{\partial t} = \frac{i}{\hbar}\frac{\Omega^*(t)dA(z,t)}{4\Delta - 2i\Gamma} - \frac{1}{2\tau}\check{\rho}_{hg}(z,t) + i\delta_{\mathrm{tot}}(z,t)\check{\rho}_{hg}(z,t),$$

$$\frac{\partial A(z,t)}{\partial z} = -i\frac{\hbar\Omega(t)\check{\rho}_{hg}(z,t)/d + A(z,t)}{2\Delta + i\Gamma}\frac{\Gamma}{2}gn(z),$$

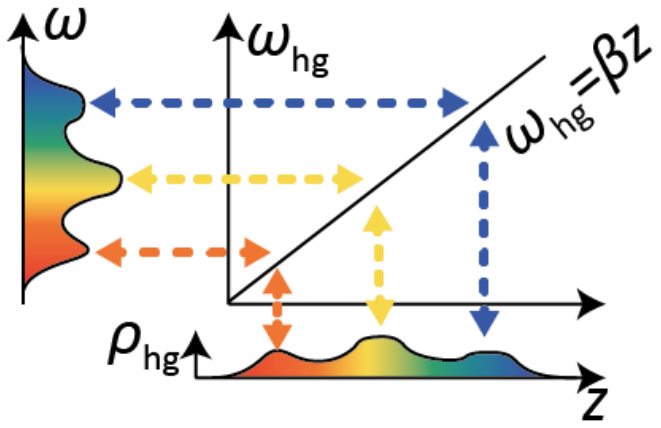


Hosseini et al., Nature 461, 241 (2009)

# Spin-wave phase modulation (GEM)

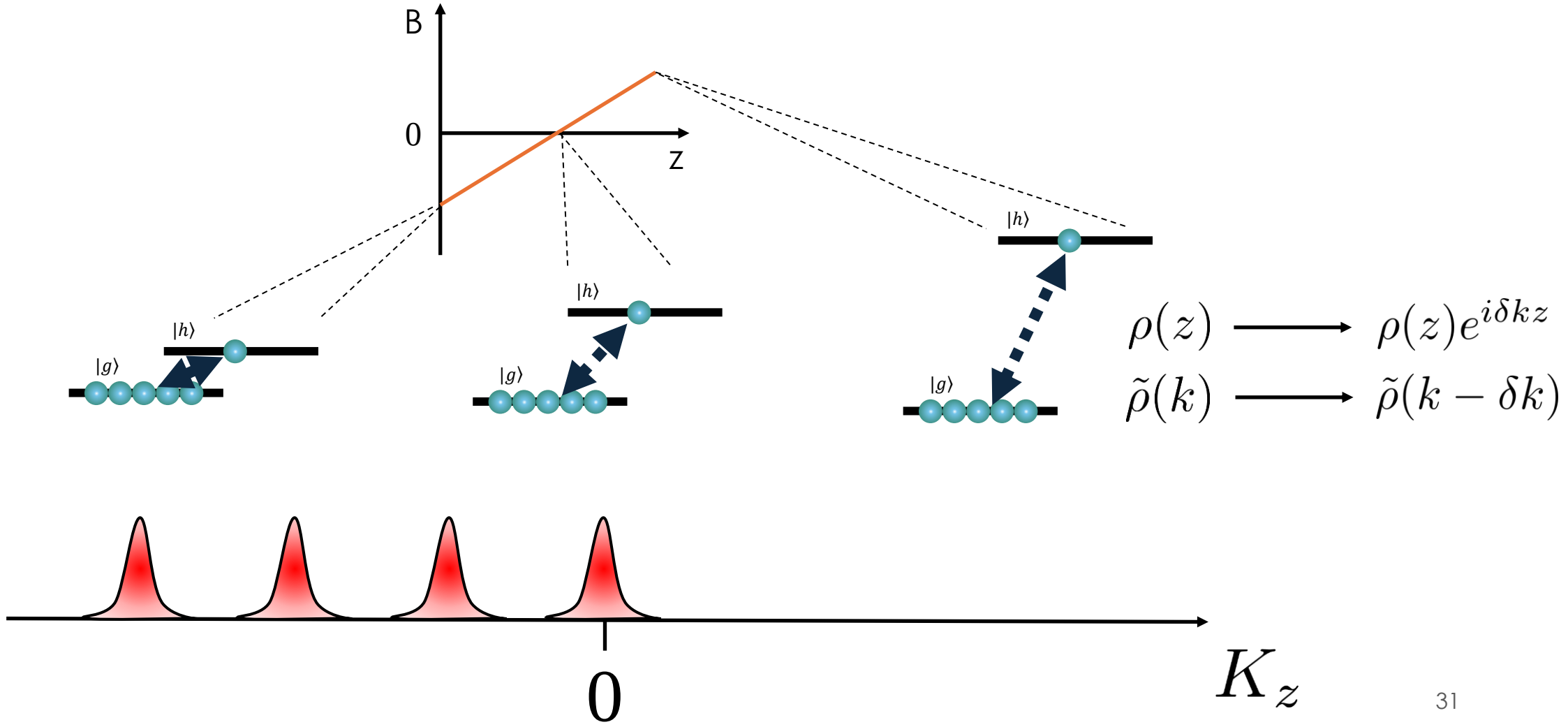

# ac-Stark spin-wave phase modulation

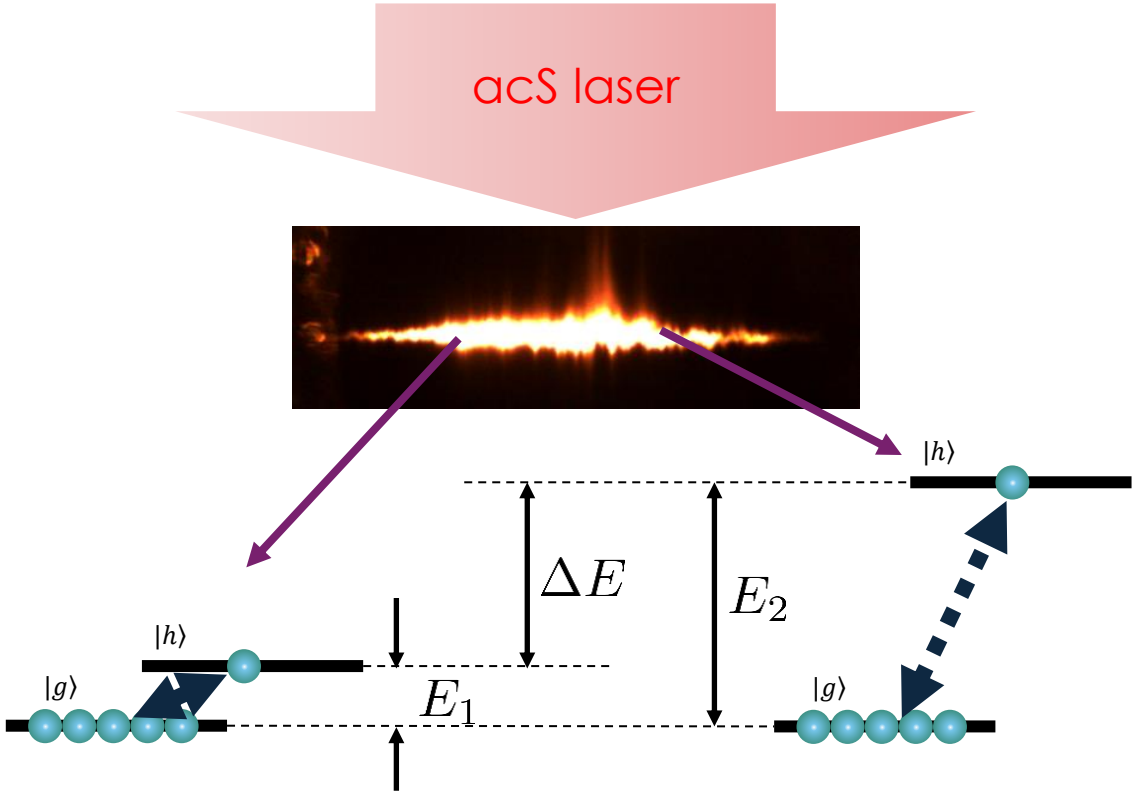


$$\Delta\varphi(y,z) = \Delta E(y,z)T/\hbar$$

Differential phase accumulated during free evolution

Fictitious magnetic fields

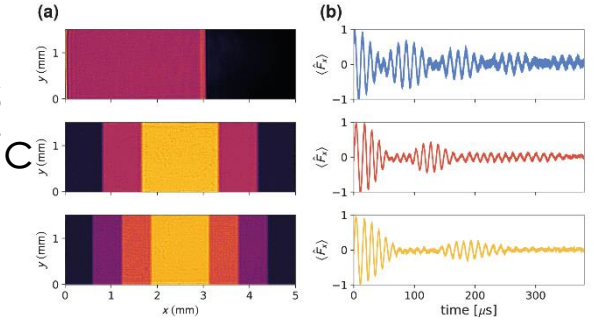


Opt. Lett. 43, 1147 (2018)

Spin-wave Hong-Ou-Mandel interference

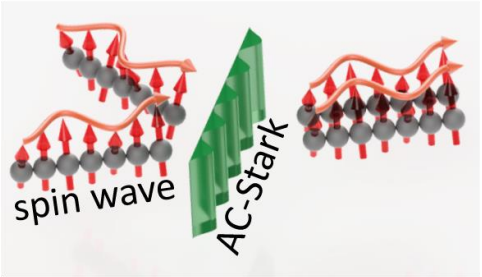


Phys. Rev. Lett. **122**, 063604 (2019)

Spin-wave processor of stored optical pulses

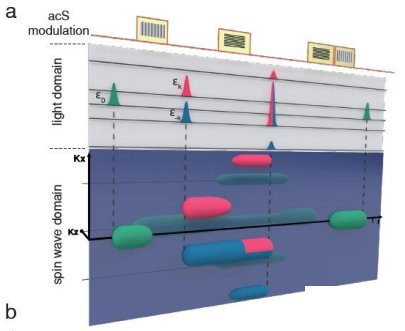


npj Quantum Information **5**, 22 (2019)

# ac-Stark GEM

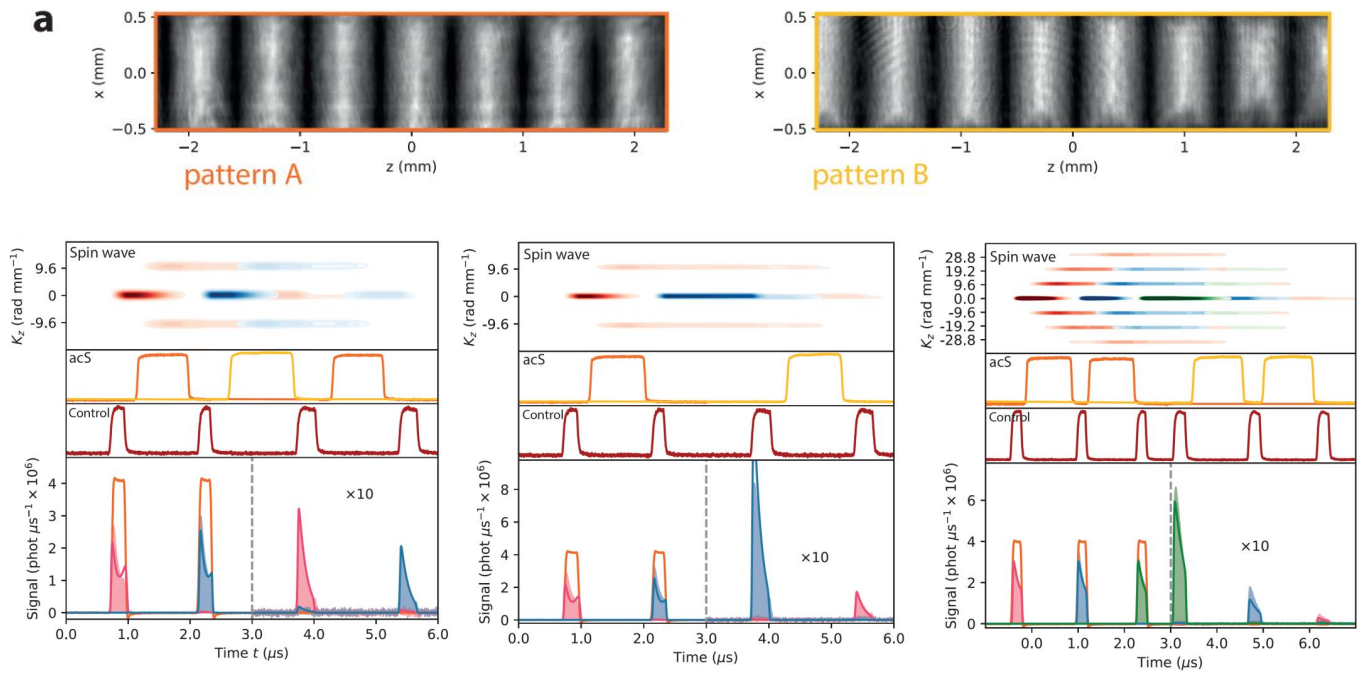
a
x (mm)
z (mm)
pattern A
pattern B
Spin wave
acS
Control
$K_z$ (rad mm$^{-1}$)
Signal (phot $\mu$s$^{-1}$ × 10$^6$)
×10
Time $t$ ($\mu$s)

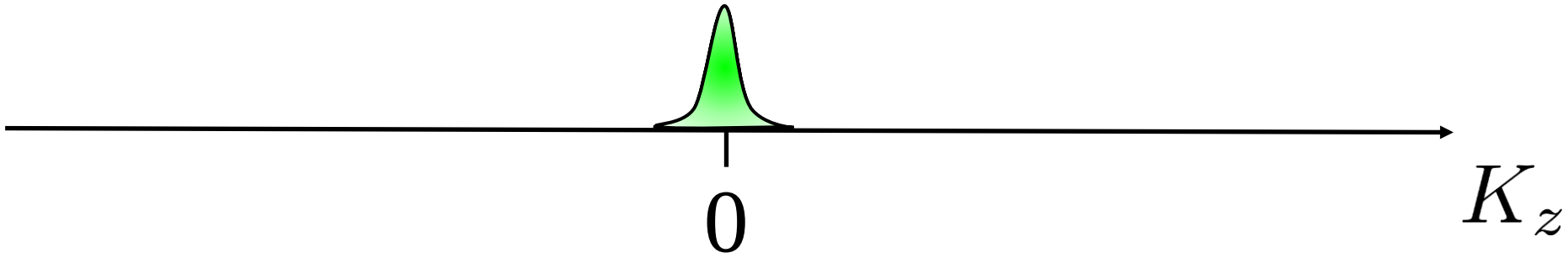
0
$K_z$

# Spin-wave splitter

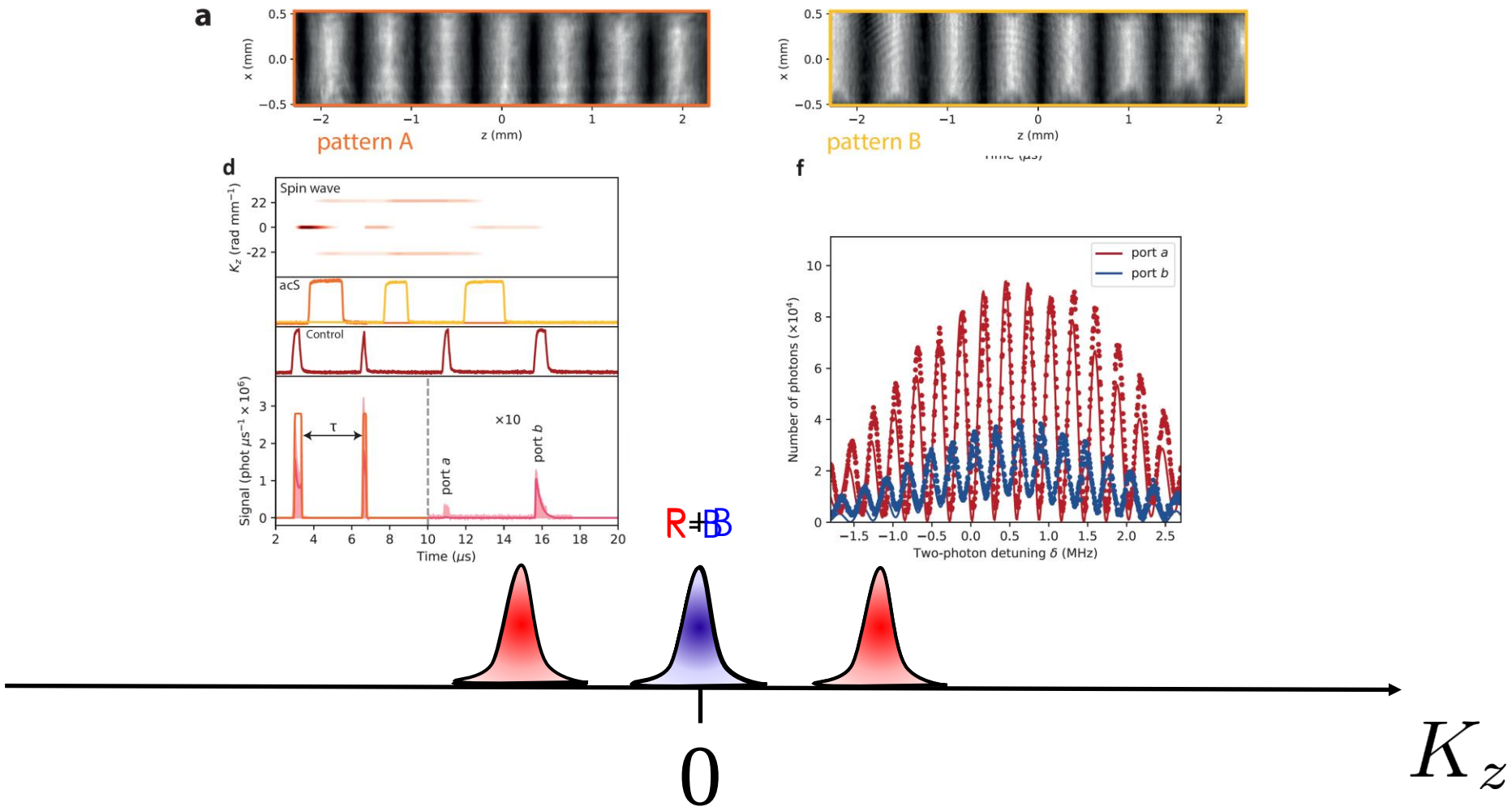

# Time-lens and spectro-spatial mapping

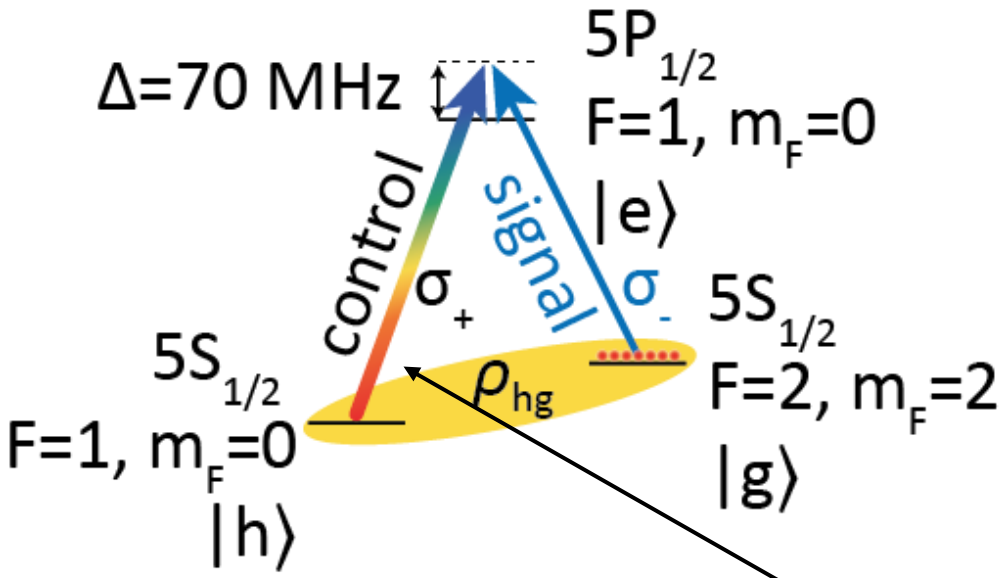


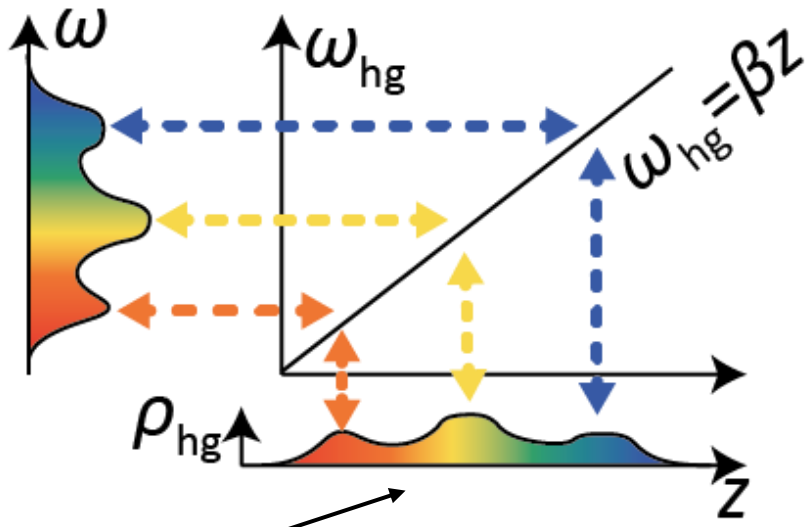


$$\rho_{hg}(z) \propto \widetilde{A}(\beta z)$$

Time-lens realized
by chirped control field

$$\delta\omega(t) = \alpha t$$

$$\begin{bmatrix} 1 & 0 \\ -\frac{1}{f_t} & 1 \end{bmatrix}$$

# Far-field temporal imaging

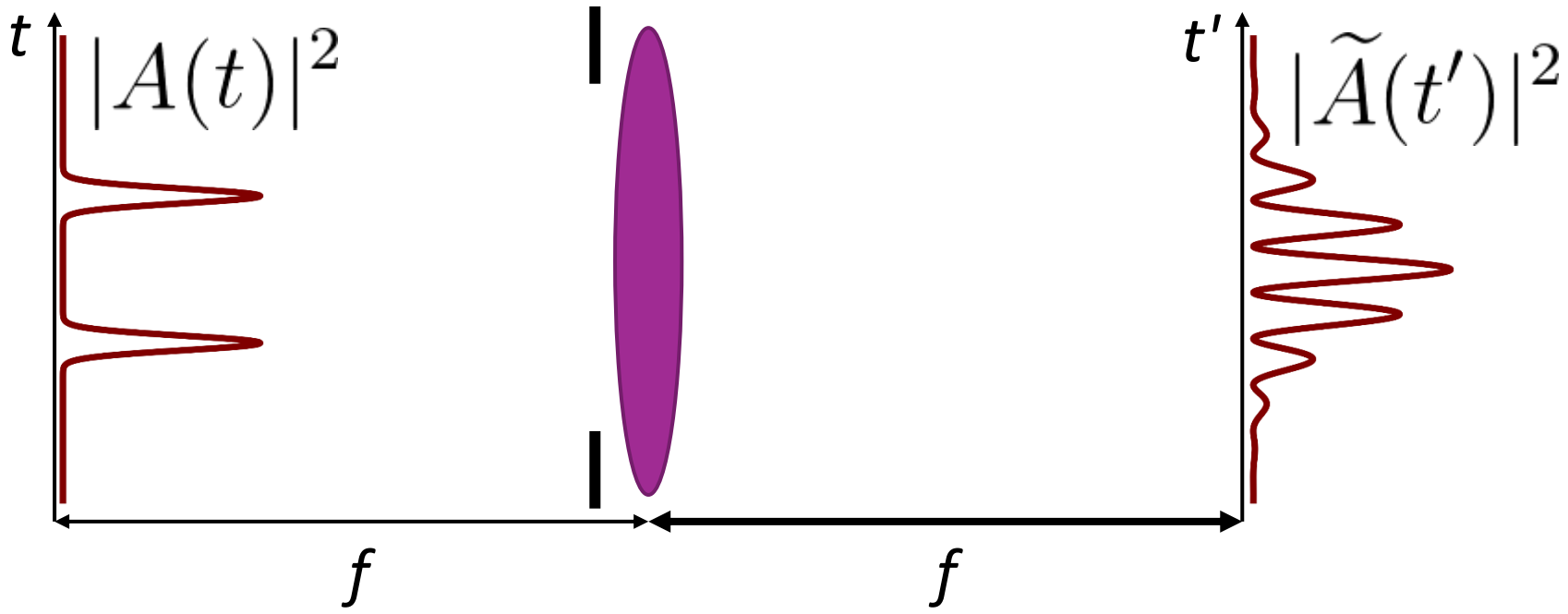


$$|\widetilde{A}(t')|^2 = |\mathcal{F}_t[A(t)](t')|^2$$

# Temporal imaging

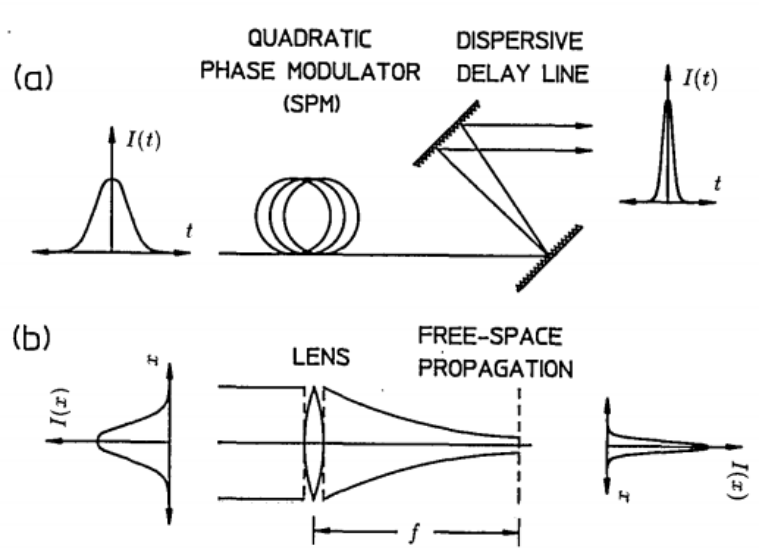


Opt. Lett. 14, 630 (1989)

- Spectral conversion
- Bandwidth manipulation
- Temporal ghost imaging
- Characterization of the time-frequency entanglement
- Manipulation of field-orthogonal temporal modes

Existing solutions are compatible with solid-state emission (high bandwith, low spectral resolution)

No solution for narrowband atomic emission

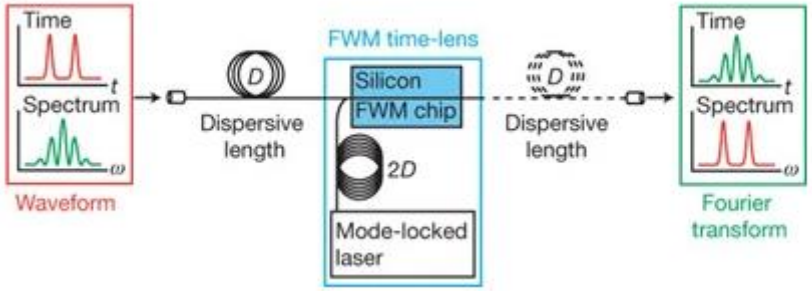


Nature 456, 81–84 (2008)

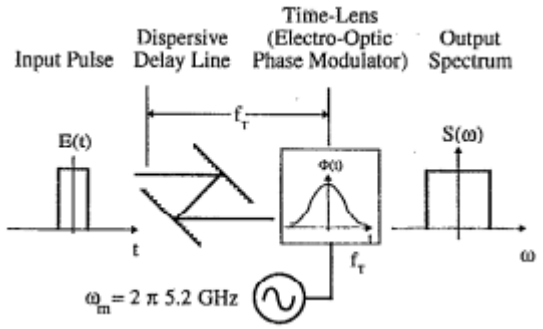


Appl. Phys. Lett. 64, 270–272 (1994)

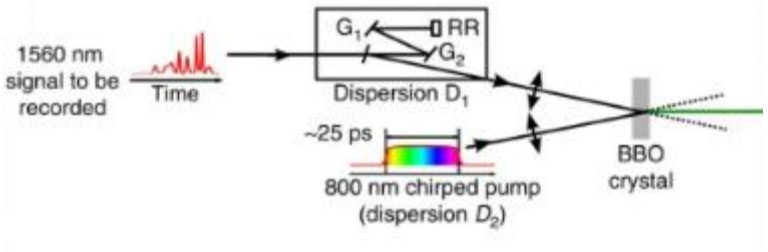


Nat. Commun. 7, 13136 (2016)

# Temporal propagation

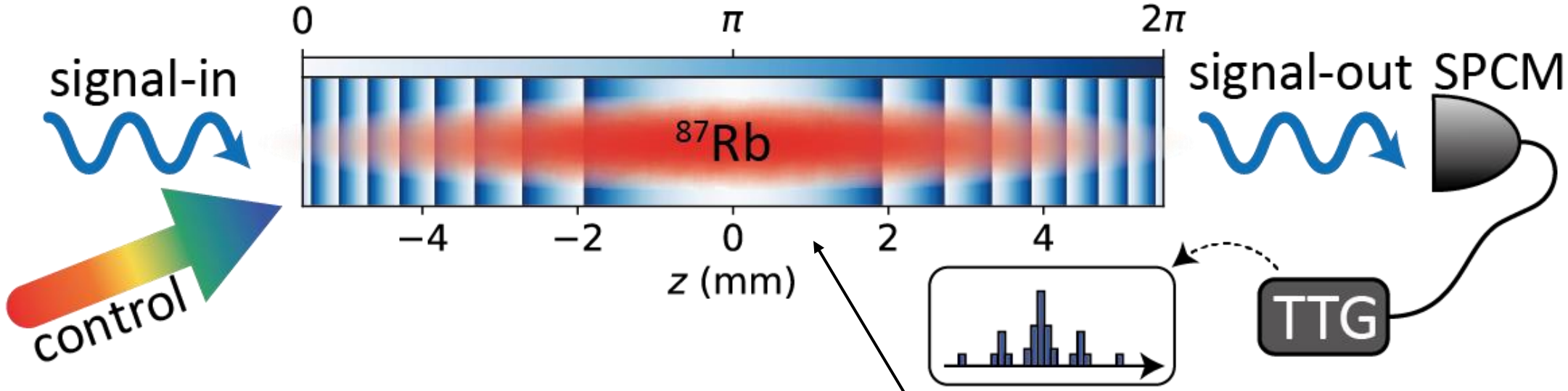


Temporal „free-space" propagation
– a quadratic phase in frequency

$$\tilde{A}(\omega) = \mathcal{F}_t[A(t)](\omega)$$

$$\tilde{A}(\omega) \rightarrow \tilde{A}(\omega)\exp[-i(f_t/\omega_0)\omega^2]$$

Thanks to spectro-spatial mapping the temporal propagation is realized by imposing a quadratic phase (Fresnel) profile onto the atomic coherence $\rho_{hg}$

Optica **7**, 203-208 (2020)

# FF-TI (QMTI) - Rotating Wigner function

$$W(t,\omega) = 1/\sqrt{2\pi}\int_{-\infty}^{\infty} A(t+\xi/2)A^*(t-\xi/2)\exp(-i\omega\xi)$$

$$\begin{bmatrix} t' \\ \frac{\omega'}{\omega_0} \end{bmatrix} = \begin{bmatrix} 1 & 0 \\ -\frac{1}{f_t} & 1 \end{bmatrix} \begin{bmatrix} 1 & f_t \\ 0 & 1 \end{bmatrix} \begin{bmatrix} 1 & 0 \\ -\frac{1}{f_t} & 1 \end{bmatrix} \begin{bmatrix} t \\ \frac{\omega}{\omega_0} \end{bmatrix} = \begin{bmatrix} 0 & f_t \\ -\frac{1}{f_t} & 0 \end{bmatrix} \begin{bmatrix} t \\ \frac{\omega}{\omega_0} \end{bmatrix}$$

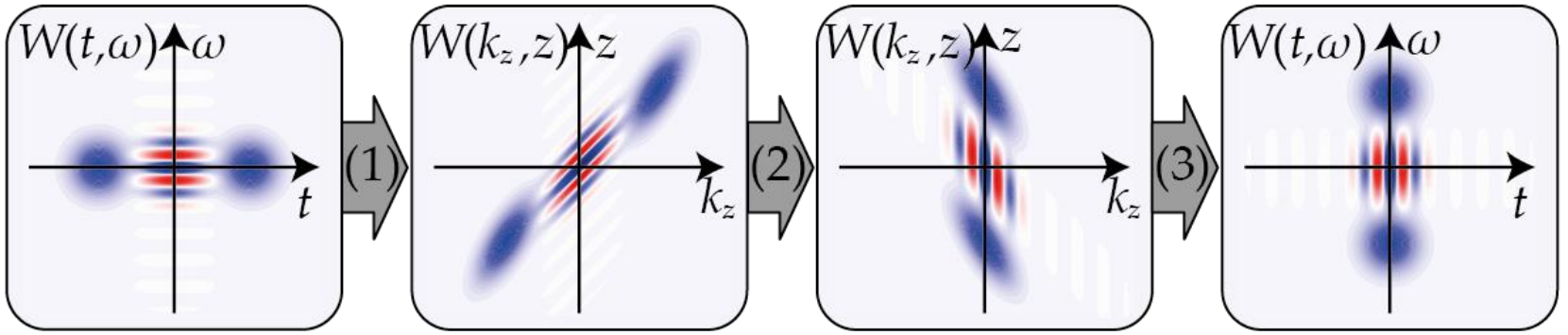


# Example input/output

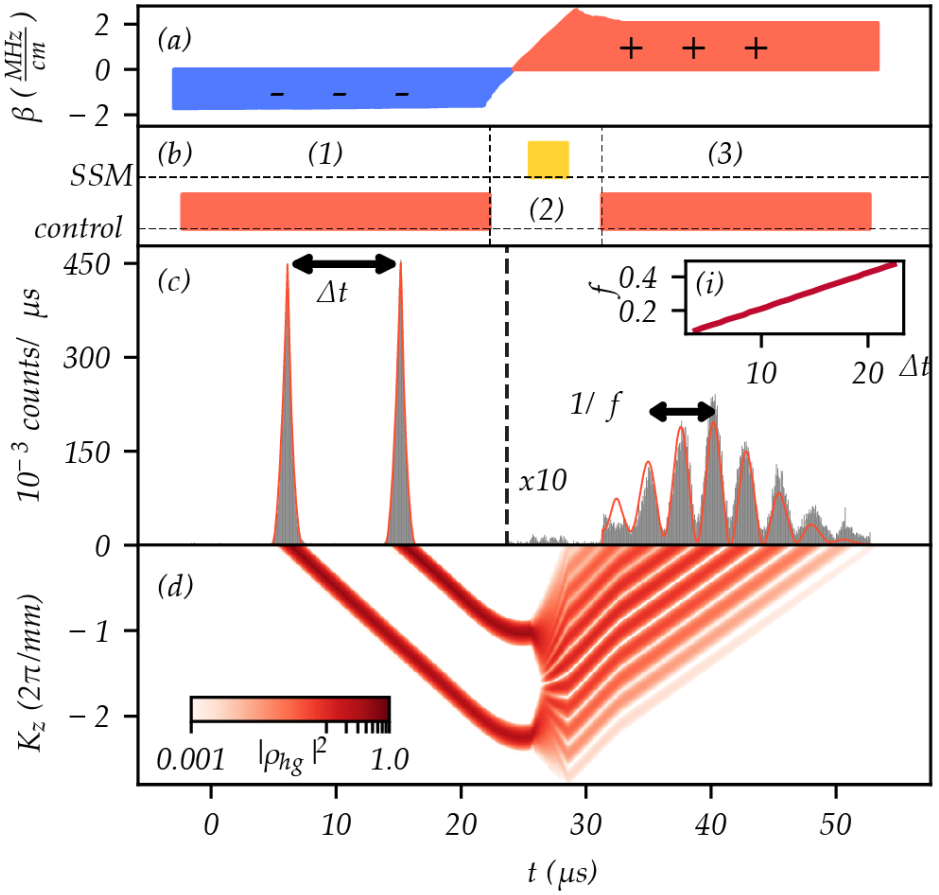


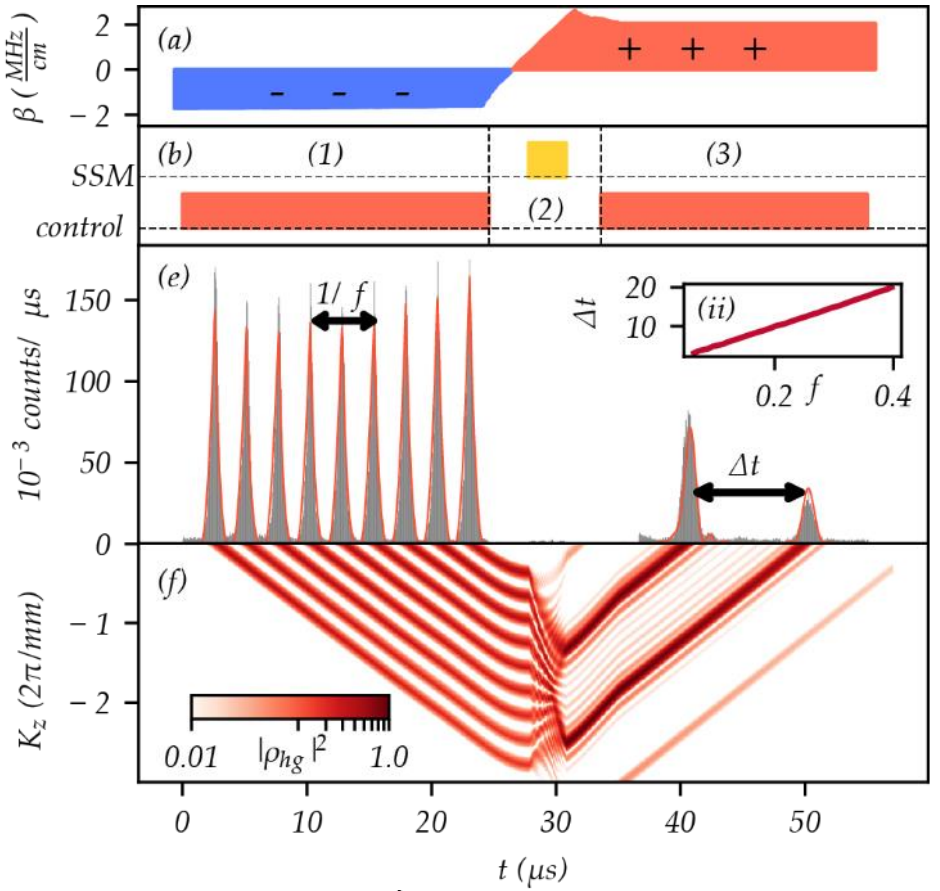


$$\left(\left(\widetilde{A}(\alpha t)\exp(-i(\alpha/2)t^2)\right) * \zeta(\beta t) * \zeta(\beta t)\right)\exp(i(\alpha/2)t^2)$$

Optica **7**, 203-208 (2020)

# Rotation by arbitrary angle = the FrFT

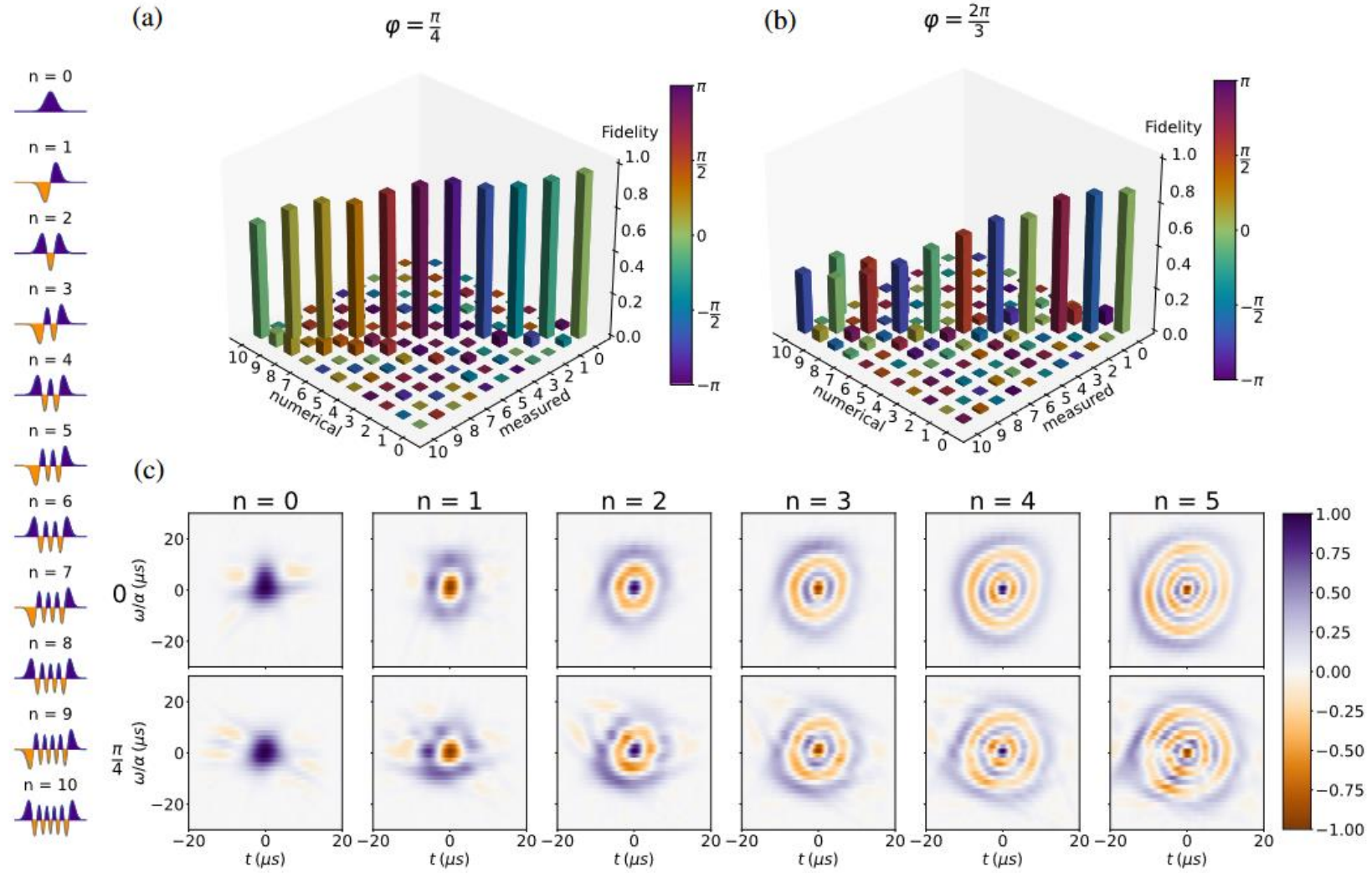


B. Niewelt et al., Phys. Rev. Lett. 130, 240801 (2023)

# Rotation by arbitrary angle = the FrFT

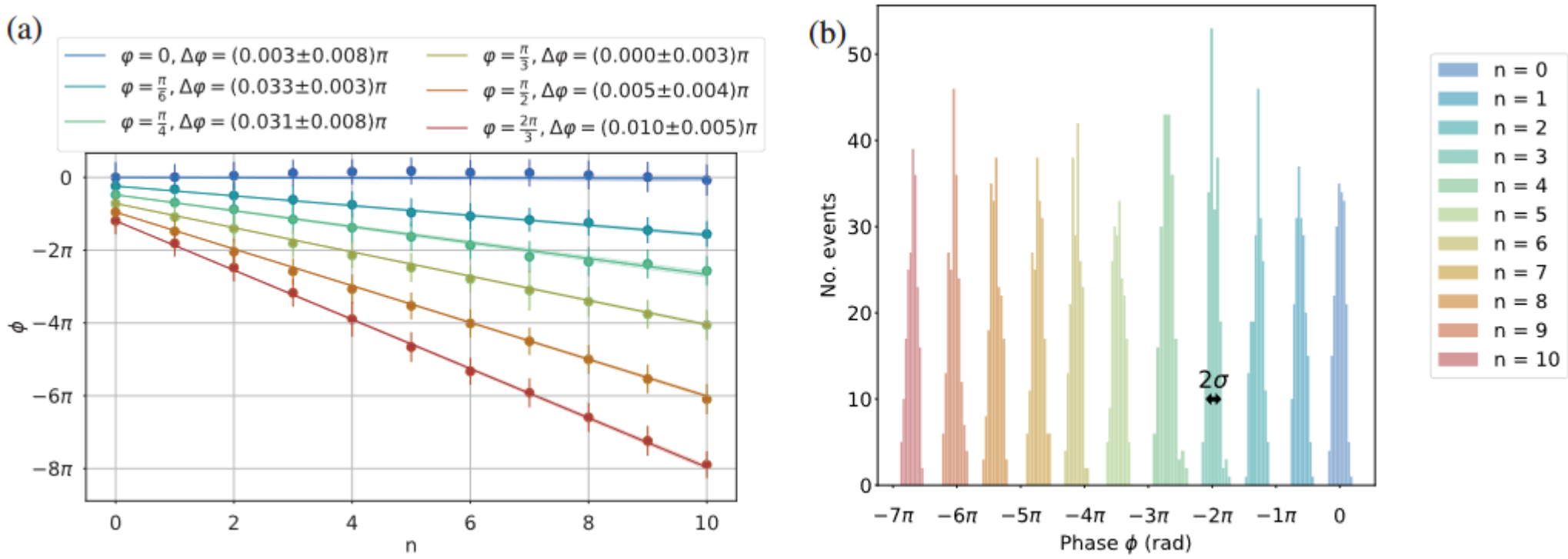


B. Niewelt et al., Phys. Rev. Lett. 130, 240801 (2023)

# Imaging resolution - Rayleigh Criterion

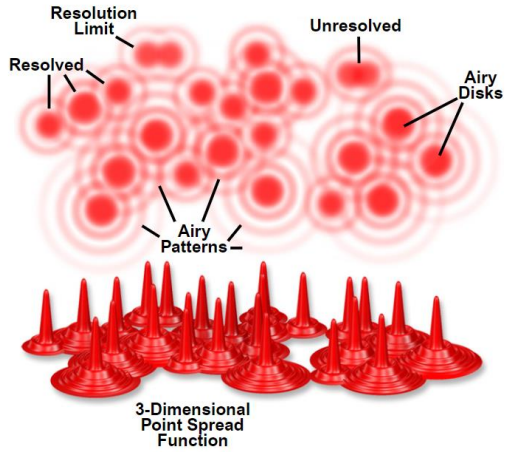


$$\theta = 1{\cdot}2197\,\frac{\lambda}{2R}$$

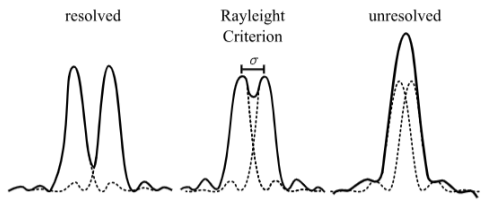


$$\sigma = \frac{0.61\lambda}{\mu \sin\gamma} = \frac{0.61\lambda}{NA}$$

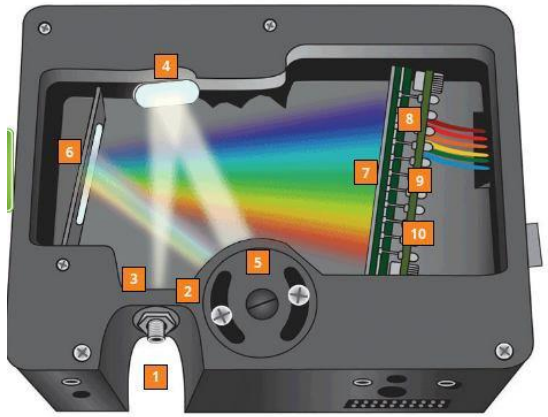


THE

LONDON, EDINBURGH, AND DUBLIN

PHILOSOPHICAL MAGAZINE

AND

JOURNAL OF SCIENCE.

[FIFTH SERIES.]

OCTOBER 1879.

XXXI. *Investigations in Optics, with special reference to the Spectroscope.* By LORD RAYLEIGH, *F.R.S.**

[Plate VII.]

§ 1. *Resolving, or Separating, Power of Optical Instruments.*

microscopyu.com oceaninsight.com

# Rayleigh Limit

Two point sources:

$$|u(x+\varepsilon/2)|^2 + |u(x-\varepsilon/2)|^2$$

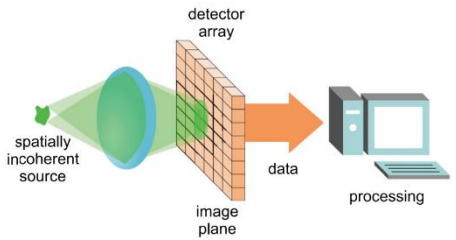


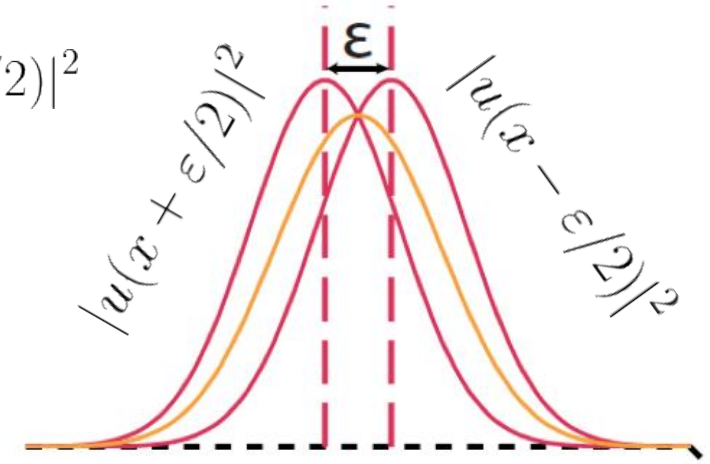


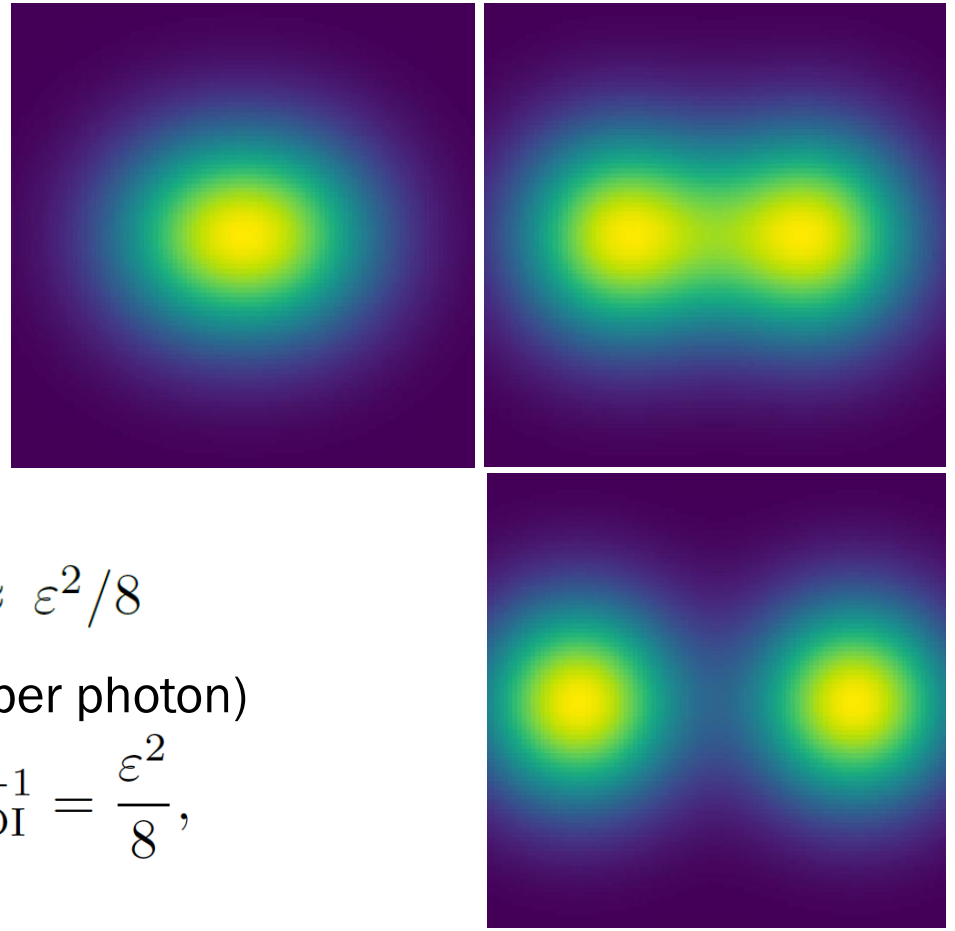

$$\mathcal{F}_{\mathrm{DI}} \approx \varepsilon^2/8$$

Cramér–Rao bound (CRB)

$$\Delta^2\hat{\varepsilon} \geq \frac{1}{\mathcal{F}}, \mathcal{F} = \int \frac{1}{p_\varepsilon(x)} \left(\frac{\partial}{\partial\varepsilon} p_\varepsilon(x)\right)^2 \mathrm{d}x$$

Precision (per photon)

$$(\Delta^2\varepsilon)^{-1}_{\mathrm{DI}} = \frac{\varepsilon^2}{8},$$

# Fisher information

$$F(\theta) = \sum_r p(r|\theta) \left( \frac{\partial}{\partial \theta} \log p(r|\theta) \right)^2$$

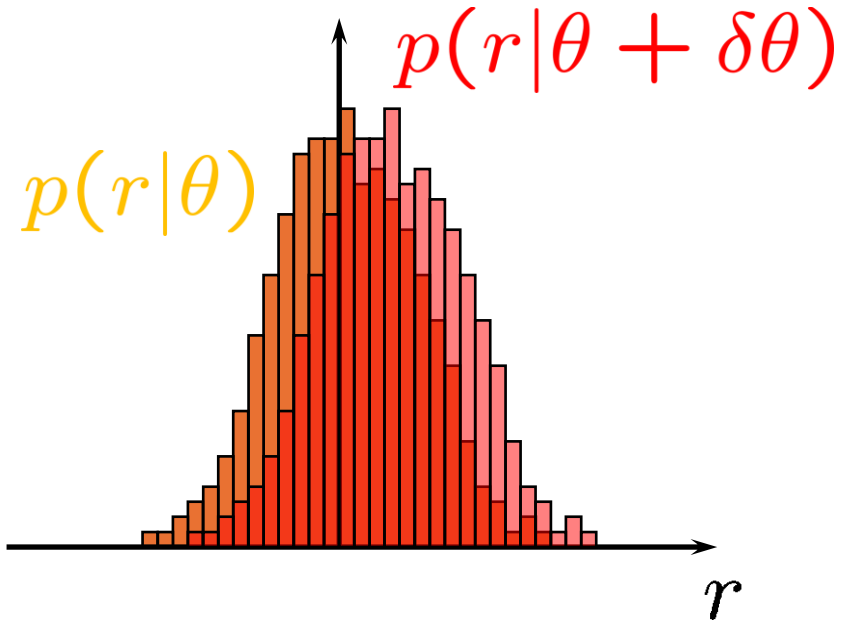


*Cramér-Rao bound:*
for unbiased estimators

$$\Delta\theta \geq \frac{1}{\sqrt{NF(\theta)}}$$

$$(\Delta^2\theta)^{-1} \leq F(\theta)N$$

# Beating the Rayleigh Limit more conventionally

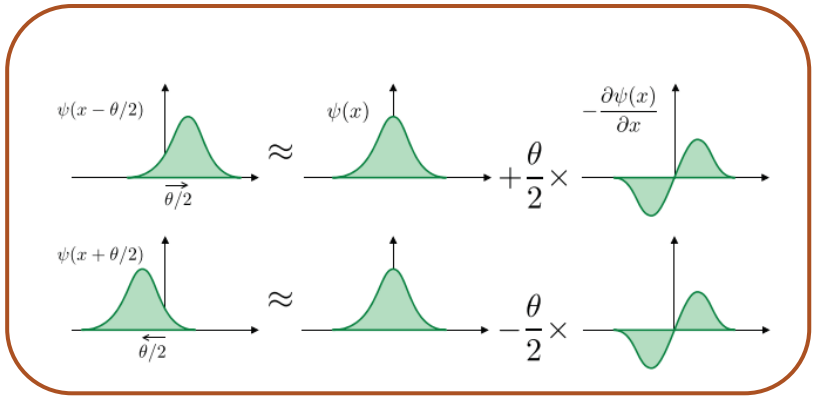


SLI
via $\mathcal{F}_{\mathrm{SLIVER}} \approx \frac{1}{4} - \frac{\varepsilon^2}{32}$ etry)

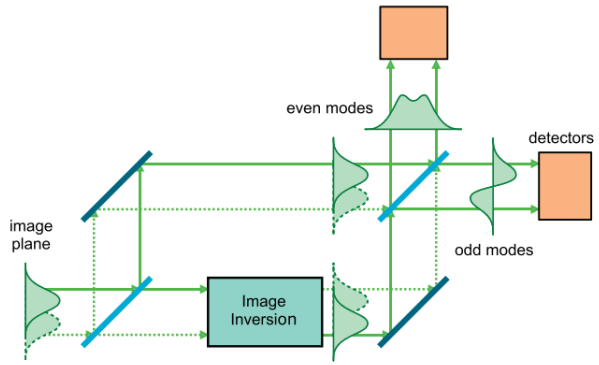


SPADE (spatial-mode demultiplexing)

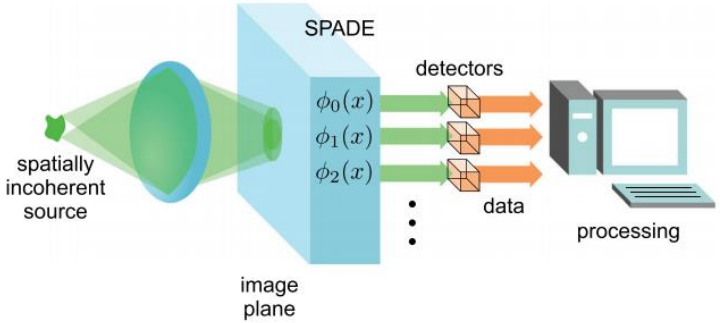


SPLICE (super-resolved position localization by inversion of coherence along an edge)

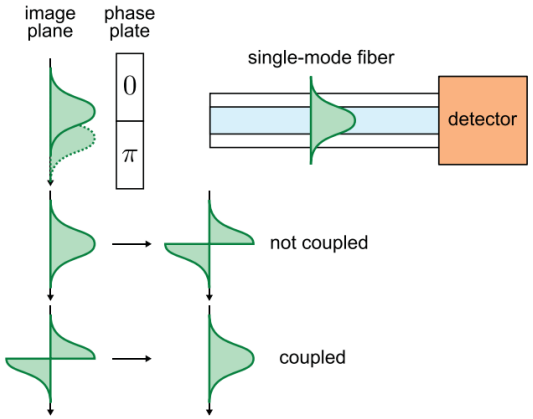


Contemporary Physics, 60:4, 279-298

# Two incoherent sources

$$\tilde{I}(\omega) = \tfrac{1}{2}\left(|\tilde{\psi}(\omega - \delta\omega/2)|^2 + |\tilde{\psi}_-(\omega + \delta\omega/2)|^2\right)$$

$$\tilde{\psi}(\omega) = \tilde{\psi}_{\blacktriangle}(\omega) = \left(\sqrt{2\pi}\sigma\right)^{-1/2} \exp\left(-\frac{\omega^2}{4\sigma^2}\right)$$

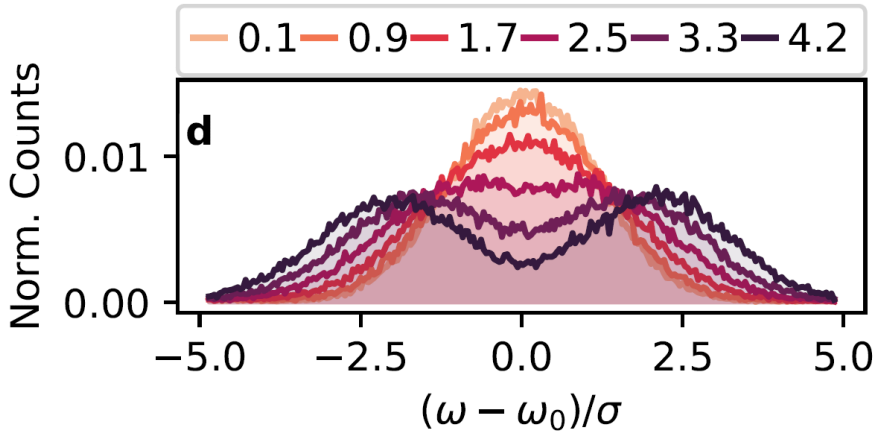


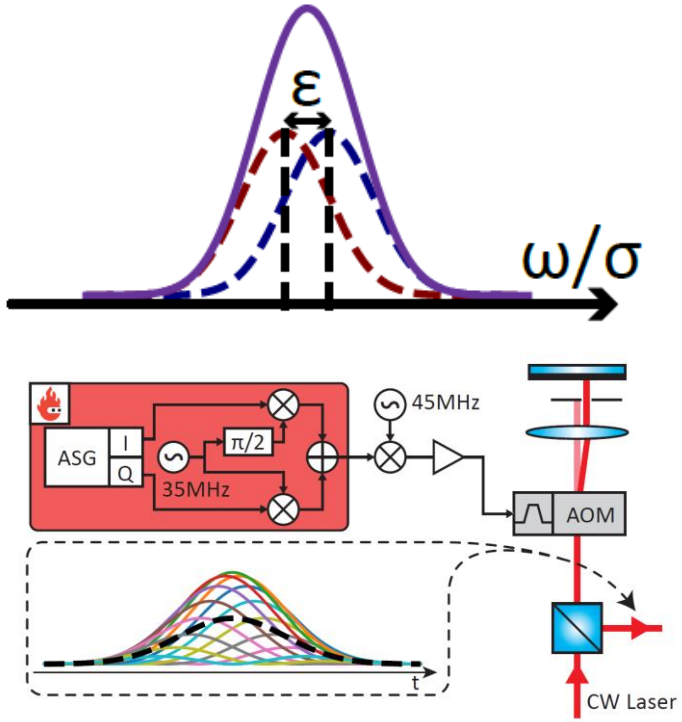


$$\mathcal{S}_\varphi(\omega) = \frac{1}{\sqrt{2}}\left(\tilde{\psi}_{\blacktriangle}(\omega - \sigma\varepsilon/2) + e^{i\varphi}\tilde{\psi}_{\blacktriangle}(\omega + \sigma\varepsilon/2)\right)$$

$$\mathcal{W}_{\mathcal{S}}(t,\omega) = \psi^2_{\blacktriangle}(t)(\tilde{\psi}^2_{\blacktriangle}(\omega - \sigma\varepsilon/2) + \tilde{\psi}^2_{\blacktriangle}(\omega + \sigma\varepsilon/2))$$

# PuDTAI
## Pulse-division time-axis-inversion interferometer

$$^1/\sqrt{2}(\mathcal{S}(\omega)+\mathcal{S}(-\omega))$$

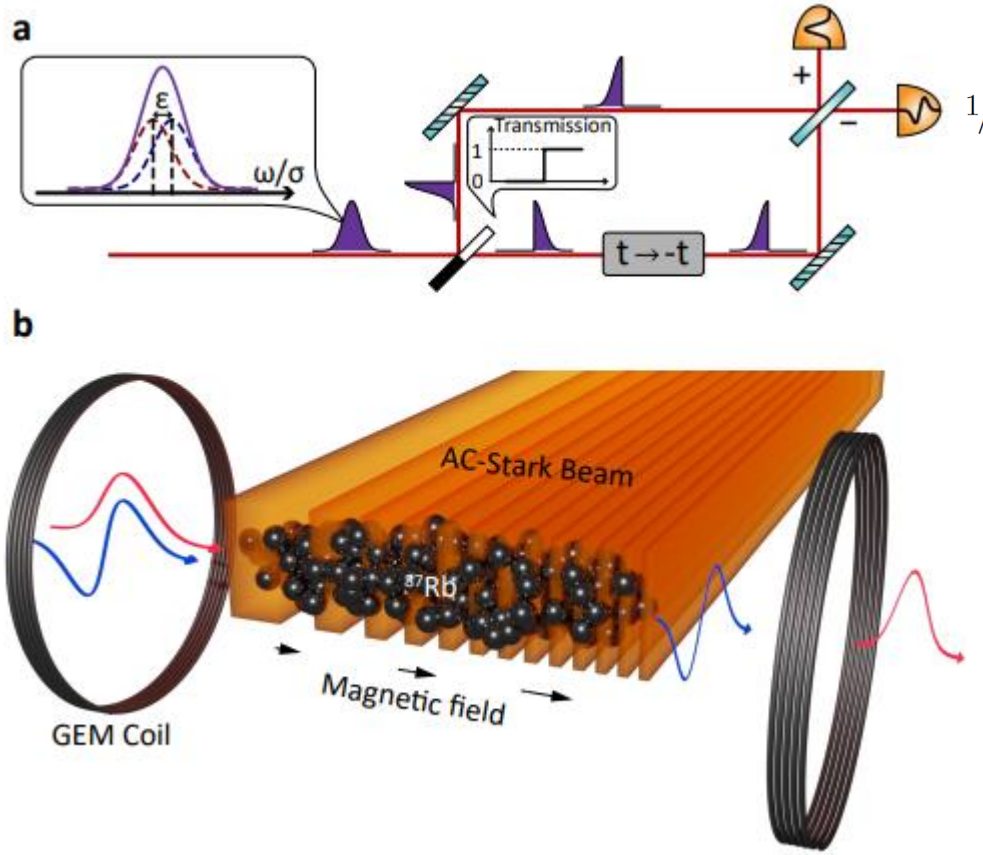


$$^1/\sqrt{2}(\mathcal{S}(\omega)-\mathcal{S}(-\omega))$$

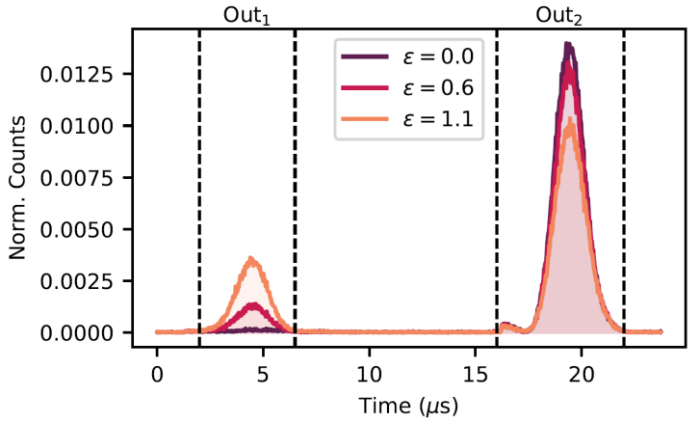


For real space imaging:
Wavefront-division image-inversion interferometer

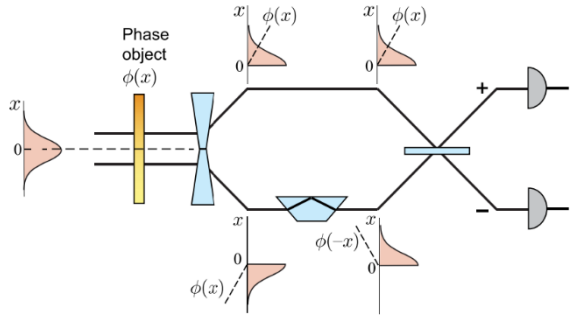


Phys. Rev. A 102, 013712 (2020)

# PuDTAI in phase space

$$\mathcal{W}(z,k_z)=\frac{1}{\sqrt{2\pi}}\int \varrho_{hg}(z+\xi/2)\varrho^*_{hg}(z-\xi/2)\exp(-ik_z\xi)\mathrm{d}\xi$$

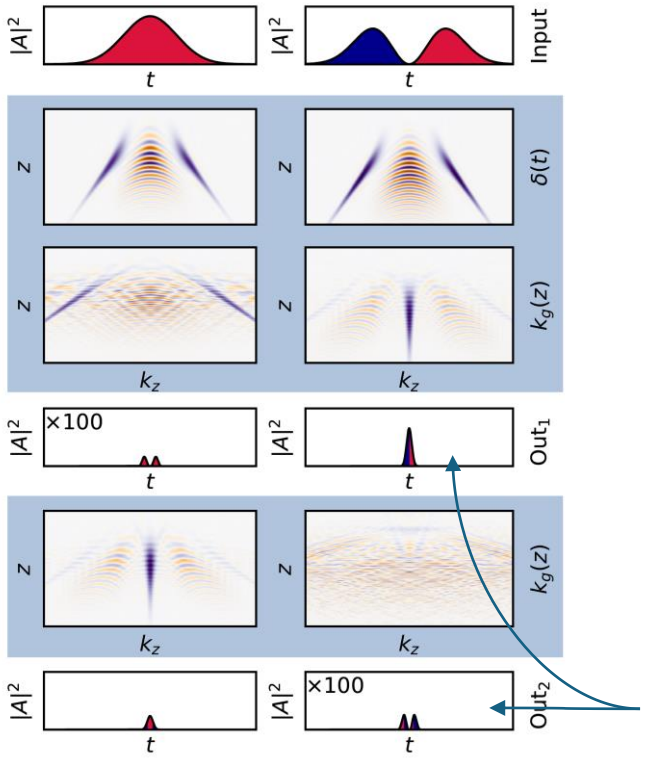


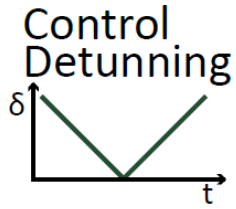


$$\delta(t) = \alpha|t|$$

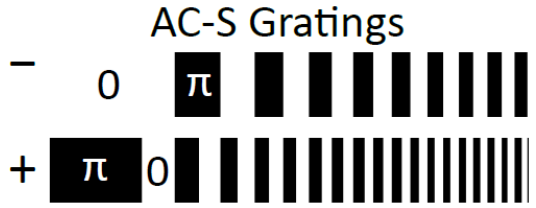


$$k_g=\zeta z \quad k_g=2\zeta z$$

The interference happens in the Fourier domain

For the first half of the pulse:

$$\mathcal{A}_-(t)=\begin{cases}\mathcal{A}(t) & t<0\\ 0 & t\geq 0\end{cases}$$

$$k_z \rightarrow k_z'=\zeta z$$

$$z \rightarrow z'=z-\frac{1}{\zeta}k_z$$

# Separation estimation

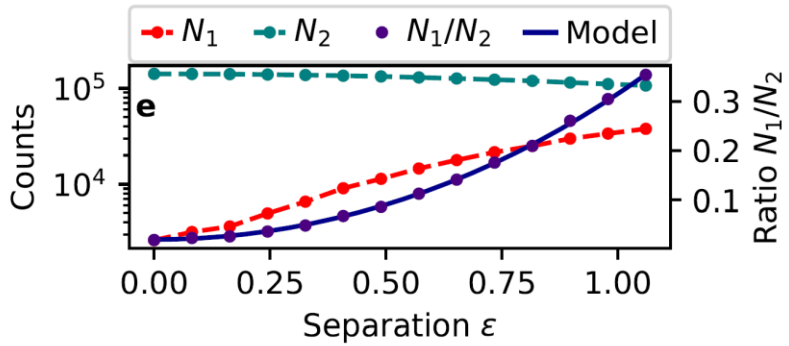


$$p_1 = \eta_1 \eta_1^{\mathfrak{A}} \frac{1}{2}\left(1 - \mathcal{V}_1 e^{-\frac{\epsilon^2}{8}}\right) \rightarrow N_1$$

$$p_2 = \eta_2 \eta_2^{\mathfrak{A}} \frac{1}{2}\left(1 + \mathcal{V}_2 e^{-\frac{\epsilon^2}{8}}\right) \rightarrow N_2$$

$$N_1, N_2 \rightarrow \hat{\varepsilon}(N_1/N_2)$$

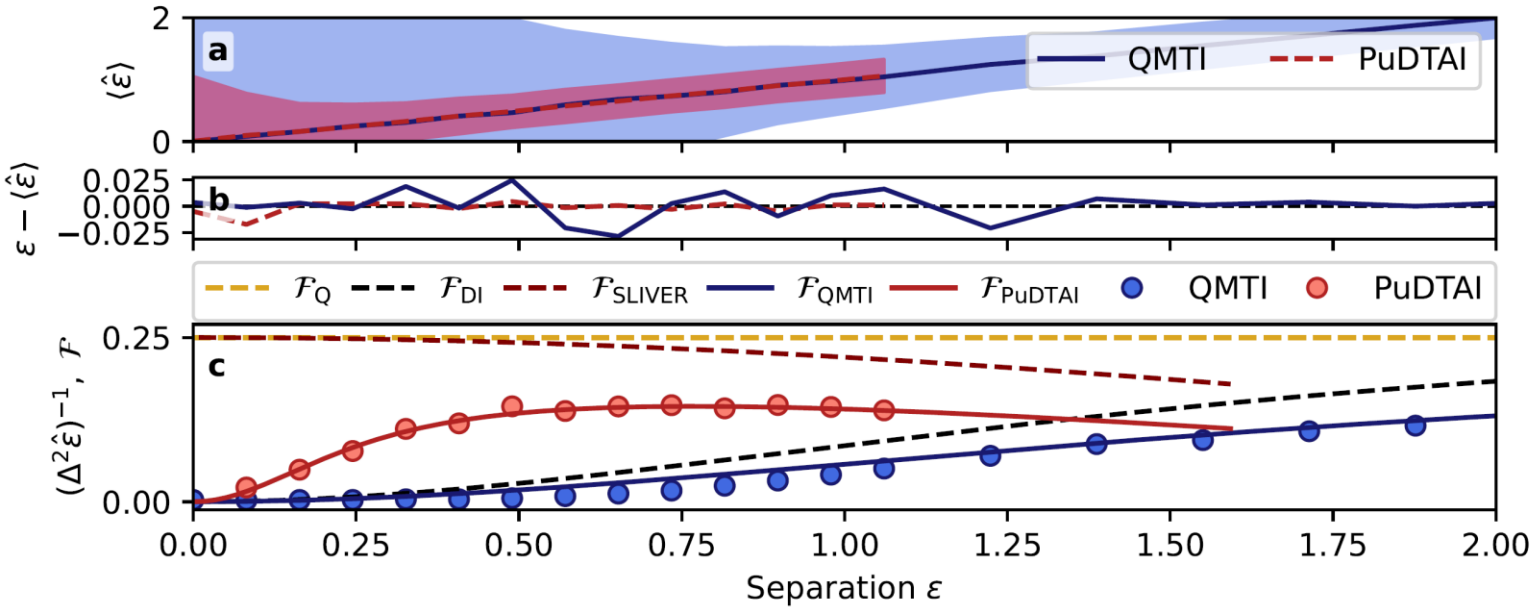


Maximum likelihood estimation in both cases

QMTI raw data:

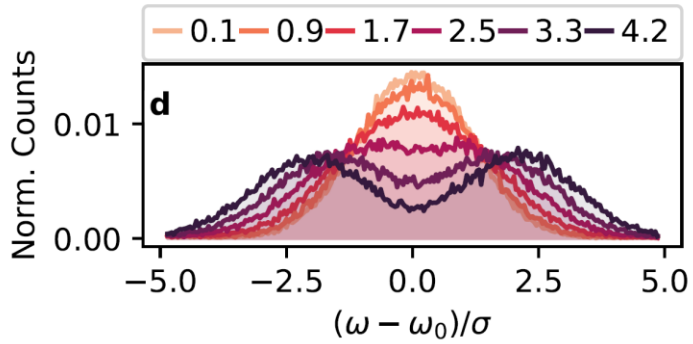

# Ultranarrowband optical spectroscopy

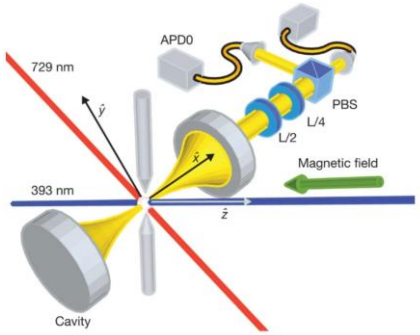


Single ions <100kHz

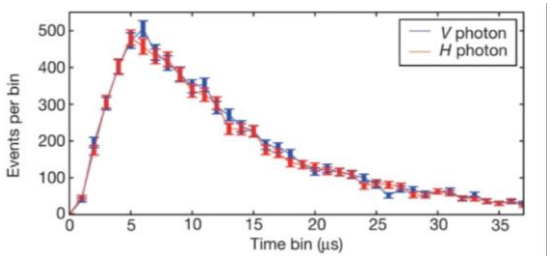


Nature **485**, 482–485(2012)

Optomechanical systems
~10kHz

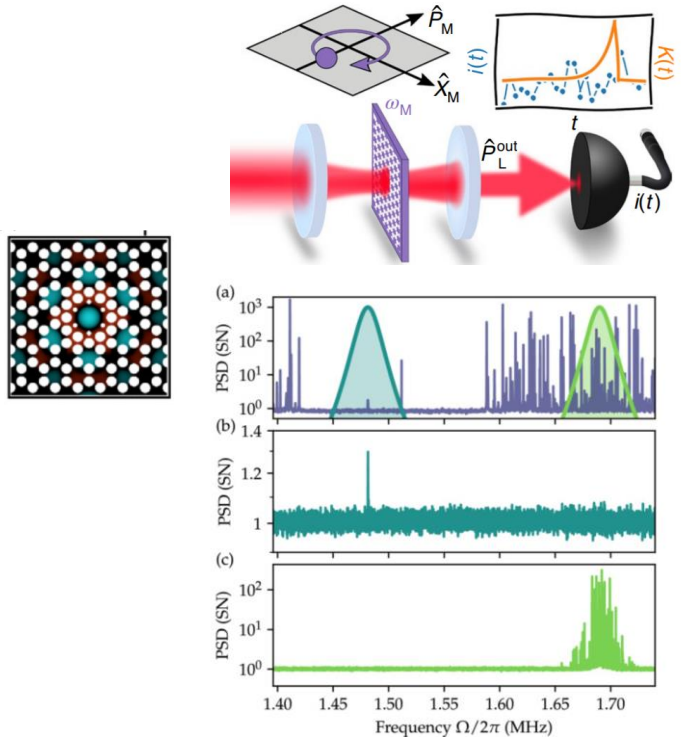


Optica **7**, 718-725 (2020)

Hot and cold atoms MHz-kHz

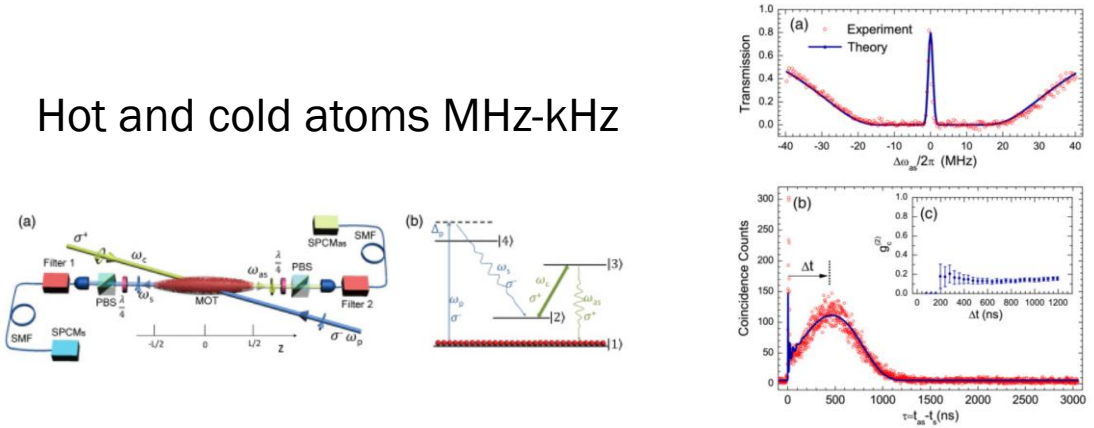


Optica **1**, pp. 84-88 (2014)

# Comparison

Our approach: PuDTAI

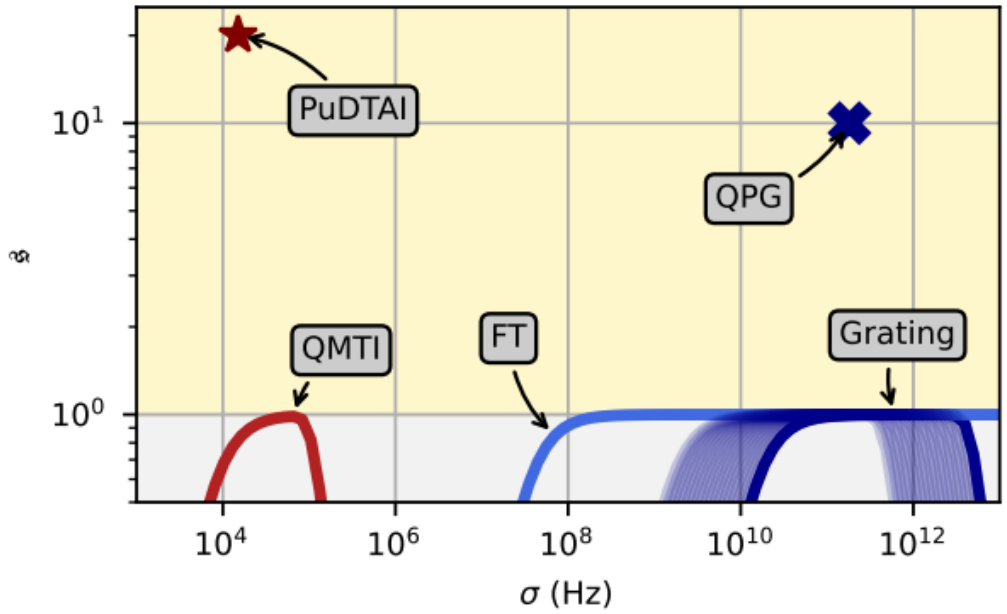


Superresolution parameter:

$$\mathfrak{s} = \lim_{\varepsilon \to 0} (\mathcal{F}/\mathcal{F}_{\mathrm{DI}})$$

Quantum Pulse Gate (QPG) - SPADE

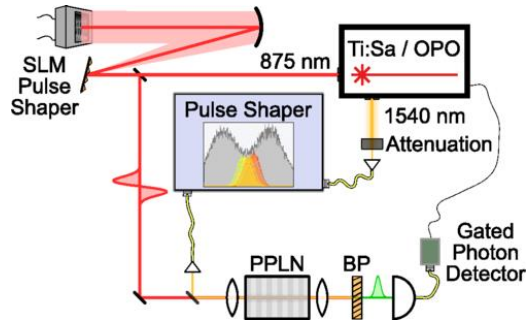


Phys. Rev. Lett. 121, 090501 (2018)

Homodyne/Heterodyne (under development)

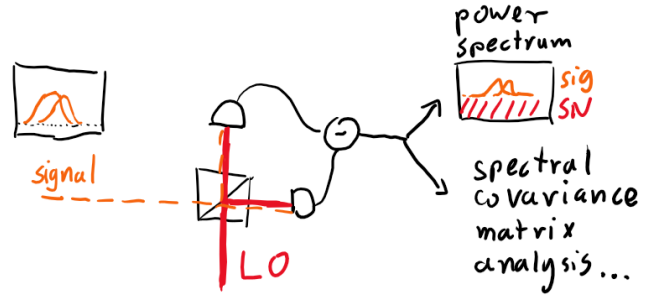


Phys. Rev. A 102, 063526 (2020)

# The three-way splitter

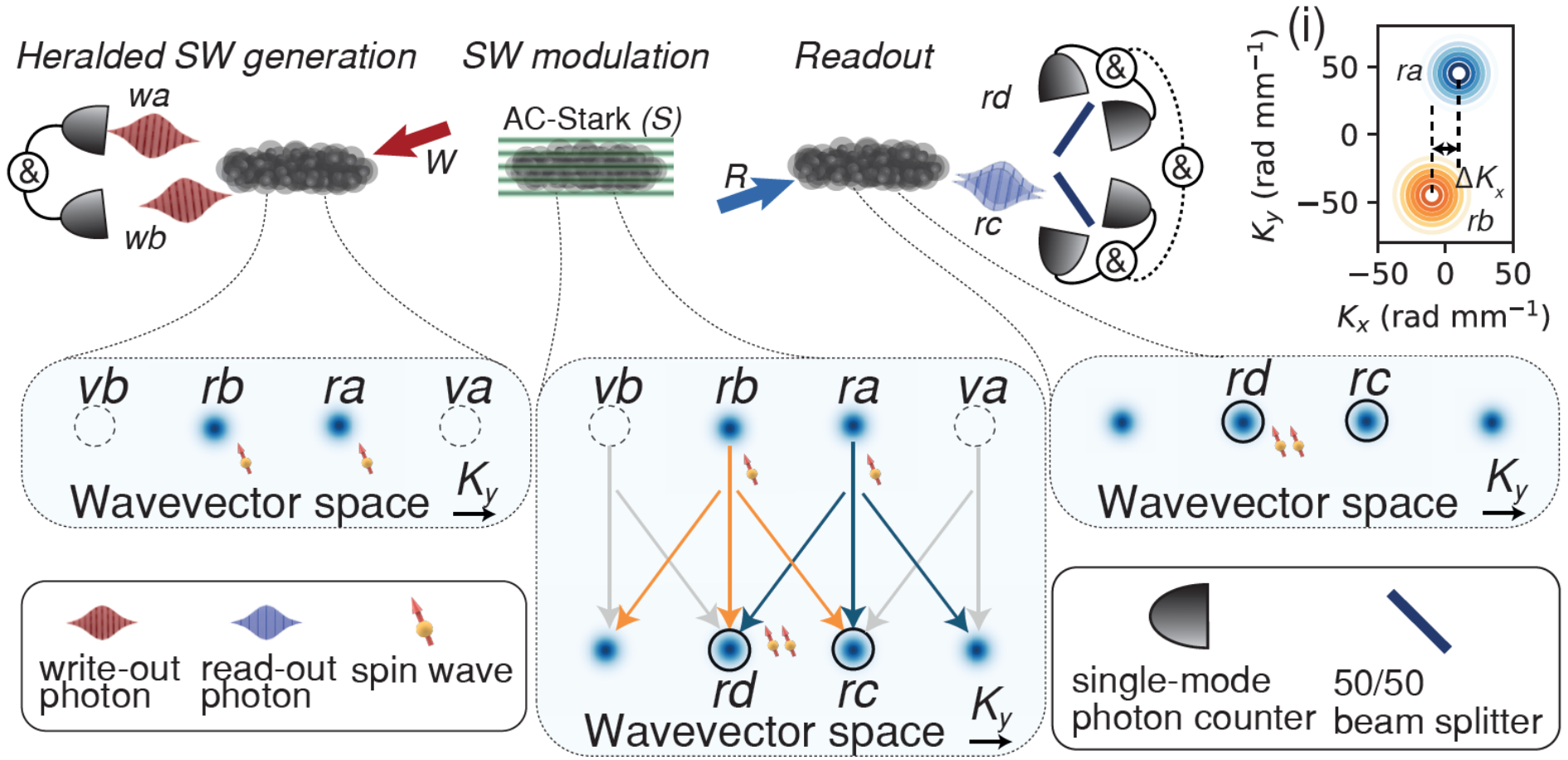


Phys. Rev. Lett. **122**, 063604 (2019)

# Hong-Ou-Mandel interference


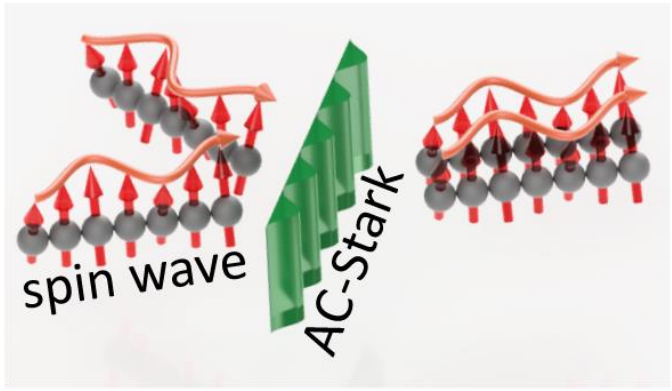


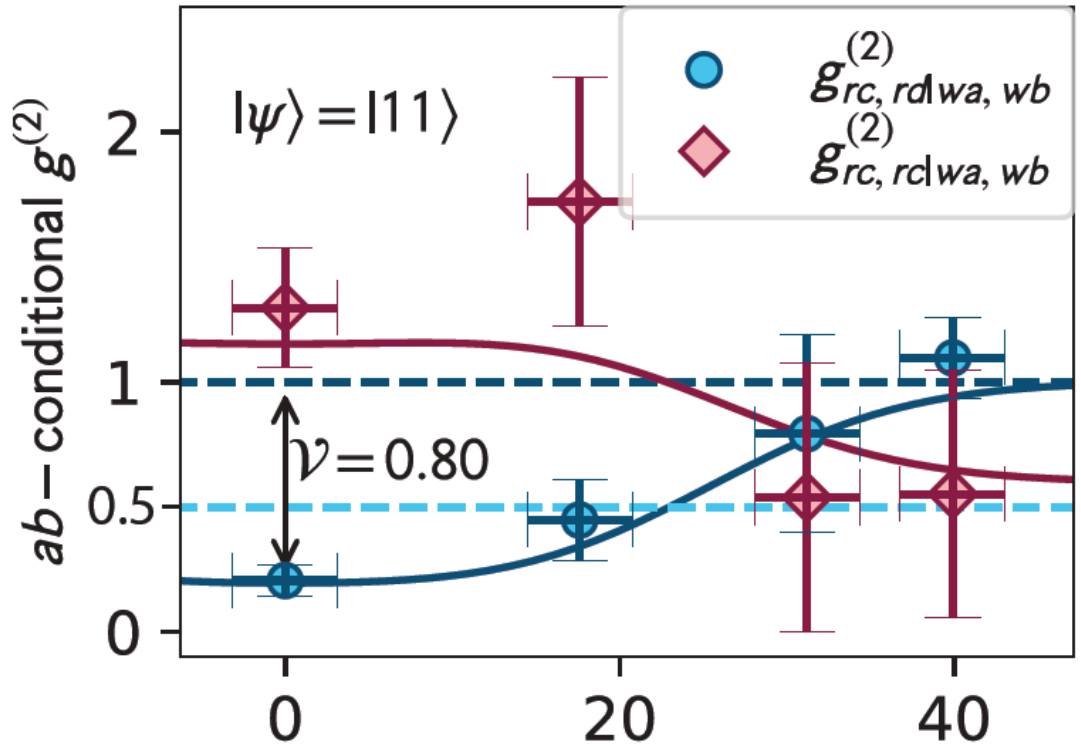


80% visibility at the moment limited by photon purity: with weak coherent states we observed interferometric visibility of >95%

Phys. Rev. Lett. **122**, 063604 (2019)

# Atom-embedded photonic (co)processor

- **Wavevector-multiplexed quantum memory**
- **Spin-wave-based interferometric processor for store**
- **Multiplexed quantum repeaters**

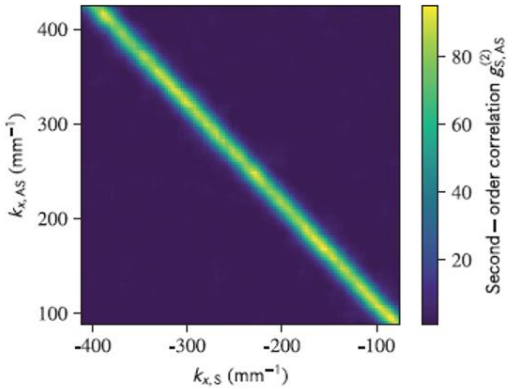


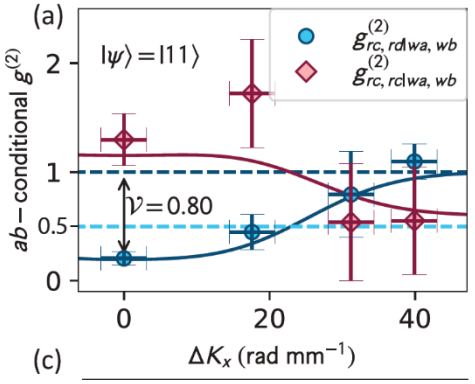


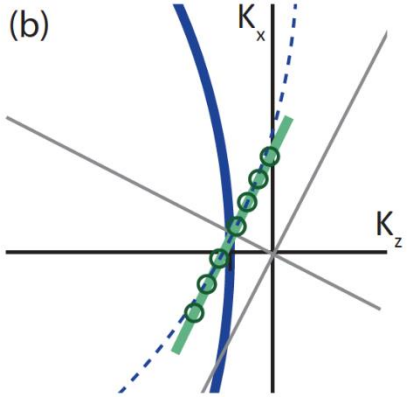


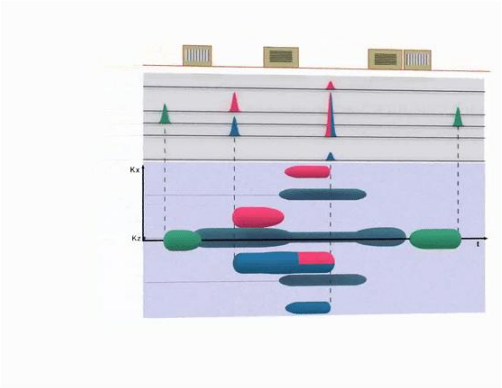

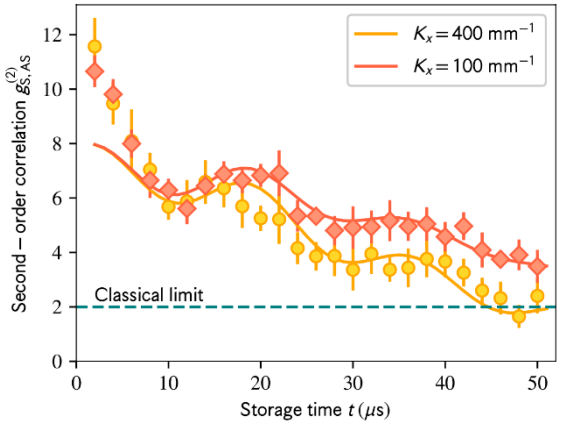

Rydberg atoms

# Rydberg atoms

- large principal quantum numbers n ≈ 15-100+
- long state lifetimes τ ≈ 15-200 μs
- long interaction radii ~μm
- microwave (and mm-wave) energy levels transitions Δf ≈ 1000-2 GHz

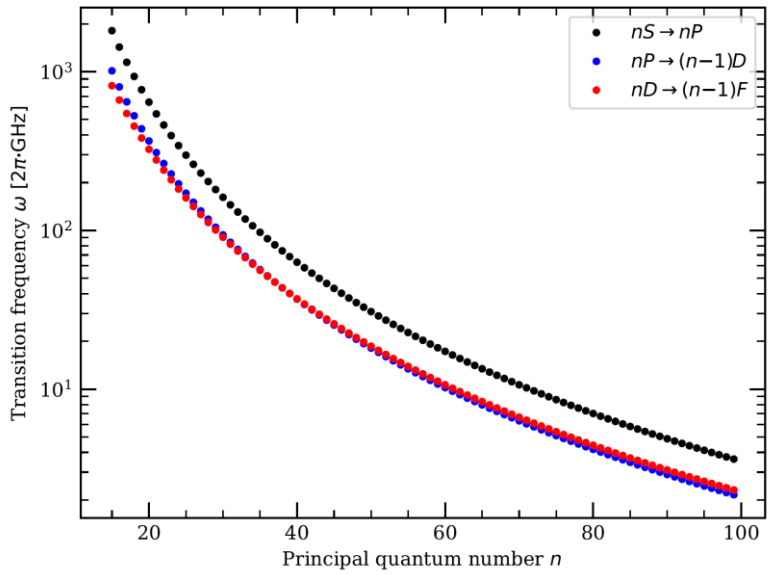


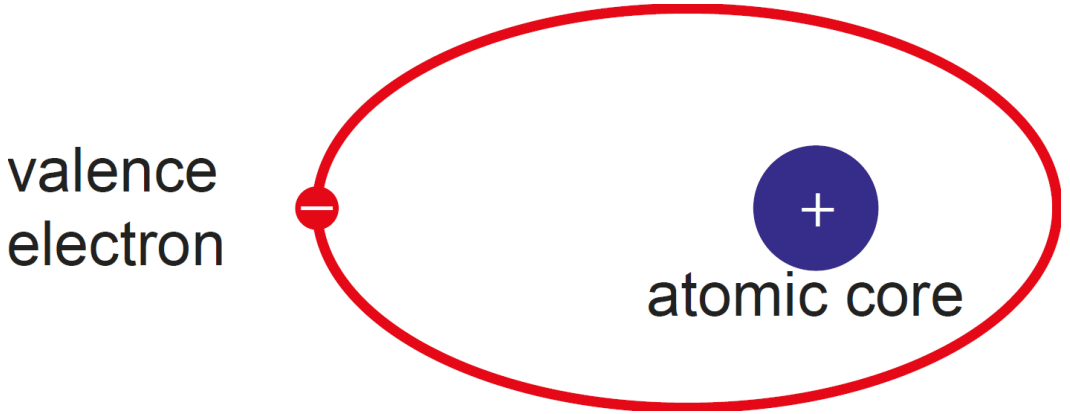

# Microwave-optical interface

5 GHz

interface?

400 THz

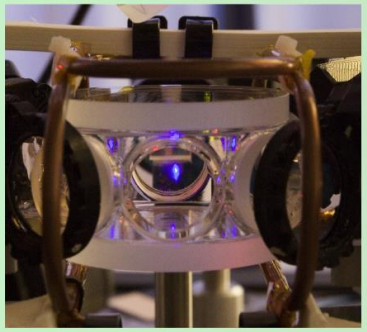

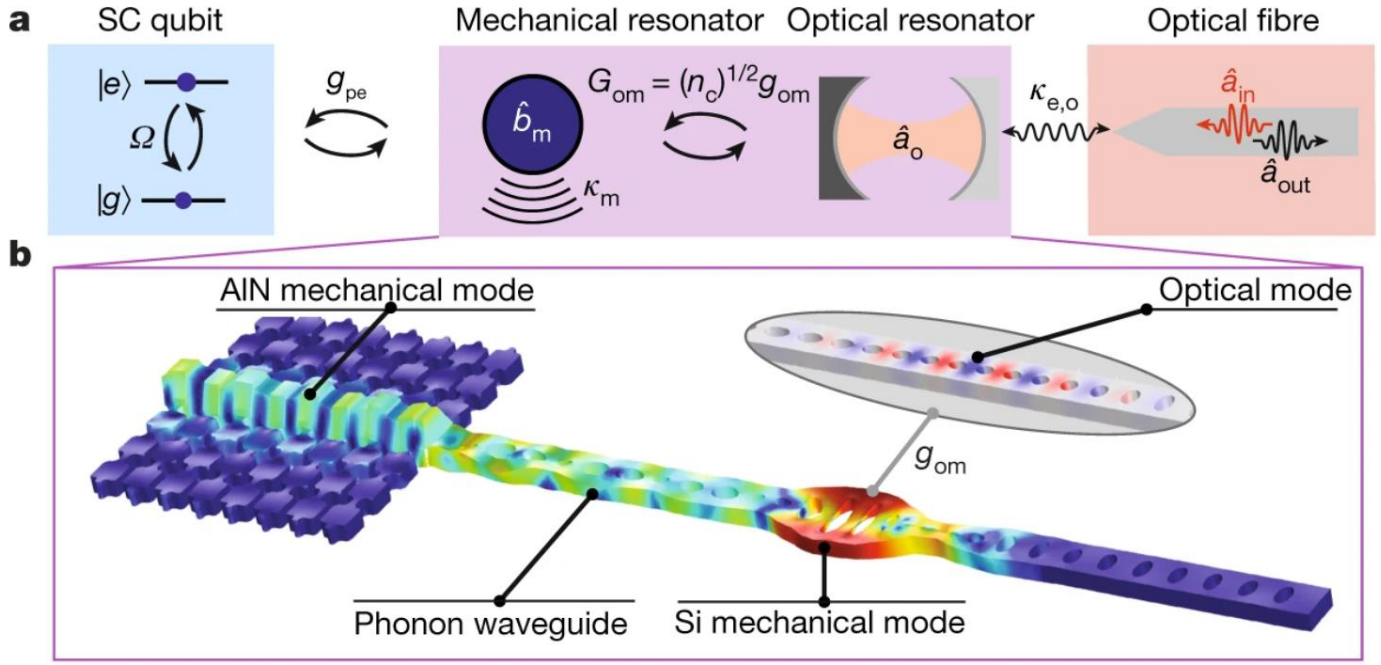


M. Mirhosseini et al. *Nature* **588**, 599–603 (2020)

# Applications of quantum transduction

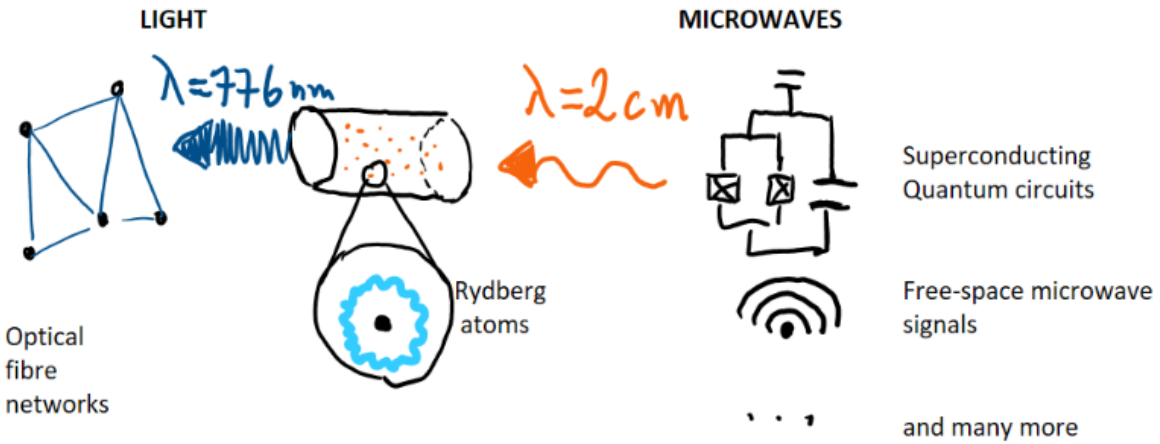


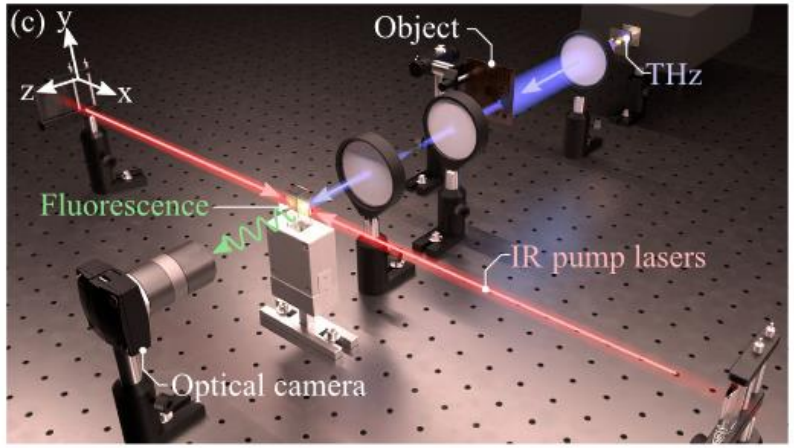


L. A. Downes et al., Phys Rev X 10, 011027 (2020) (Durham)


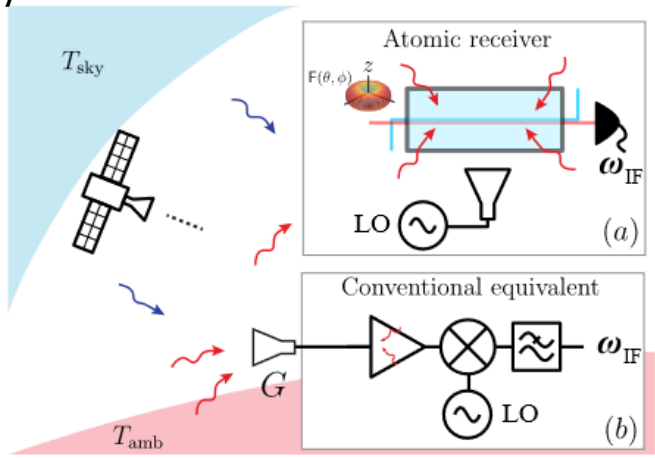


G. Santamaria Botello et al., arXiv:2209.00908 (CU Boulder)

# Microwave detection

## GHz & THz imaging

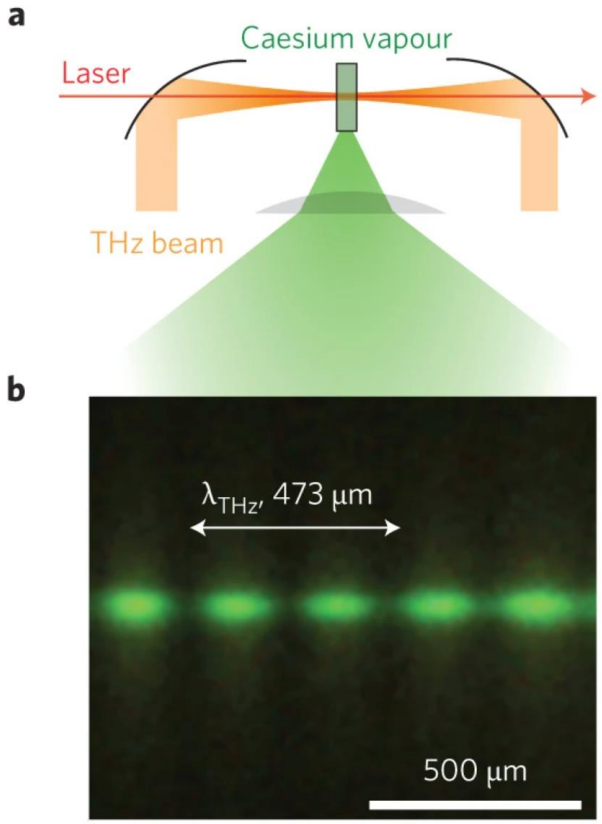


C.G. Wade et al. *Nat. Phot.* **11**, 40–43 (2017)

## Microwave astronomy

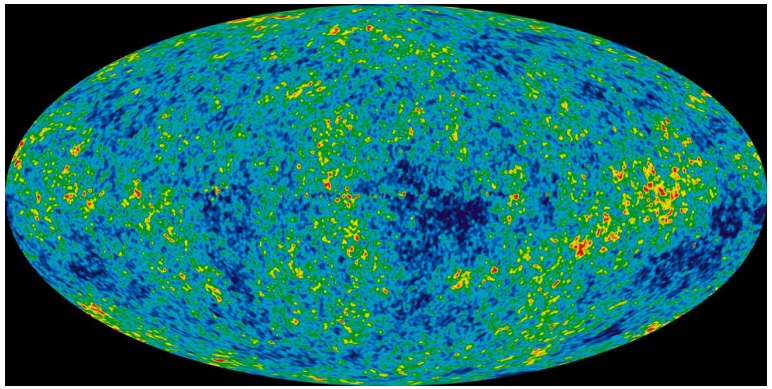

source:
https://upload.wikimedia.org/wikipedia/commons/3/3c/Ilc_9yr_moll4096.png

## Next-gen microwave sensing and communication

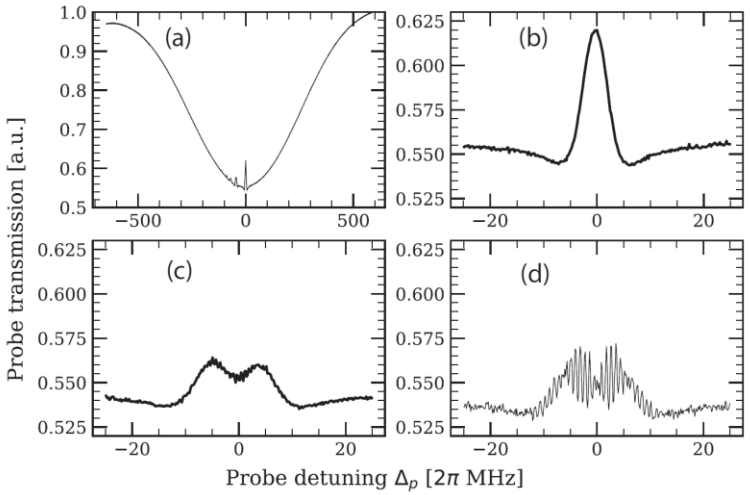


S. Borówka et al. *Appl. Opt.* **61** (29), 8806-8812 (2022)

# Other approaches - examples

Λ system

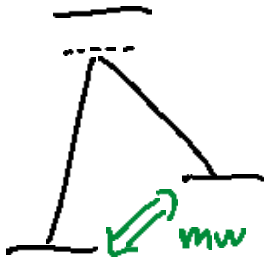


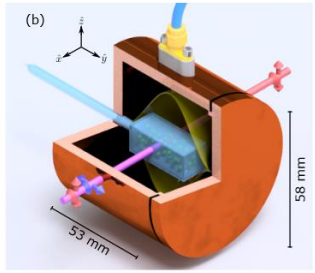


(very low dipde moment)

Ground state atoms, RE ions, …
2305.19221(Alberta, Canada)

Opto-magnonics

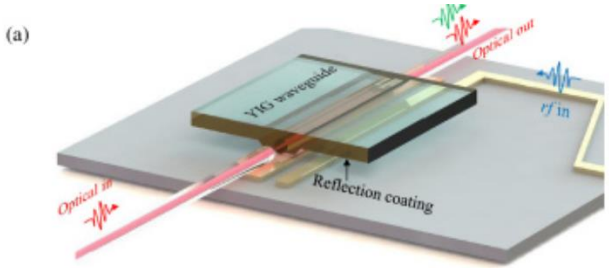


Optica 7, 10, 1291 (2020)
(Yale)

opto-electro-mechanics

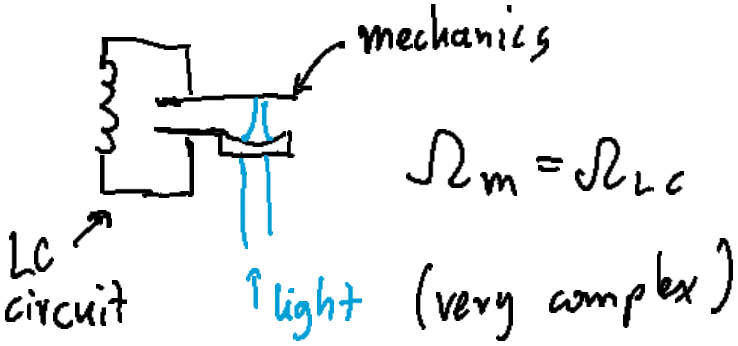


$\Omega_m = \Omega_{LC}$

(very complex)

Si or SiN resonators, …

Nature Phys. **16**, 69–74 (2020)
(Delft)

Electro-optics

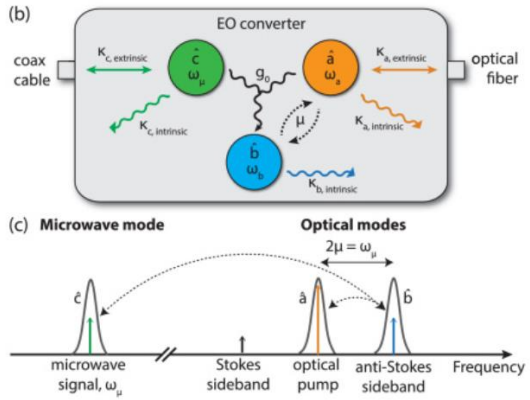


LN resonator, …

Optica 7, 12, 1737-1745 (2020)
(Stanford)

# Other approaches

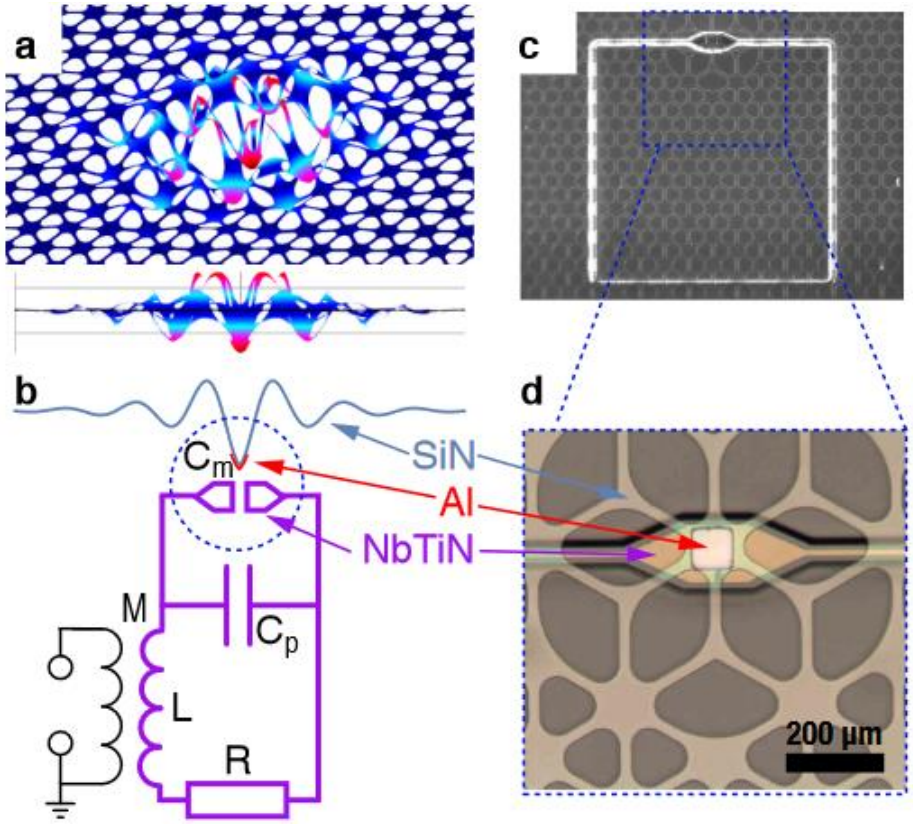


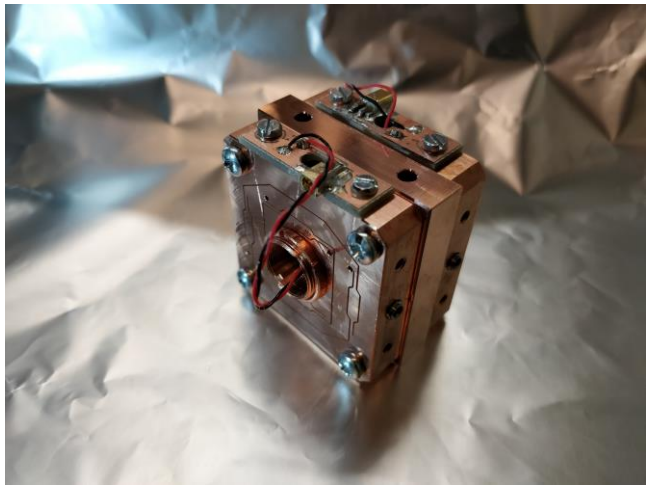

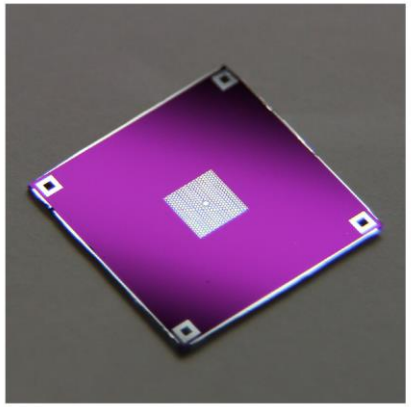

membrane

Nat. Commun. 13, 1507 (2022) (NBI Copenhagen)
A. Schliesser

I. Galinskiy, Y. Tsaturyan, MP, E. S. Polzik, Optica 7, 718 (2020)
R.A. Thomas, MP, et al., Nature Physics 17, 228–233 (2021)
I. Galinskiy, G. Enzian, M. Parniak, E. S. Polzik, Phys Rev. Lett. 133, 173605 (2024)

# Rabi frequency and EIT sensing

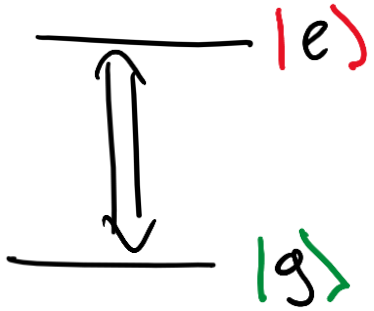


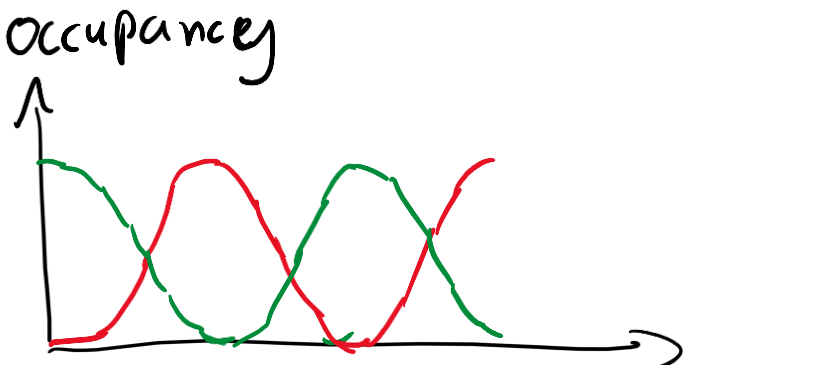


period = 1/Rabi frequency

$$\Omega_R = \frac{E \cdot d}{\hbar}$$

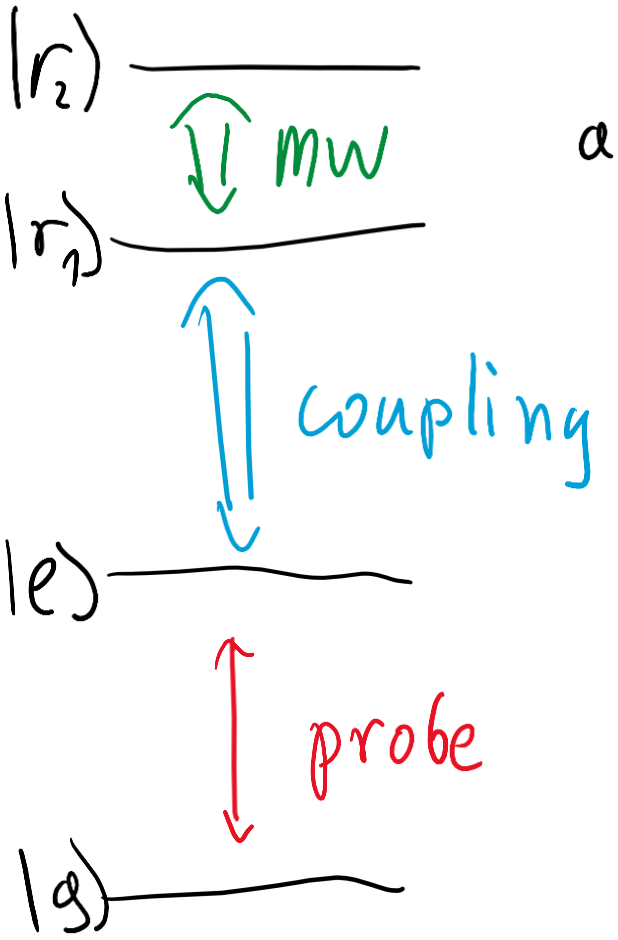


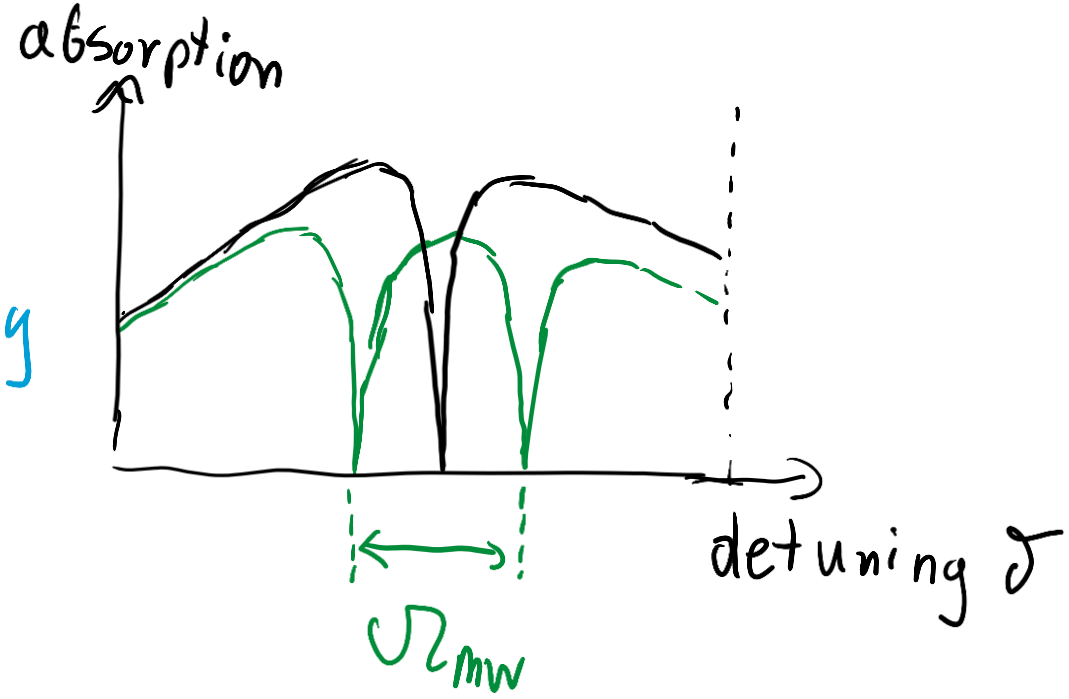

# Rydberg electrometry

Frequency splitting
- Rabi frequency -
**measured with respect to a frequency reference**

$$\Omega = \frac{d_x E_0}{\hbar}$$

Electric field amplitude **E**
Dipole moment **d**

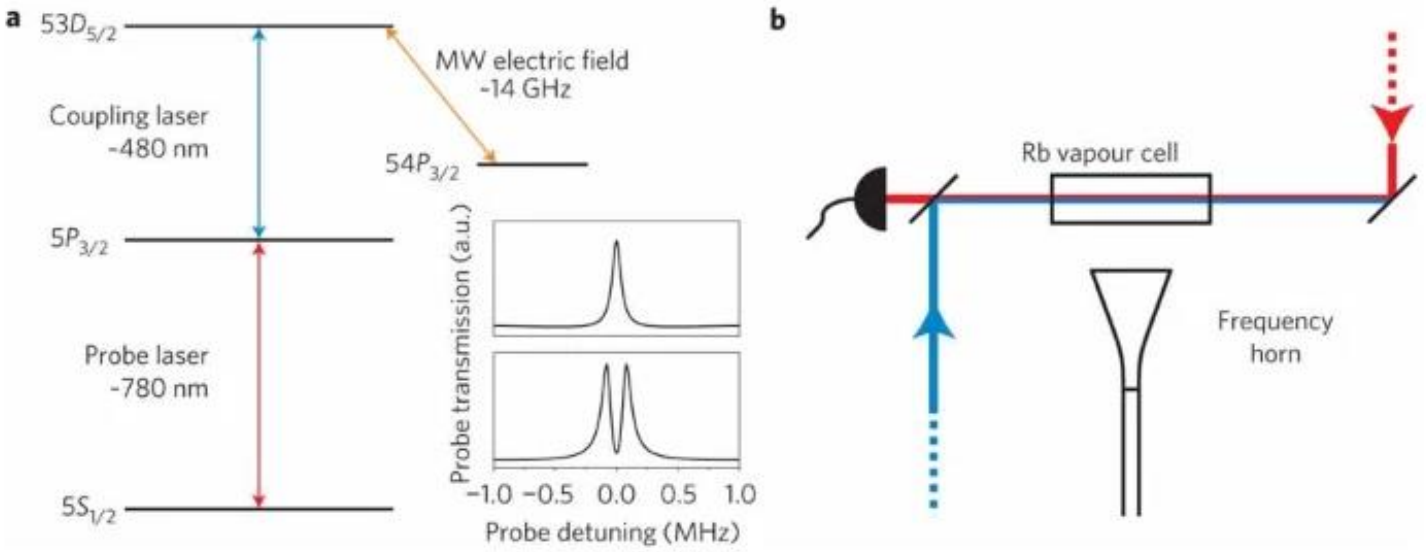


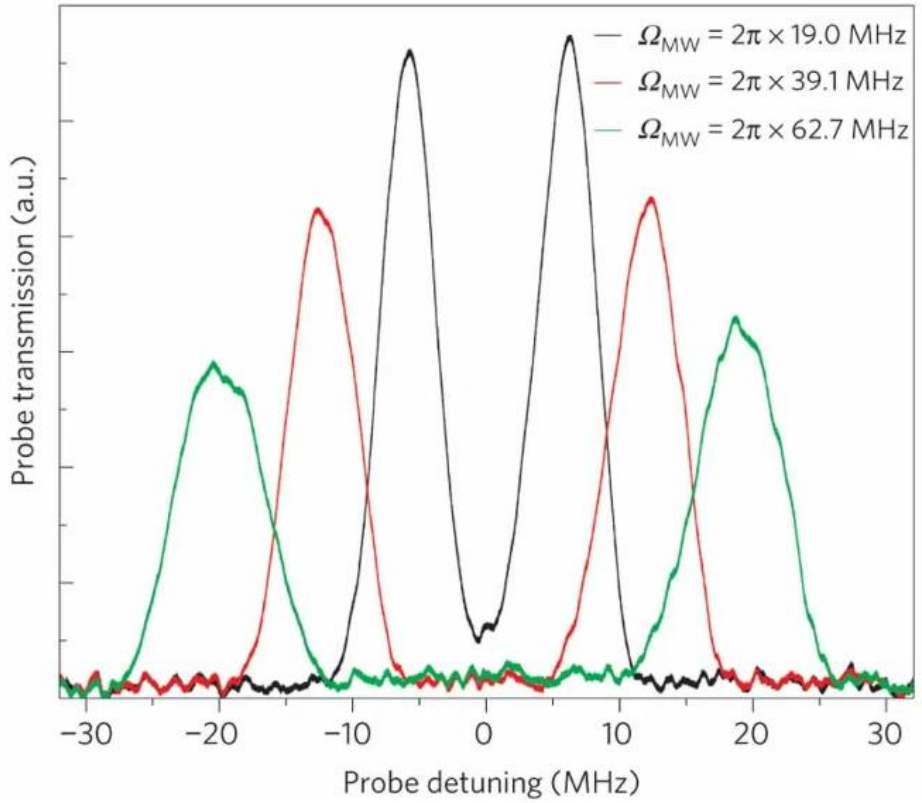


*Sedlacek et al., Nature Physics* **8**, 819–824 (2012) (Oklahoma/Stuttgart)

# Practical electrometers

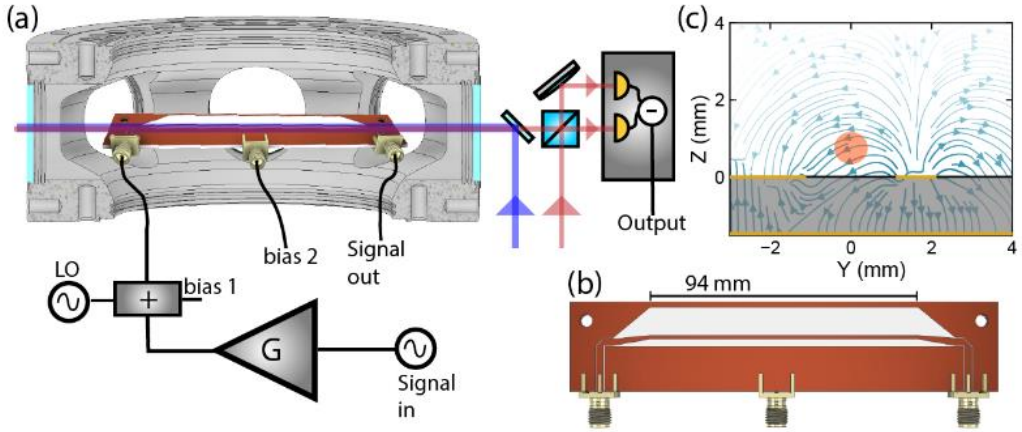


D. Meyer et al., PR Applied **15**, 014053 (2020) (ARL Maryland)

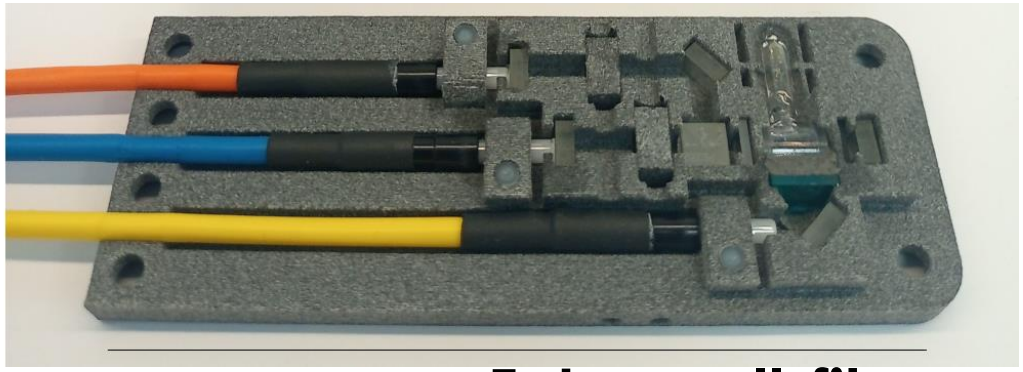

**Future: all-fiber laser system?**

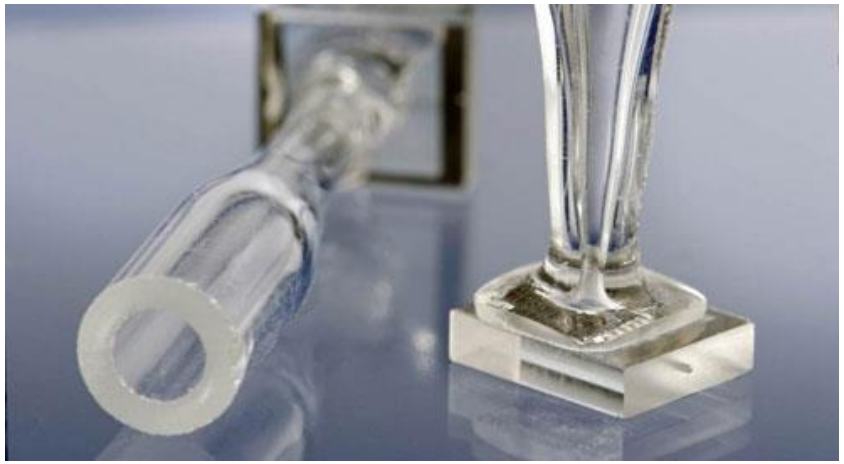

Soon: smaller cel

Future: miniaturized assembly

Example atomic magnetometer by our collaborators from University of Copenhagen
H. Stærkind et al., arXiv:2208.00077 (2022)

**Potential: all-glass/fiber/plastic microwave receiver, insensitive to EMI**

# Microwave-to-optical conversion

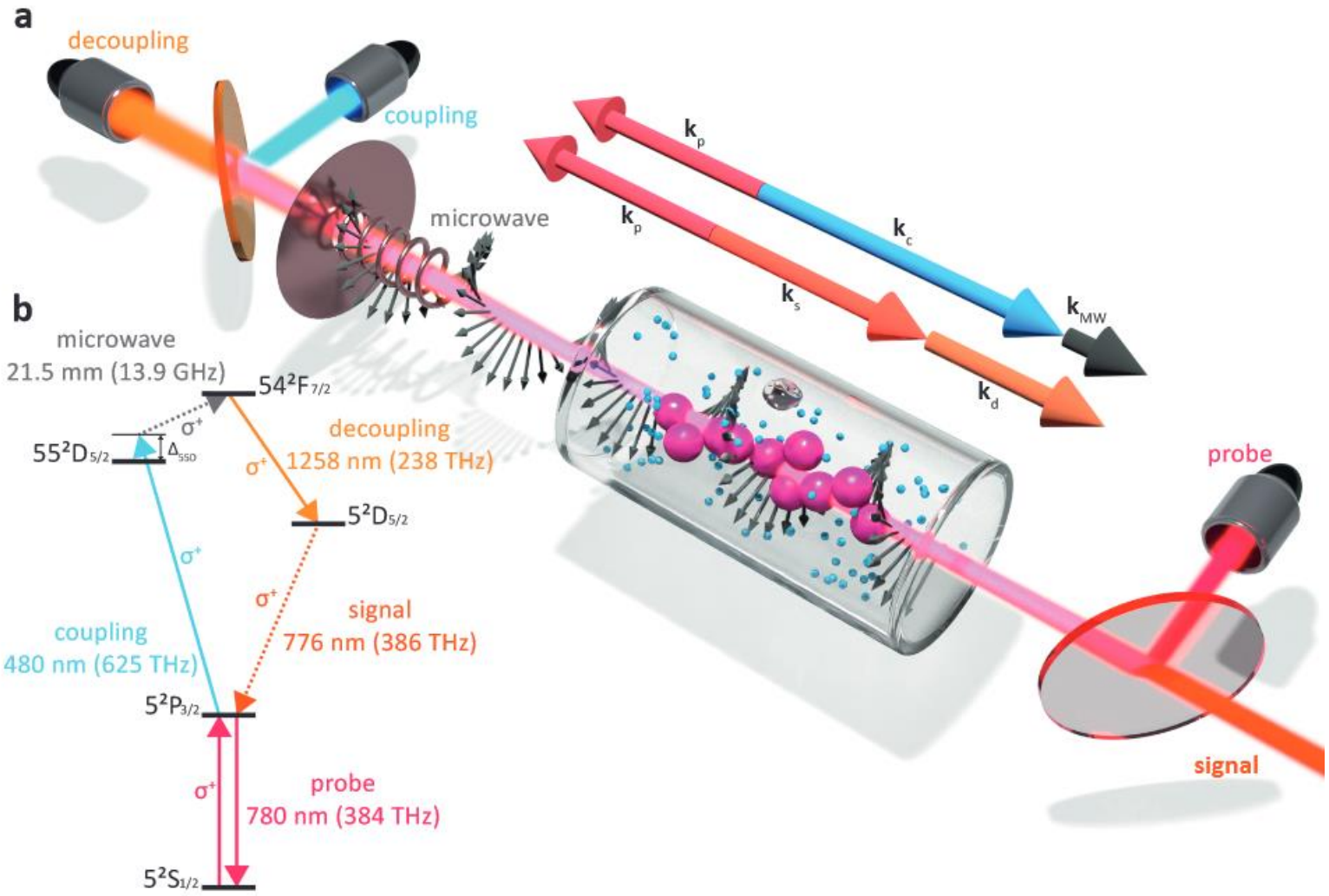


S. Borówka,
U. Pylypenko, M. Mazelanik, **MP**,
**Nature Photonics 18, 32-38 (2024)**

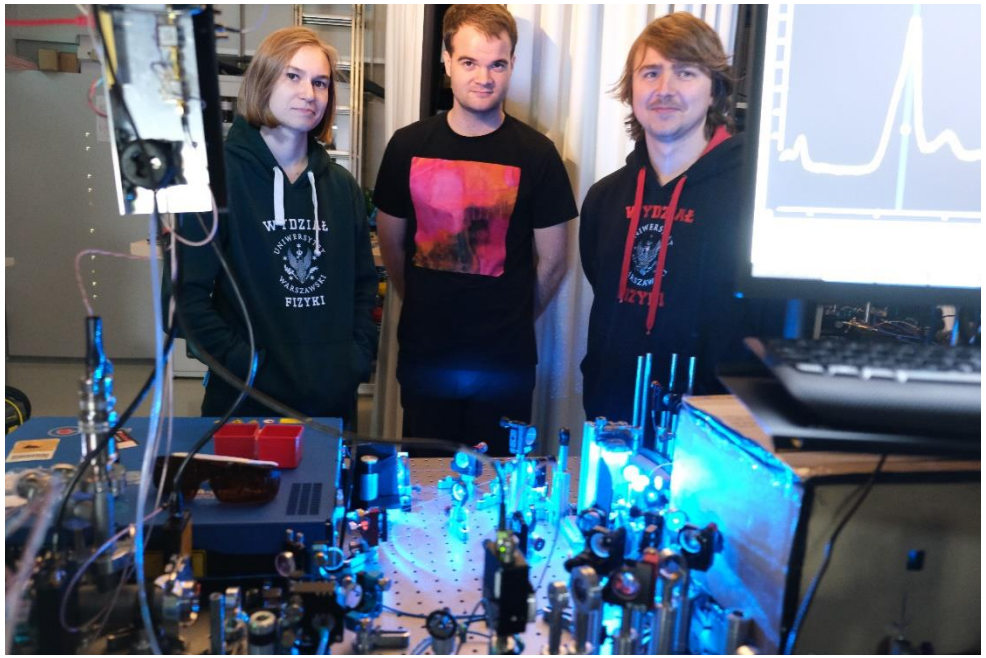

# Experimental setup

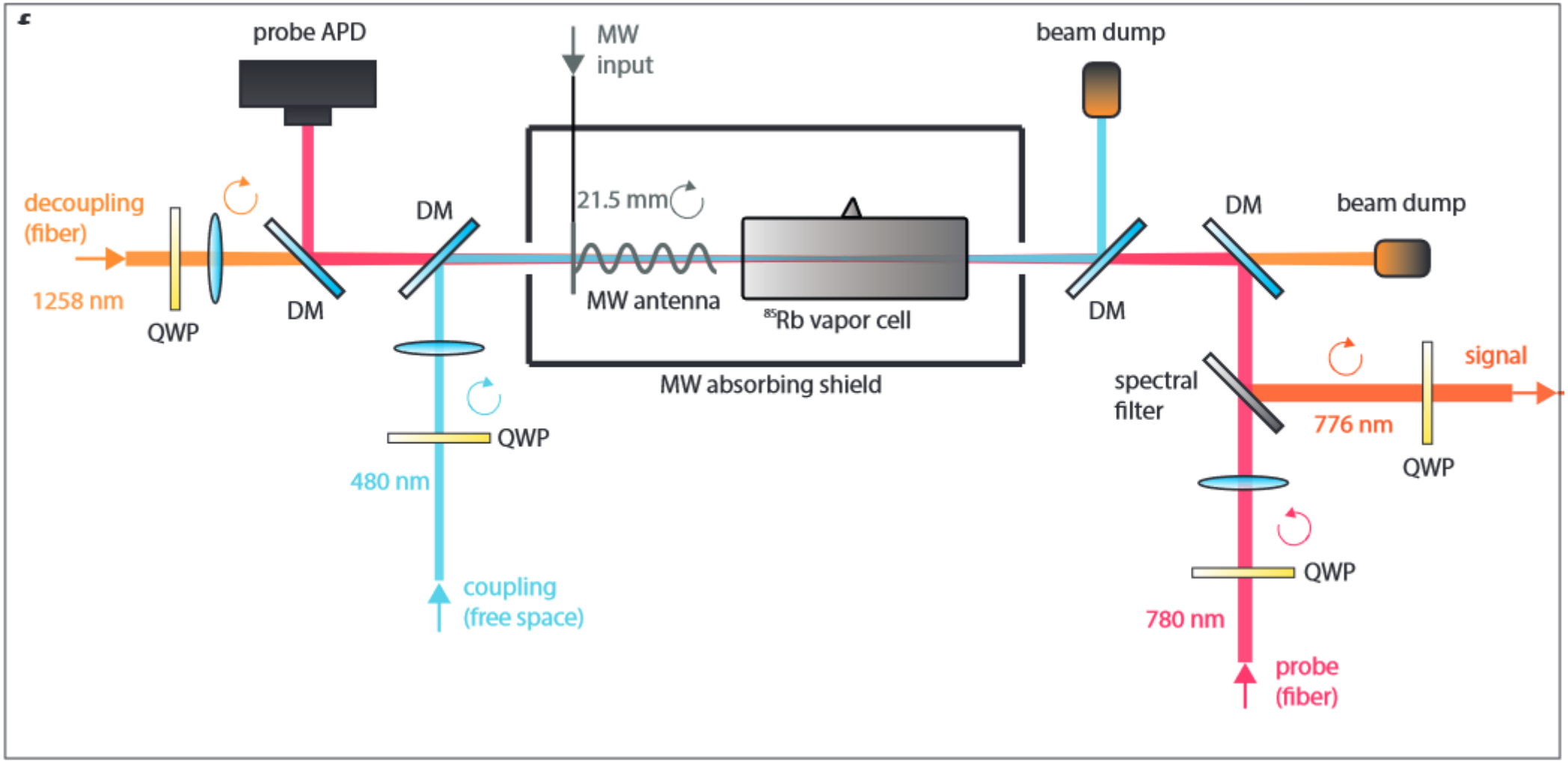


S. Borówka et al. C*ontinuous wideband microwave-to-optical converter based on room-temperature Rydberg atoms*, *Nat. Phot.* **18**, 32–38 (2024)

# Experimental setup

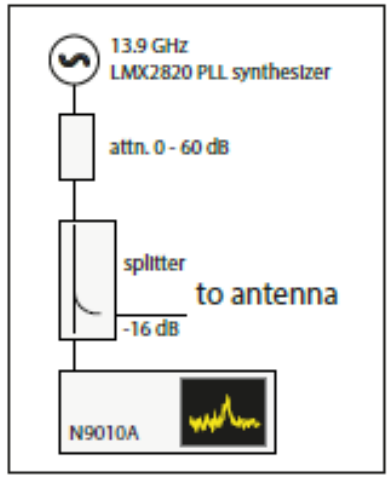


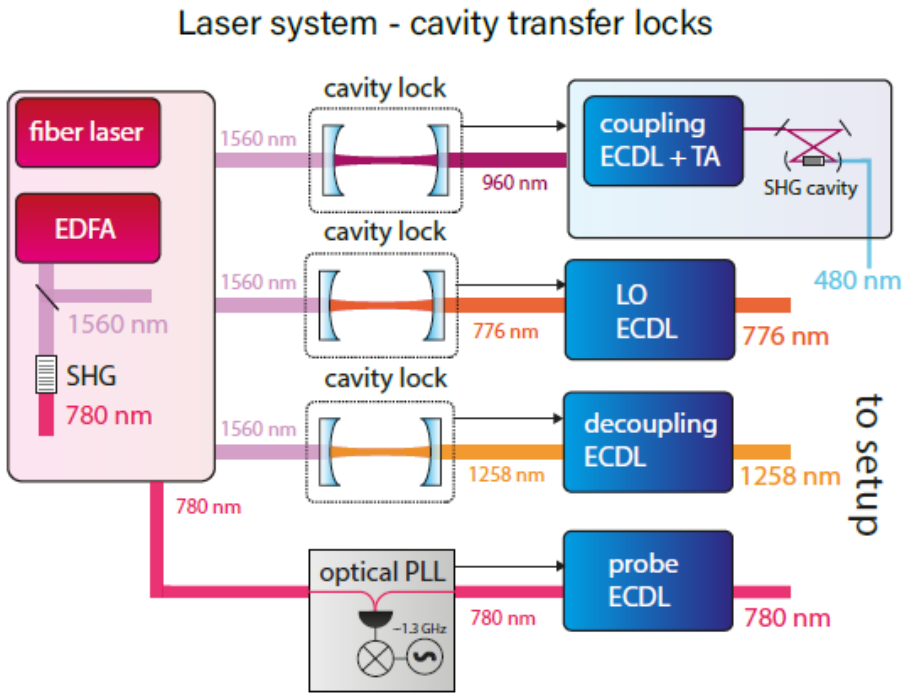


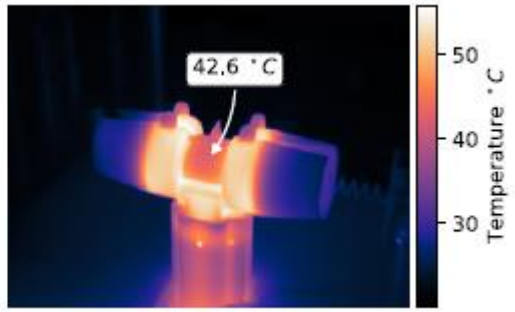


3D printed plastic heater with air-channels

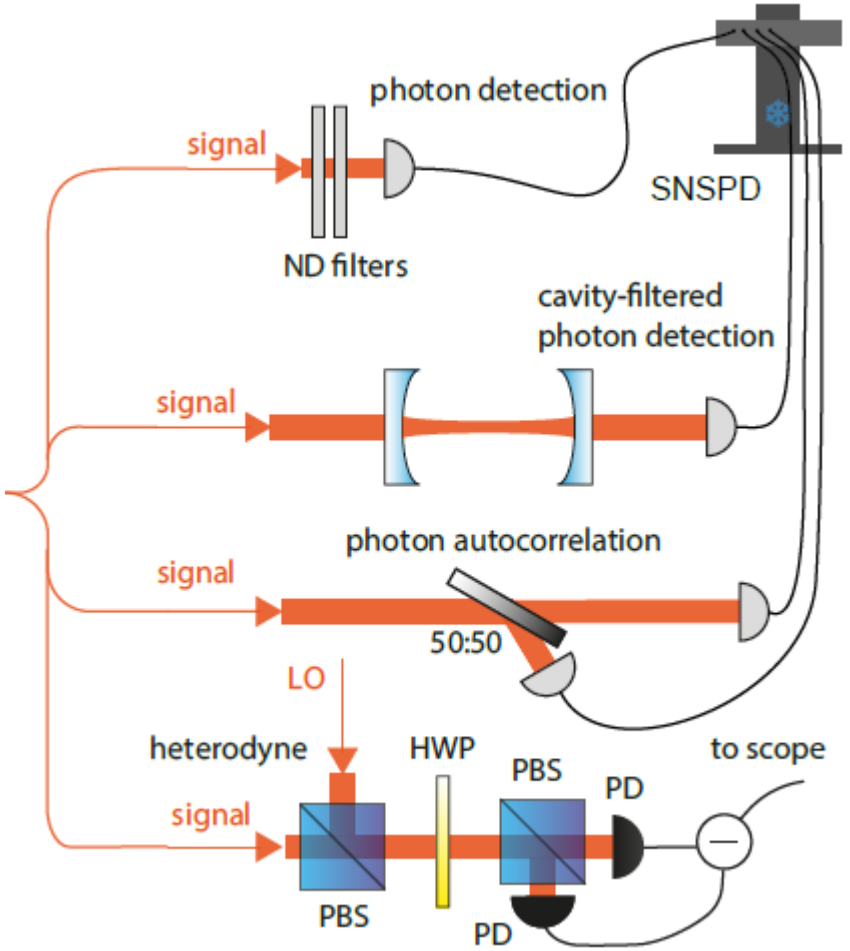


S. Borówka et al. C*ontinuous wideband microwave-to-optical converter based on room-temperature Rydberg atoms*, *Nat. Phot.* **18**, 32–38 (2024)

# EIT & conversion

Simulation

Experiment

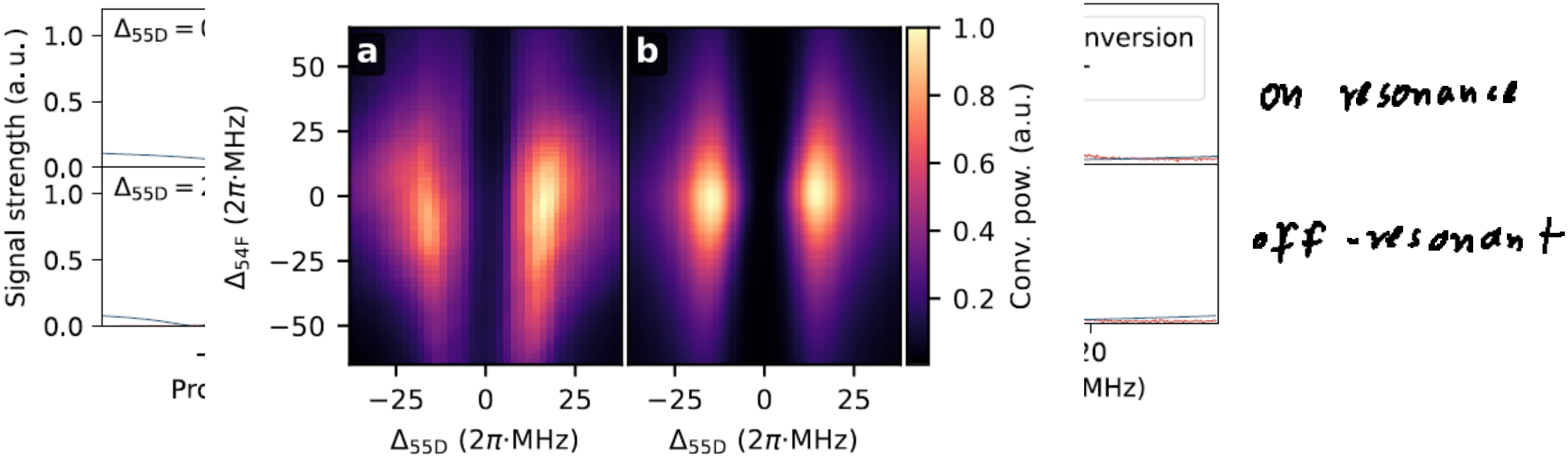


S. Borówka et al. C*ontinuous wideband microwave-to-optical converter based on room-temperature Rydberg atoms*, *Nat. Phot.* **18**, 32–38 (2024)

# Photon counting and efficiency

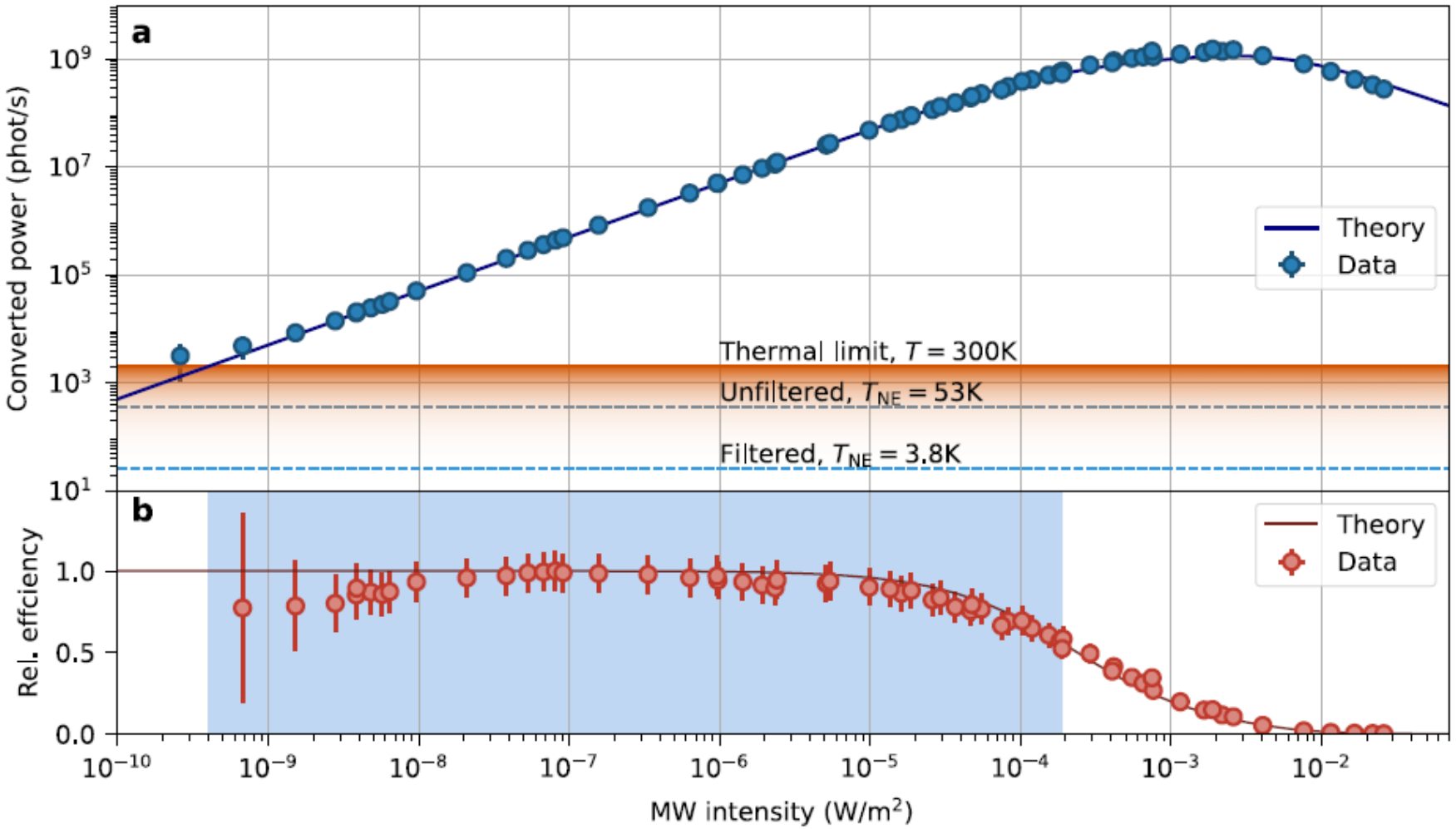


S. Borówka et al. C*ontinuous wideband microwave-to-optical converter based on room-temperature Rydberg atoms*, *Nat. Phot.* **18**, 32–38 (2024)

# Approaching the thermal limit

## Theoretical

4.11 nVcm$^{-1}$Hz$^{-1/2}$

## Measured

3.98 nVcm$^{-1}$Hz$^{-1/2}$

## Theory of black-body radiation

$$\langle E_{\mathrm{eff}}^2 \rangle = \frac{\omega^2 \langle \mathcal{E} \rangle}{\pi^2 c^3 \varepsilon_0} \frac{1}{4\pi} \int_0^{2\pi} \mathrm{d}\phi \int_0^{\pi} \mathrm{d}\theta \sin(\theta) |\eta(\theta)|^2,$$

$$\langle \mathcal{E} \rangle = \frac{\hbar\omega}{e^{\hbar\omega/k_{\mathrm{B}}T} - 1},$$

$$|\eta(\theta)|^2 = \left( \cos\left(\frac{\theta}{2}\right)^4 + \sin\left(\frac{\theta}{2}\right)^4 \right) |\eta_{\mathrm{phm}}(\theta)|^2.$$

Polarization

Phase matching

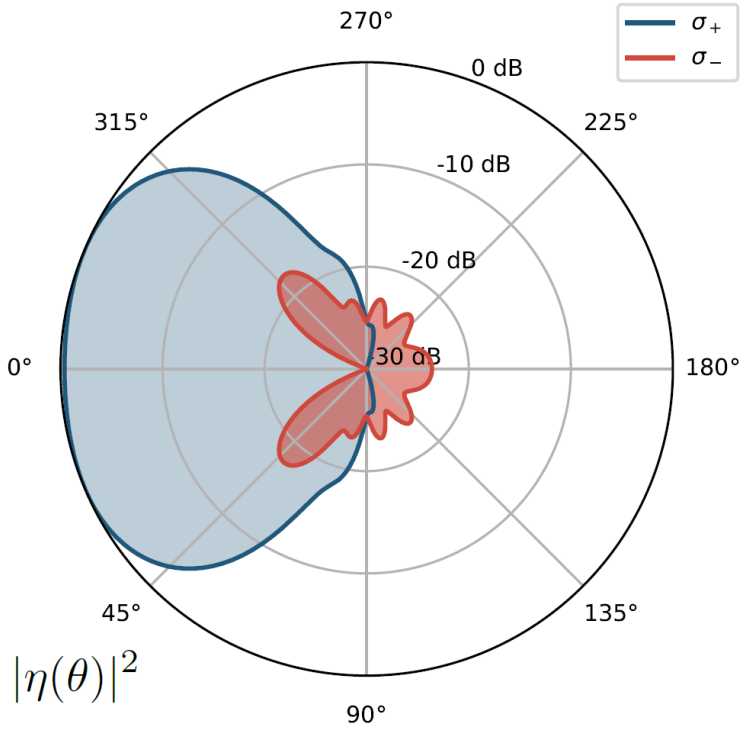


S. Borówka et al. C*ontinuous wideband microwave-to-optical converter based on room-temperature Rydberg atoms*, *Nat. Phot.* **18**, 32–38 (2024)

# Conversion bandwidth

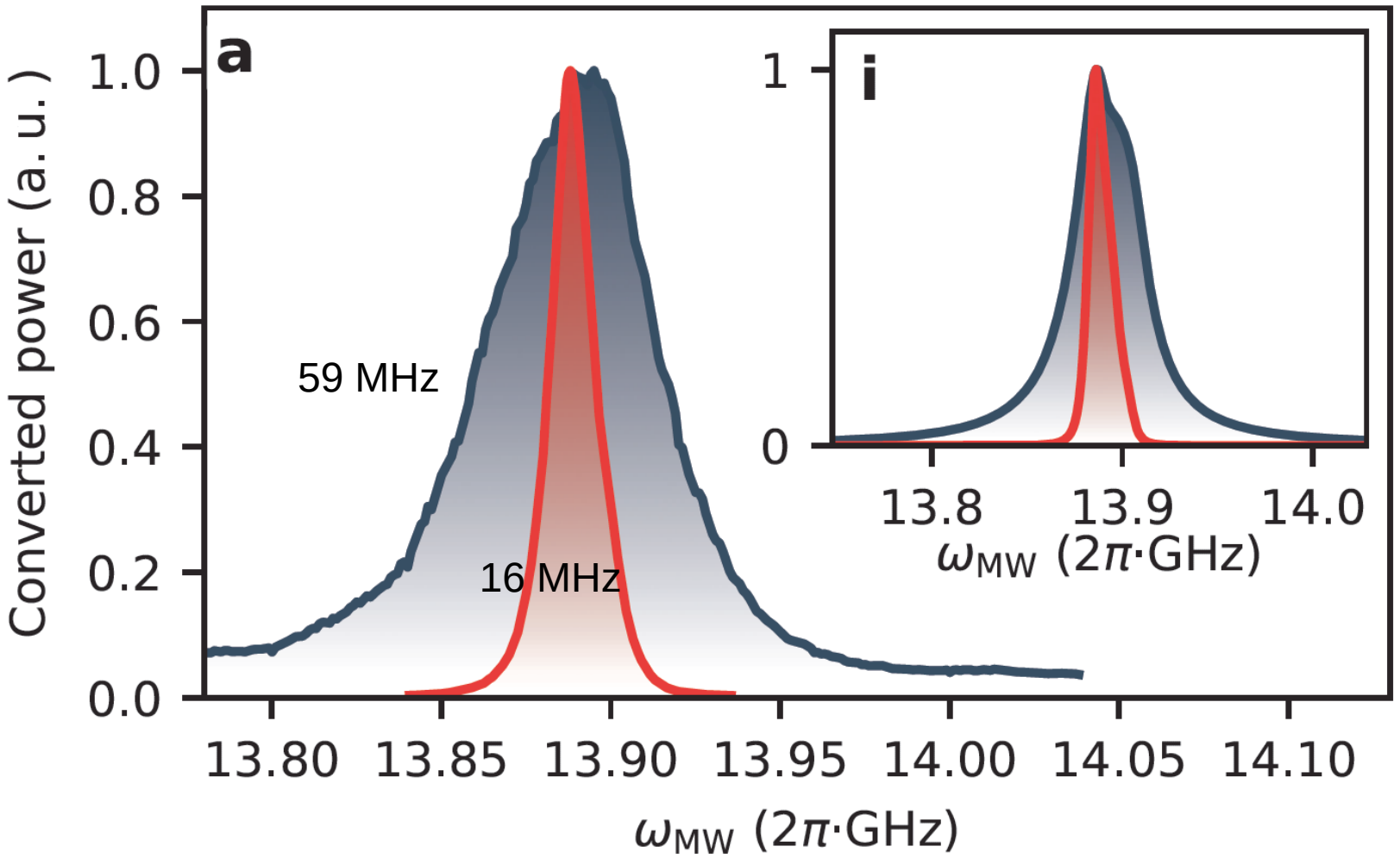


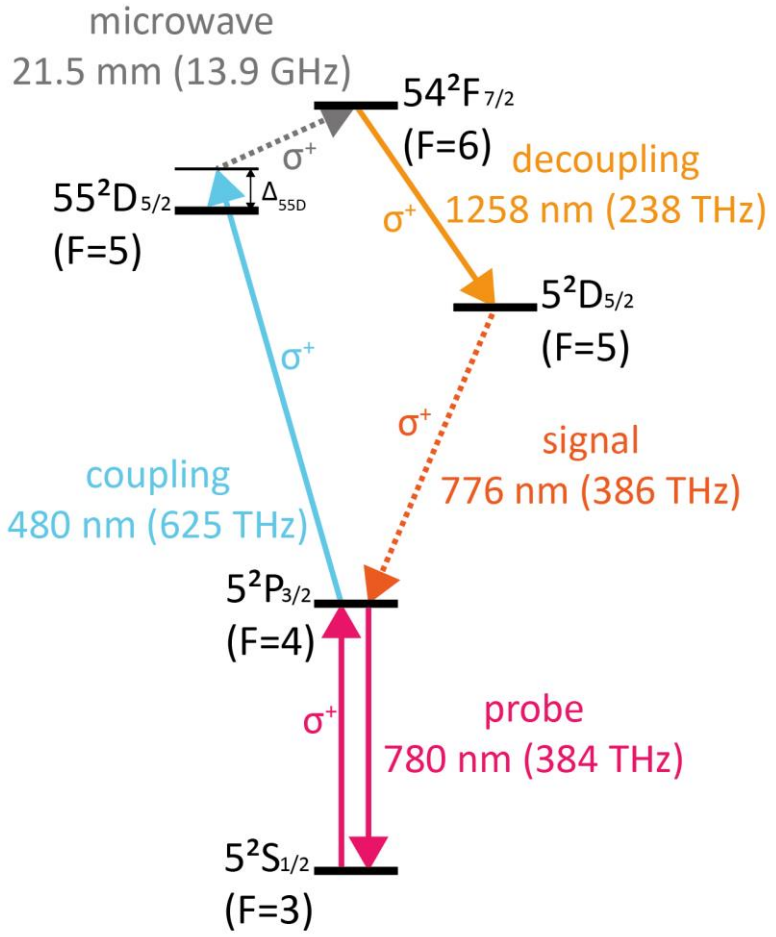


S. Borówka et al. C*ontinuous wideband microwave-to-optical converter based on room-temperature Rydberg atoms*, *Nat. Phot.* **18**, 32–38 (2024)

# Bandwidth

**Tunable bandwidth (single laser)**

**Instantenous bandwidth**

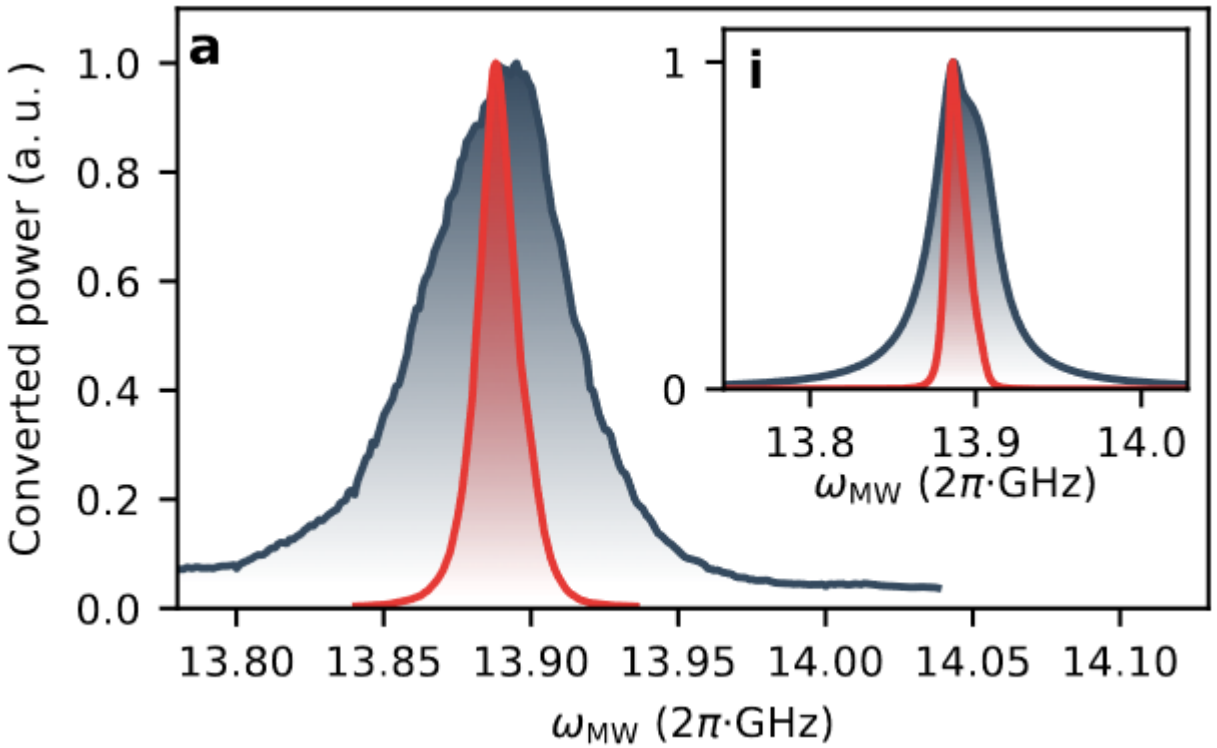


**Wiener-Khinchin theorem!**

$$g_{\mathrm{th}}^{(1)}(\tau) = \frac{1}{2\pi}\int_{-\infty}^{\infty} |S(\omega)|^2\, e^{-i\omega\tau}\,\mathrm{d}\omega,$$

$$g^{(2)}(\tau) = 1 + \frac{1}{4}\left(\left|g_{\mathrm{th}}^{(1)}(\tau) + e^{-i\omega\tau}\right|^2 - 1\right),$$

S. Borówka et al. C*ontinuous wideband microwave-to-optical converter based on room-temperature Rydberg atoms*, *Nat. Phot.* **18**, 32–38 (2024)

# Second-order correlation

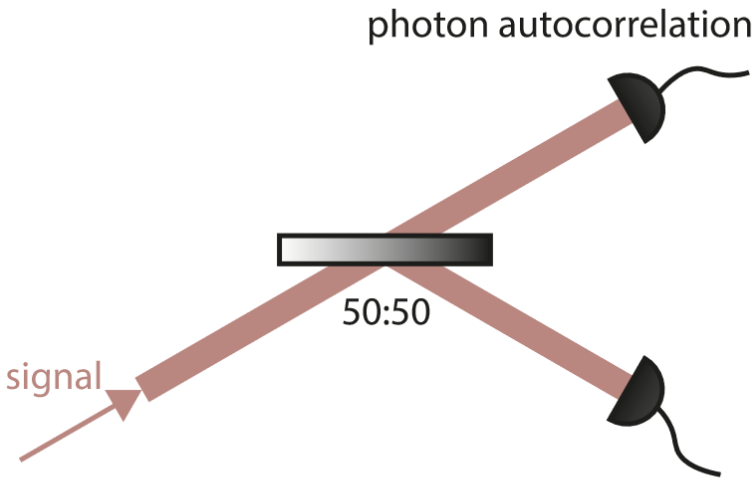


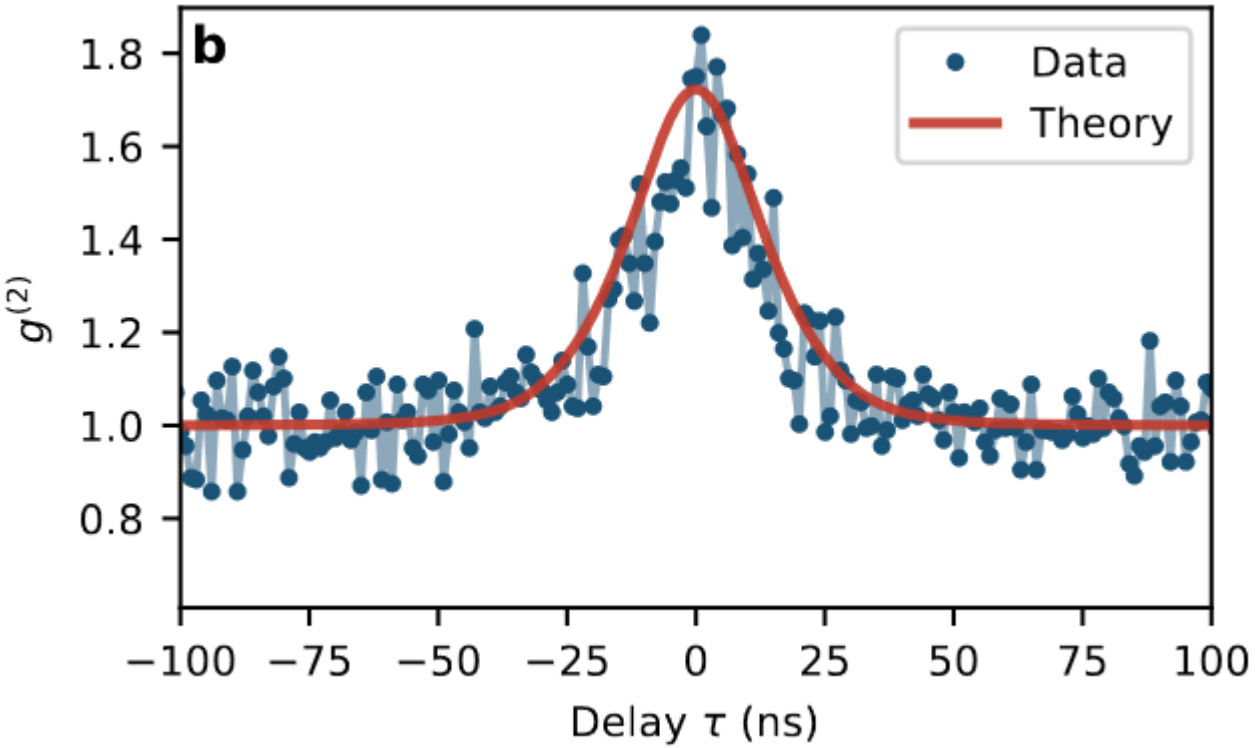


S. Borówka et al. C*ontinuous wideband microwave-to-optical converter based on room-temperature Rydberg atoms*, *Nat. Phot.* **18**, 32–38 (2024)

# Second-order correlation

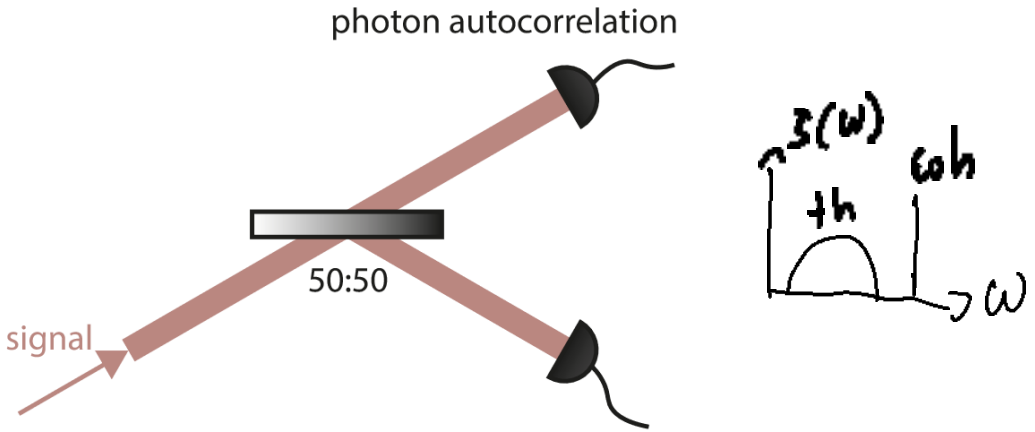





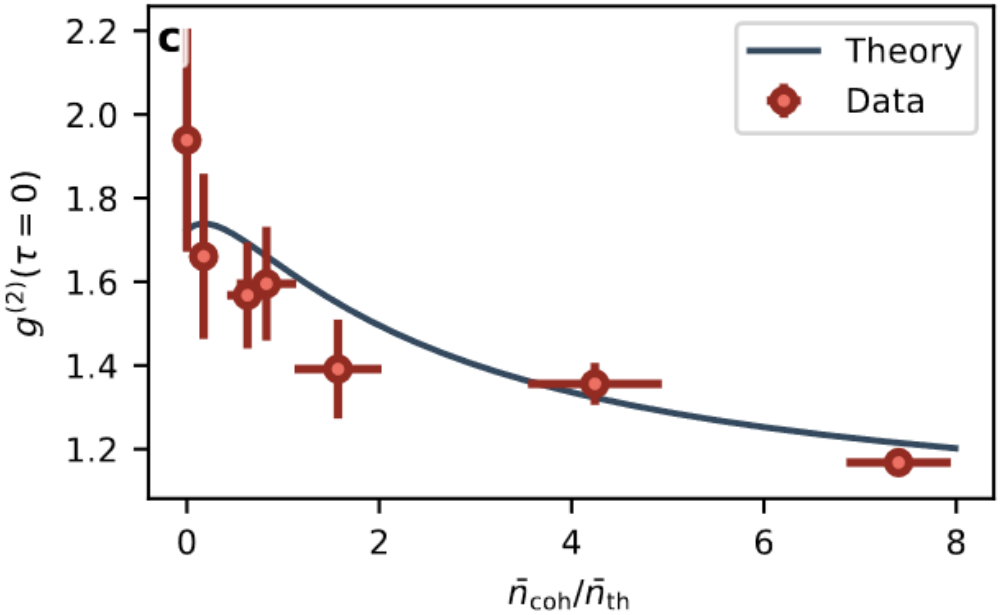


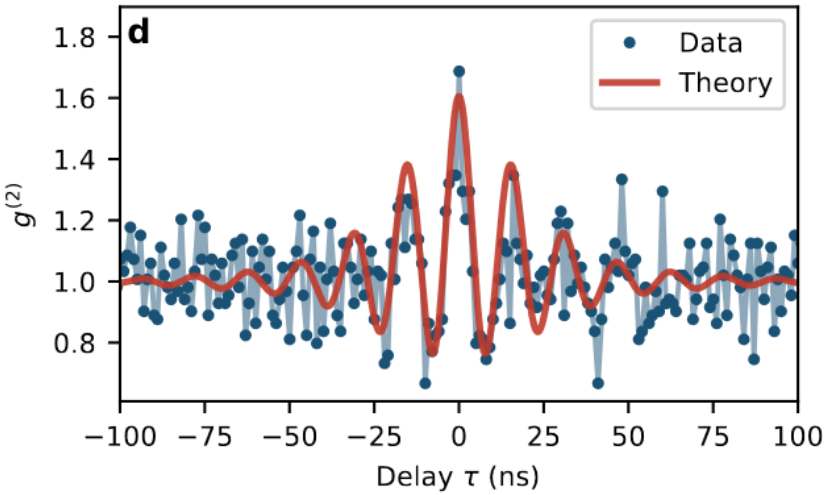


$$g^{(2)}(\tau) = 1 + \frac{\left|\bar{n}_{\mathrm{th}} g^{(1)}_{\mathrm{th}}(\tau) + \bar{n}_{\mathrm{coh}} e^{-i\omega\tau}\right|^2 - \bar{n}^2_{\mathrm{coh}}}{\left(\bar{n}_{\mathrm{th}} + \bar{n}_{\mathrm{coh}} + \bar{n}_{\mathrm{noise}}\right)^2}$$

S. Borówka et al. *Continuous wideband microwave-to-optical converter based on room-temperature Rydberg atoms*, *Nat. Phot.* **18**, 32–38 (2024)

# Conversion @130 GHz

Rydberg transition
34D to 32F

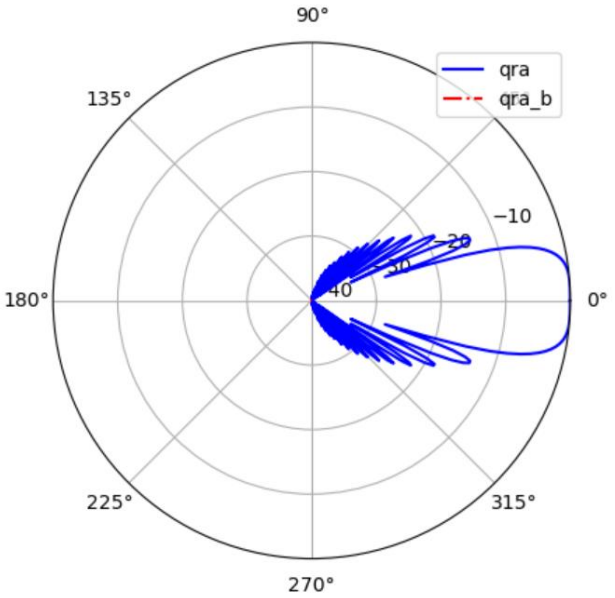


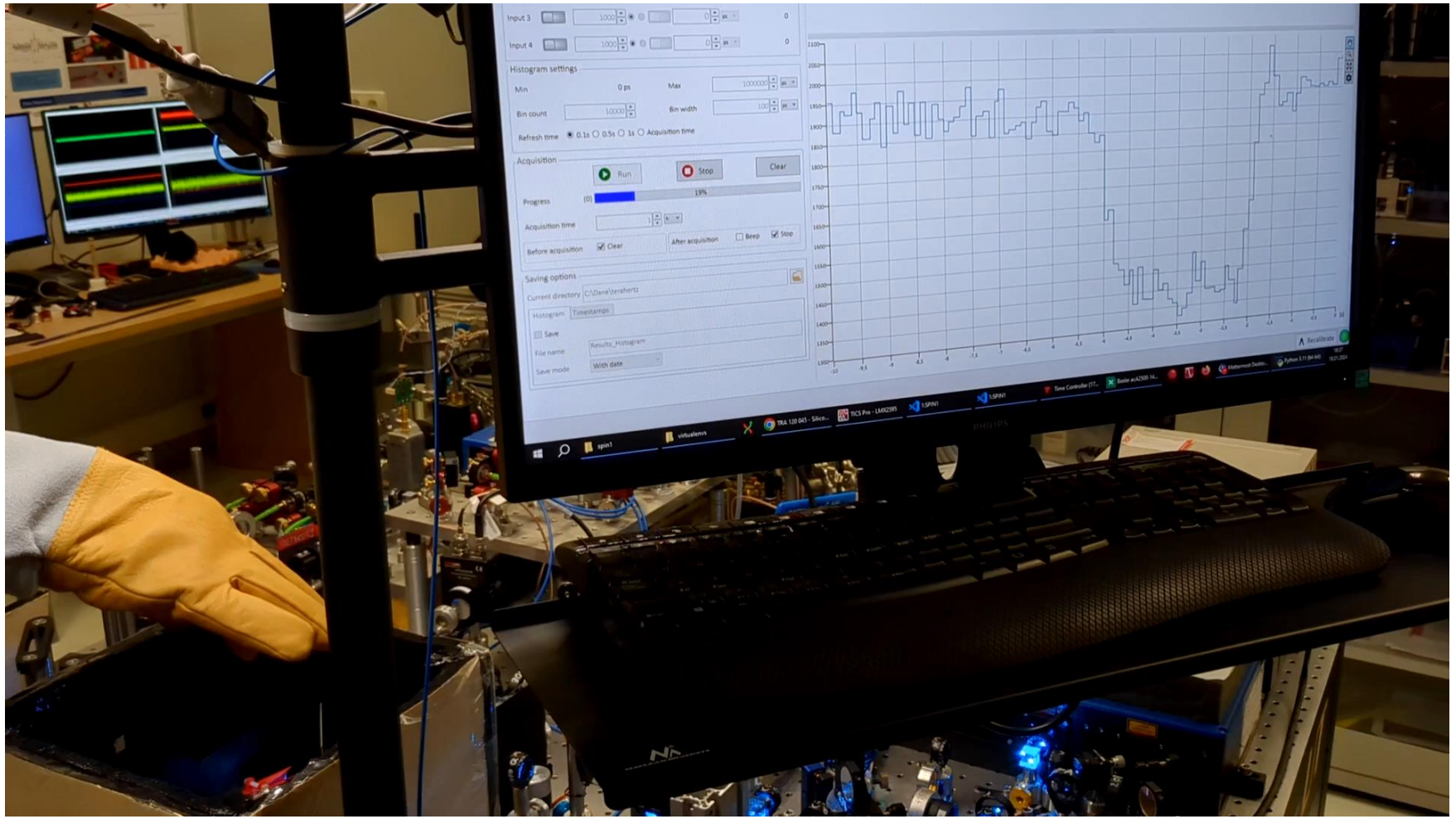


Sebastian Borówka, et al. Phys. Rev. Applied **22**, 034067 (2024)

# Conversion @130 GHz – THz "optics" and "photonics"

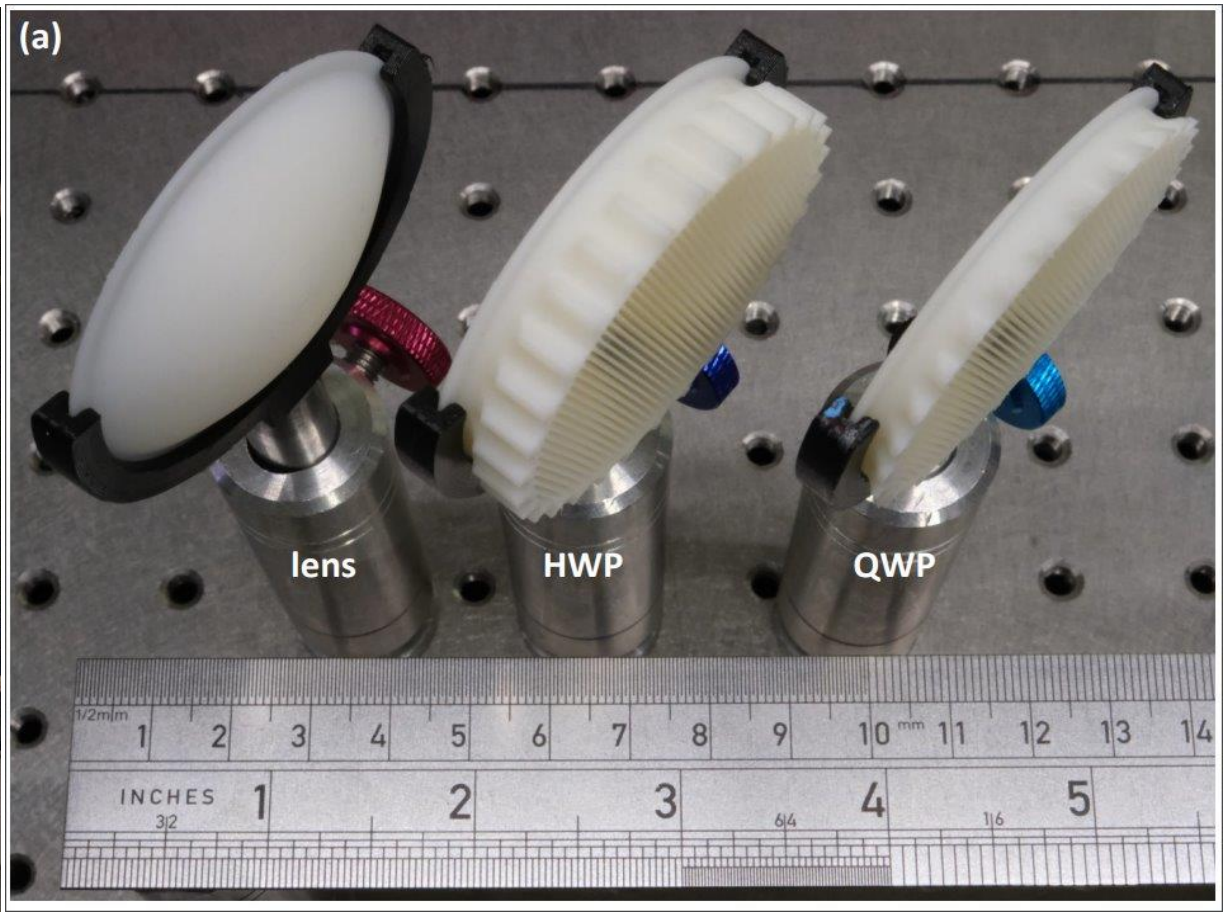


Sebastian Borówka, et al. Phys. Rev. Applied **22**, 034067 (2024)

# THz "photonics"

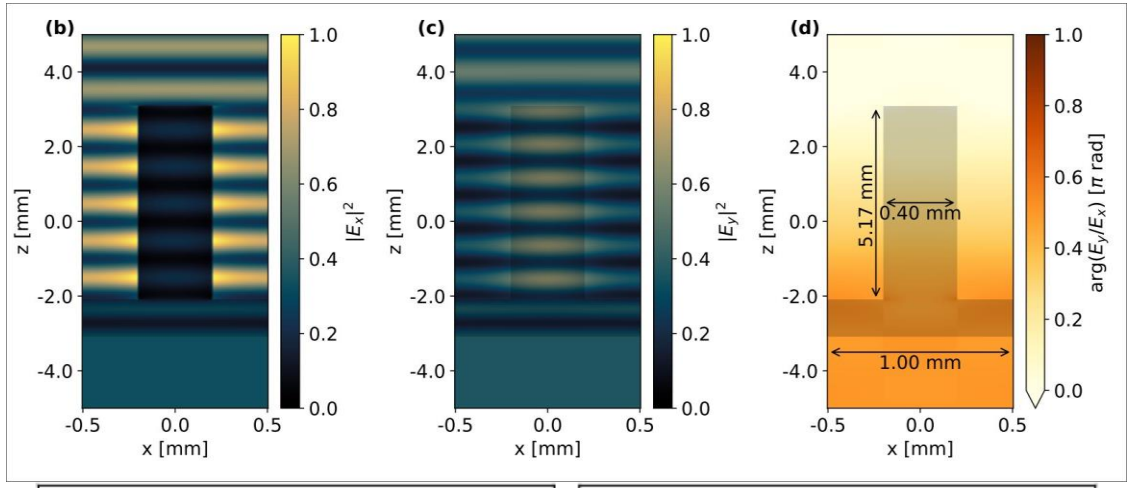


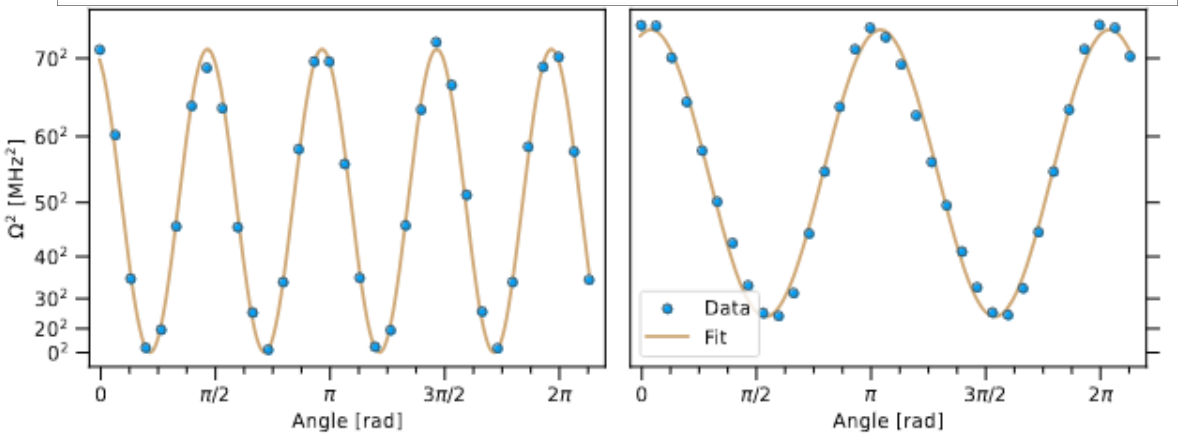


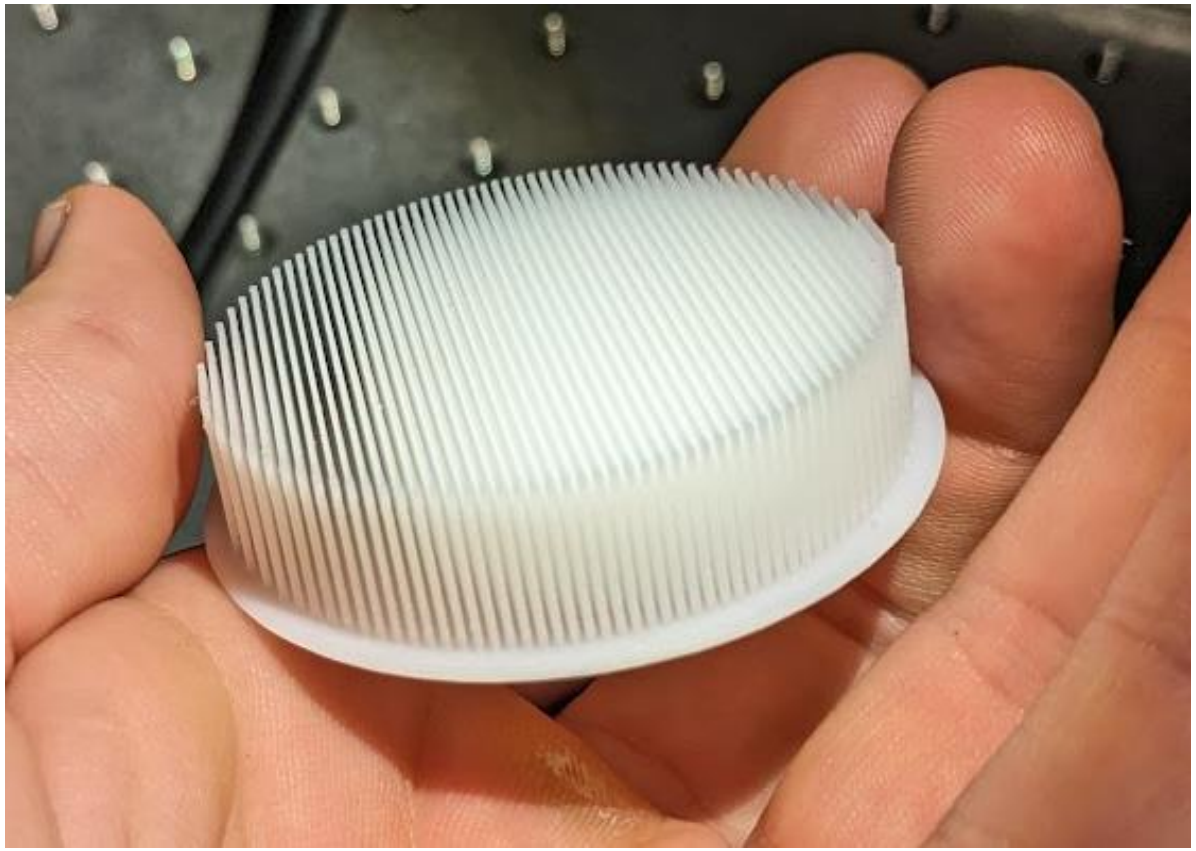

Computed using https://github.com/flexcompute/tidy3d

Sebastian Borówka, et al. Phys. Rev. Applied **22**, 034067 (2024)

# Callibration of a chip source for automotive applications (TRA120)

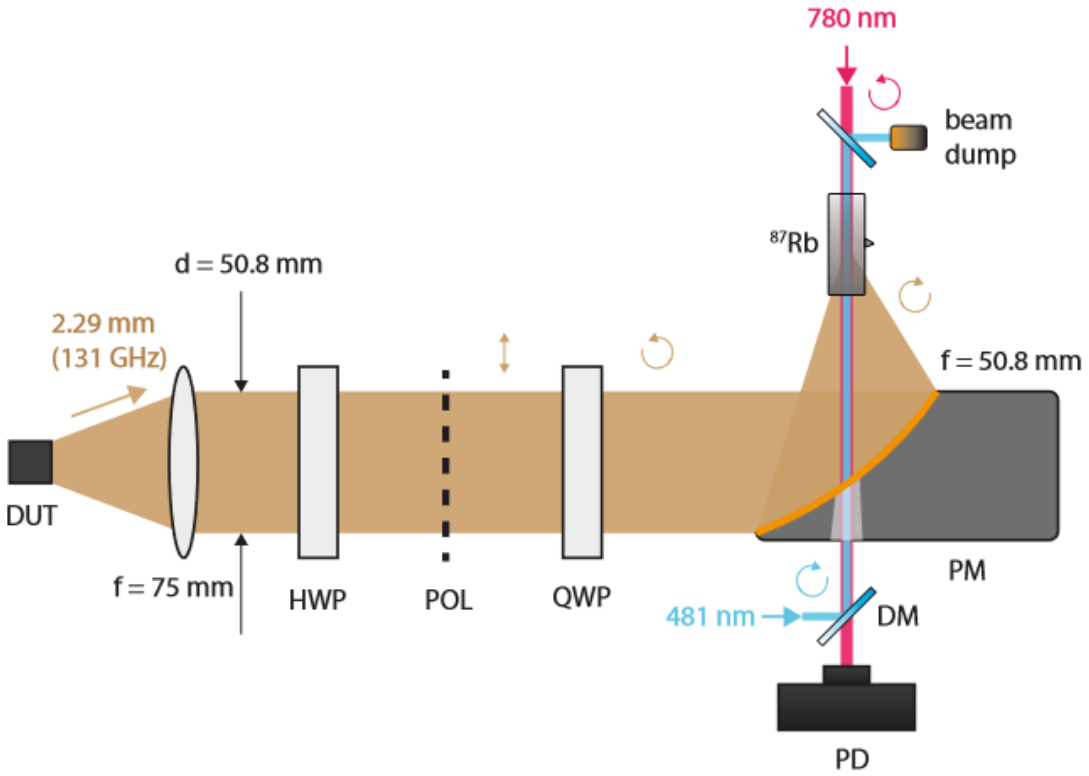


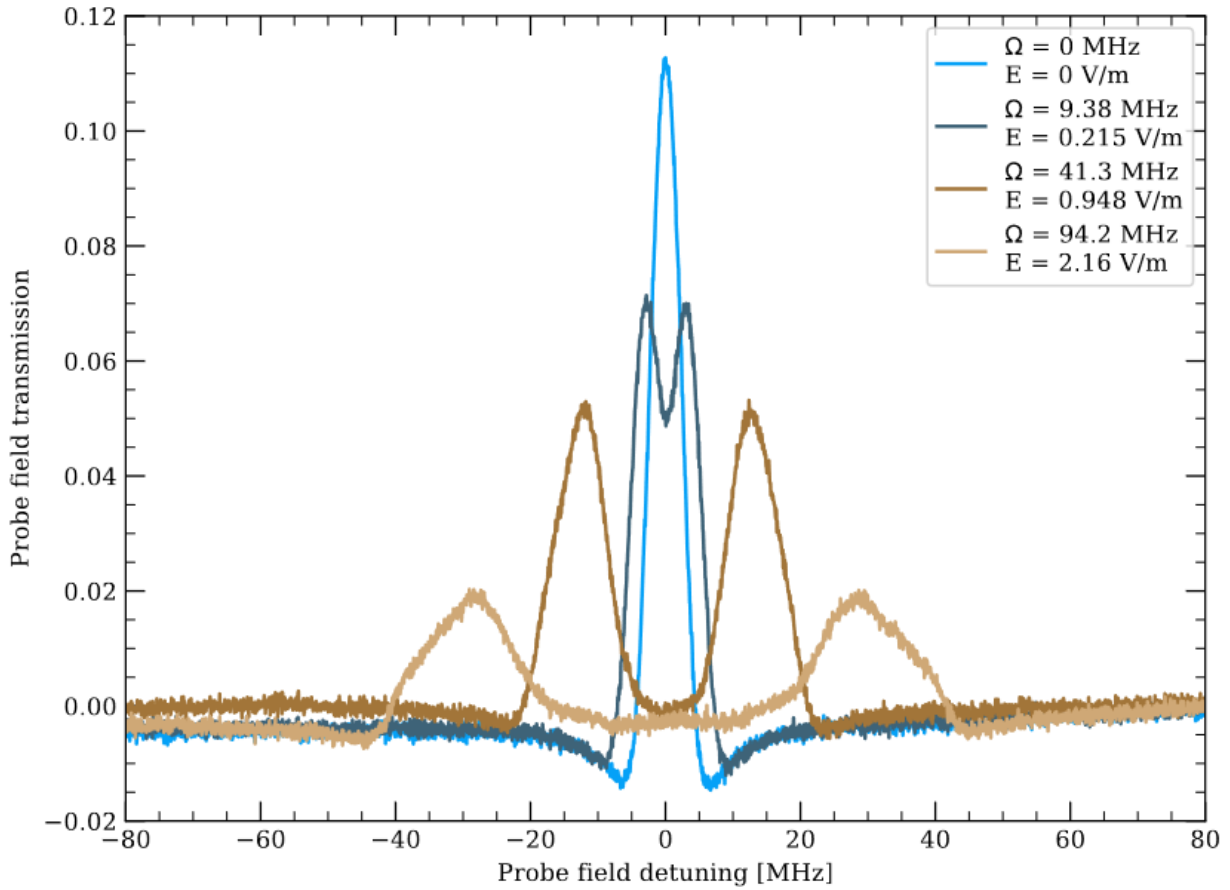


Sebastian Borówka, et al. Phys. Rev. Applied **22**, 034067 (2024)

# Phase sensitive detection – microwave mixer

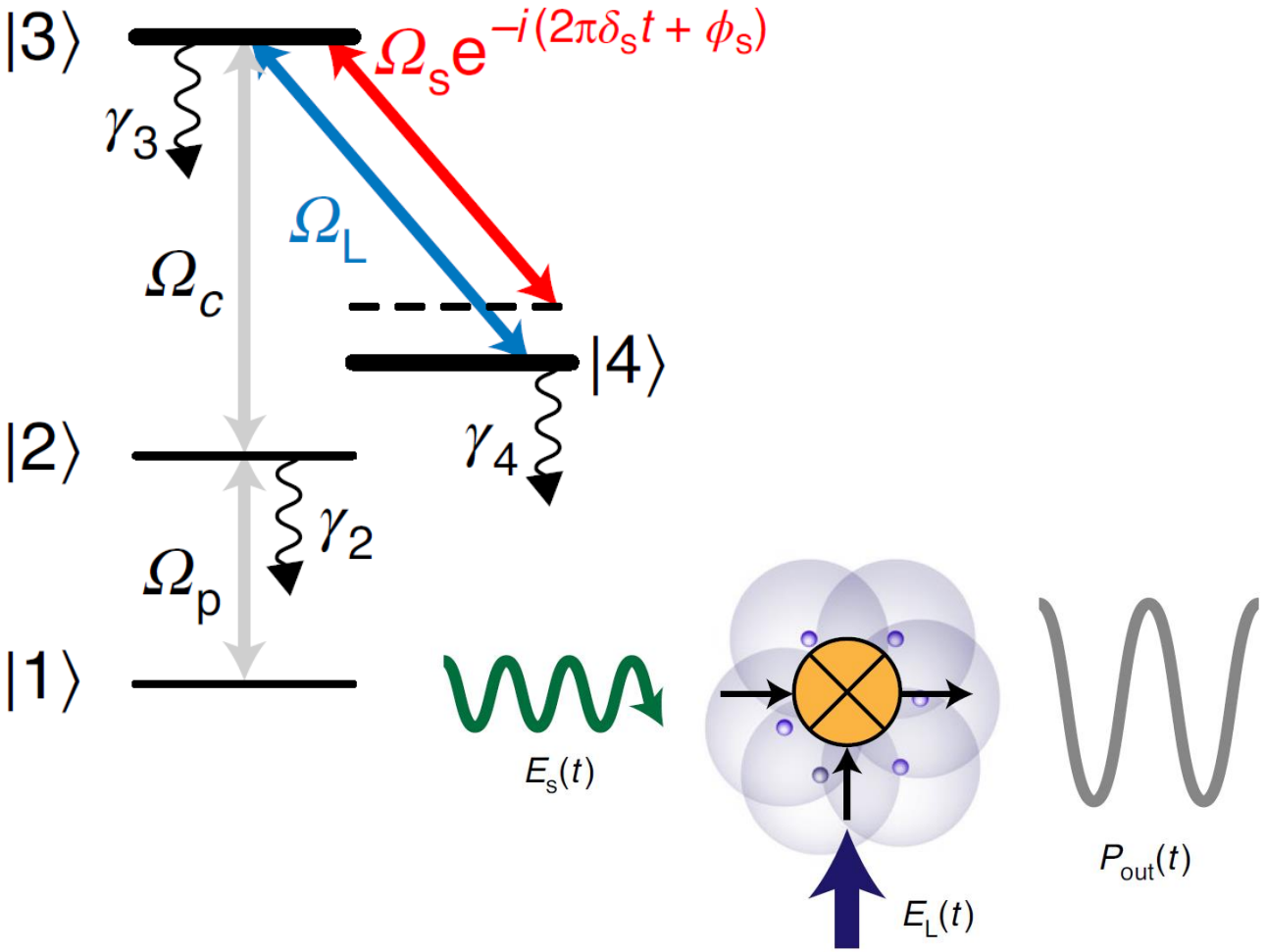


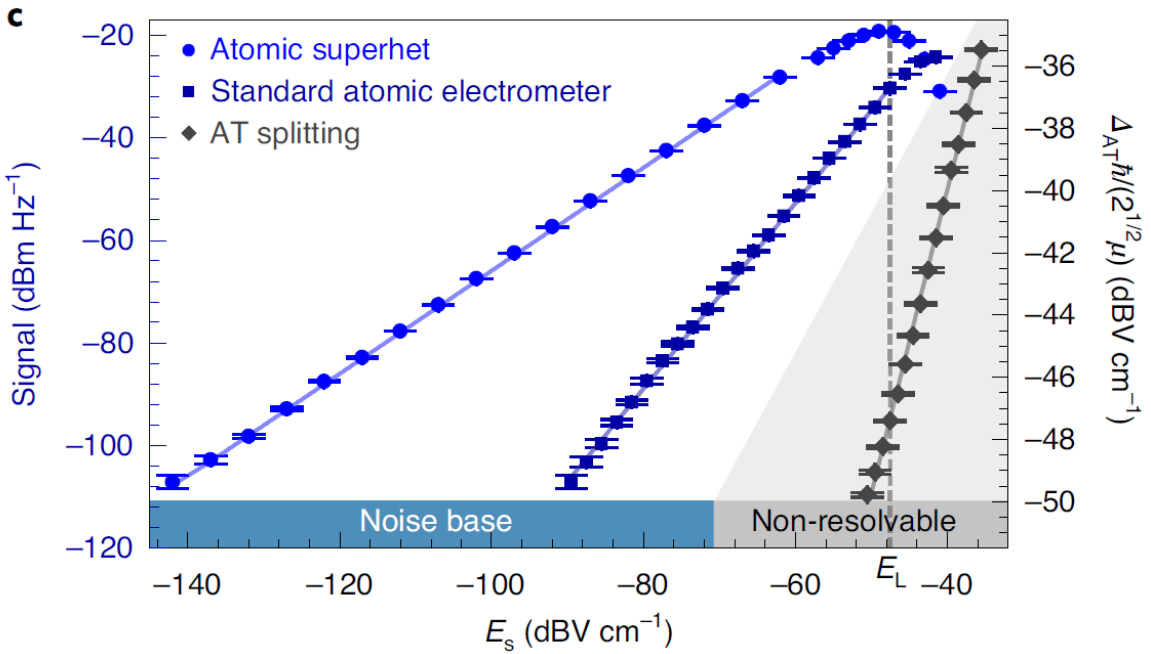


M. Jing et al. *Nat. Phys.* **16**, 911–915 (2020)

# All optical superheterodyne – optically biased detection

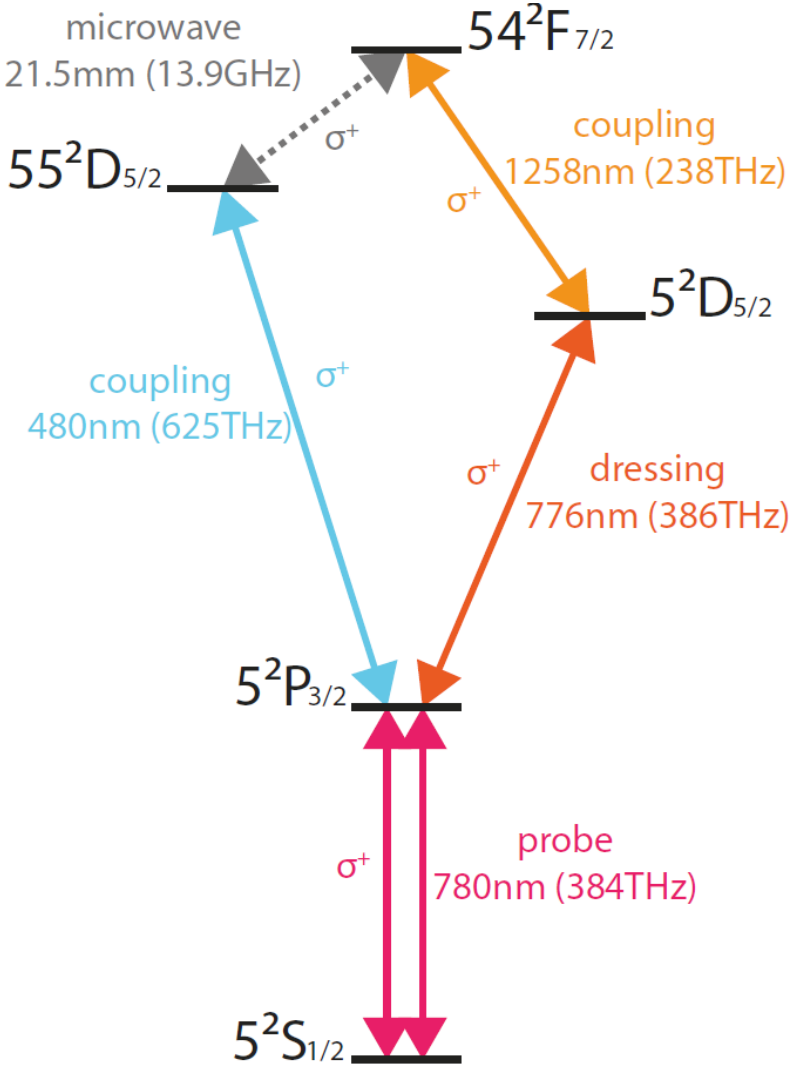


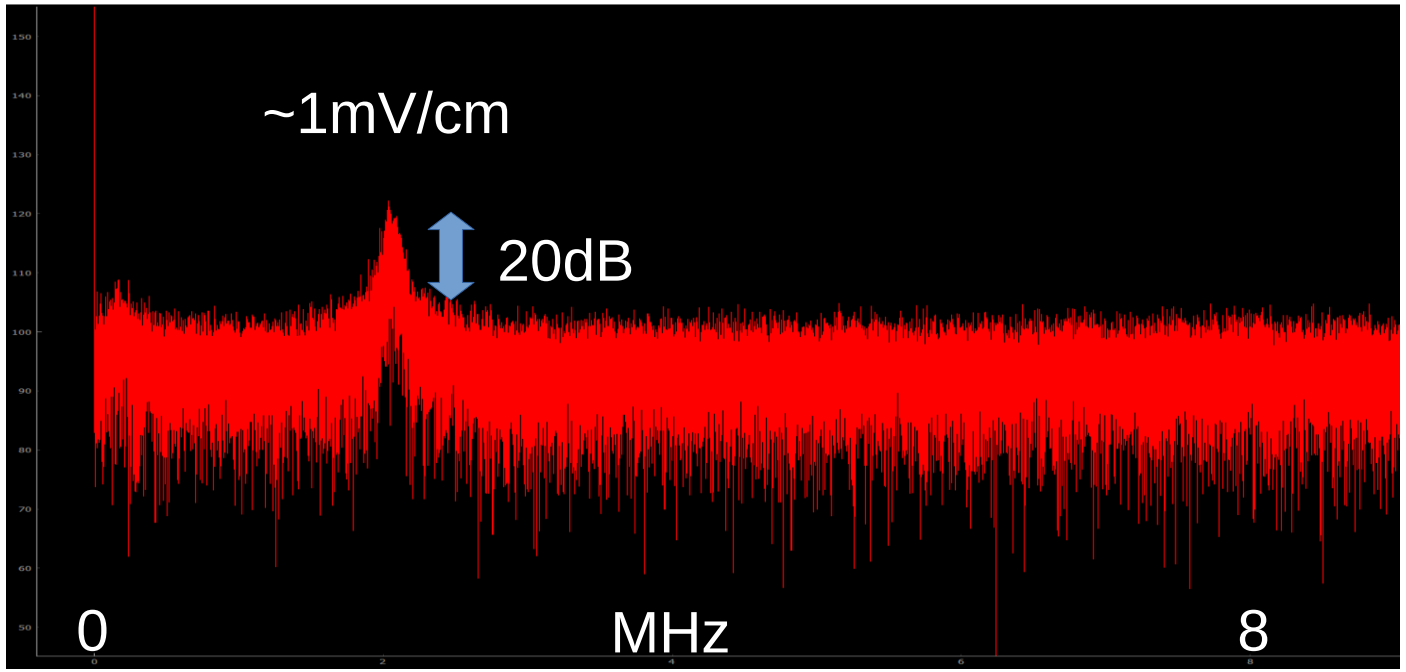


$$\phi = \phi_{480} + \phi_{776} + \phi_{1258}$$

Laser phase fluctuations transferred to the signal :(
Can we solve it without investing in ultra-stable lasers?

# Noise-compensated detection

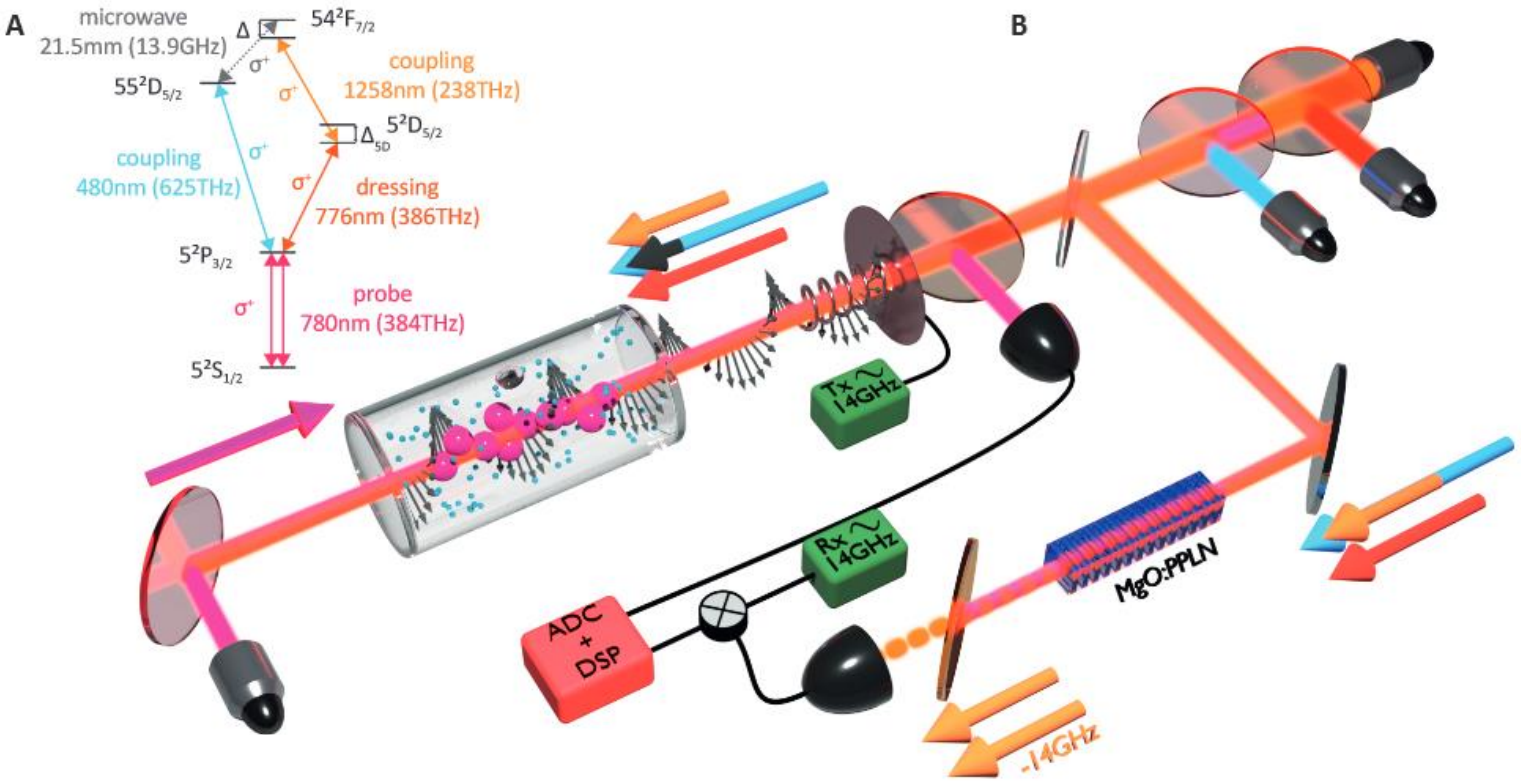


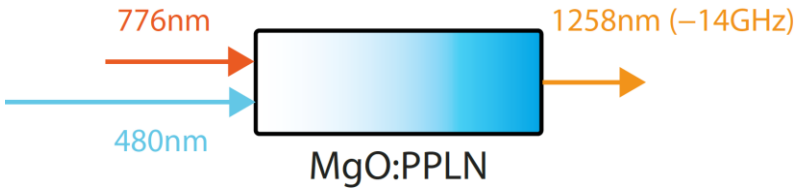


$$\phi_{480} + \phi_{776}$$

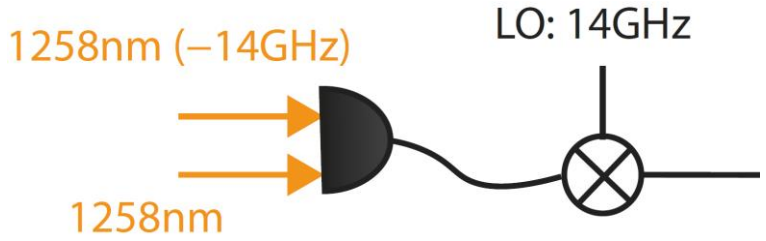


$$\phi_{480} + \phi_{776} + \phi_{1258}$$

S. Borówka, M. Mazelanik, W. Wasilewksi, M. Parniak, **arXiv:2403.05310**

# Phase compensation and sensitivity comparison

signal

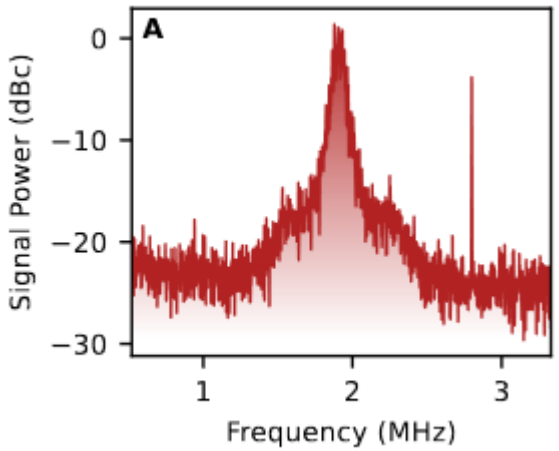


reference

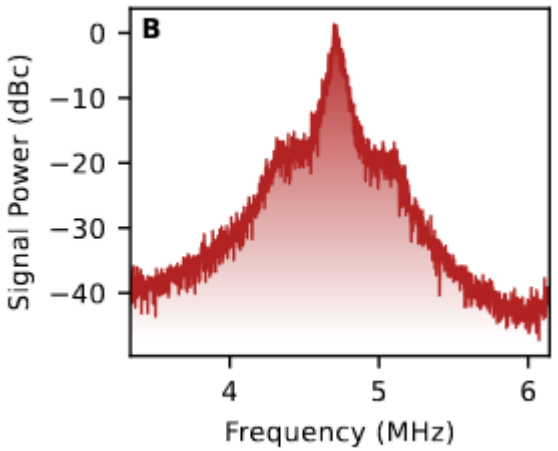


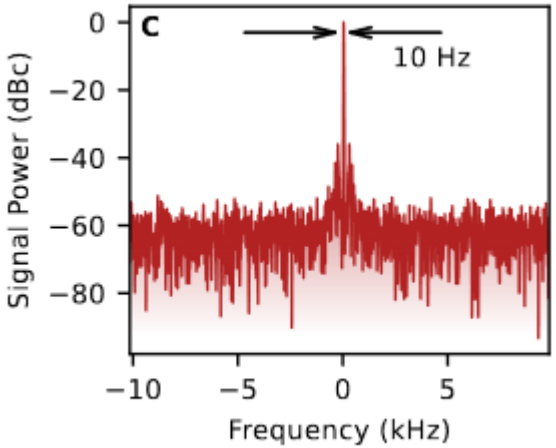


Improvement from
20dB to 60dB SNR

**arXiv:2403.05310**

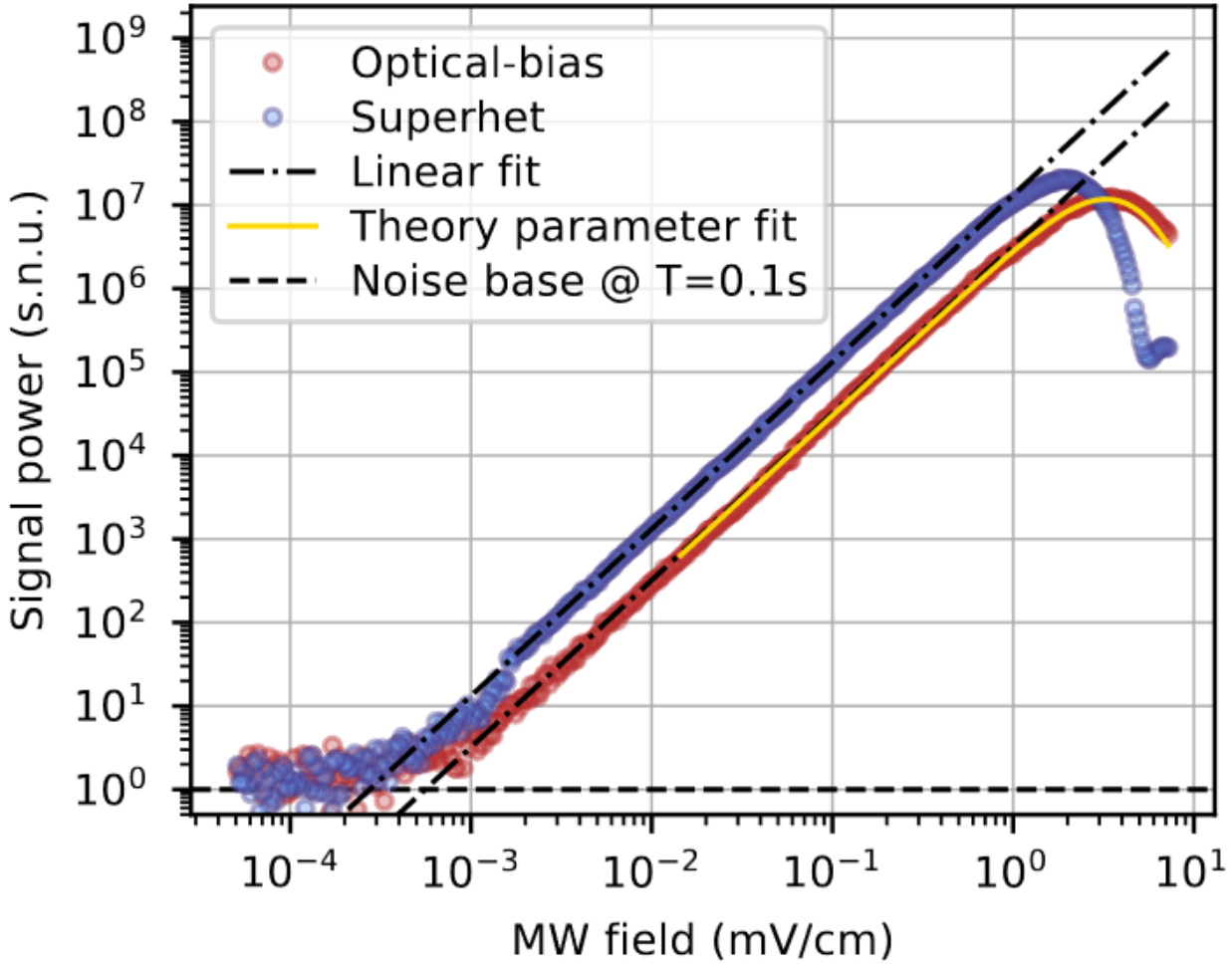

# Microwave sensing with cold Rydberg atoms

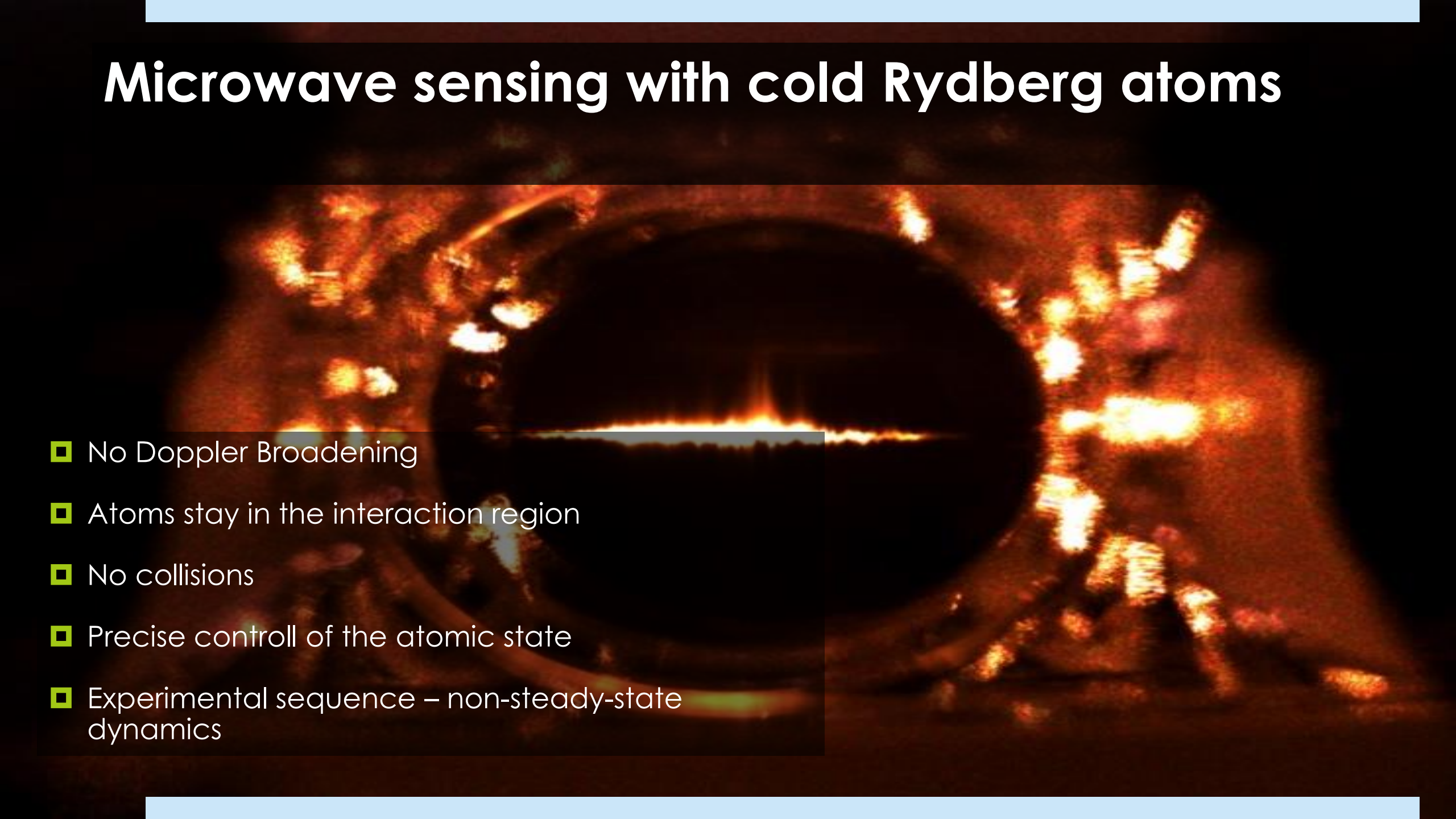

- No Doppler Broadening
- Atoms stay in the interaction region
- No collisions
- Precise controll of the atomic state
- Experimental sequence – non-steady-state dynamics

# Collective excitations in the ground state - interface

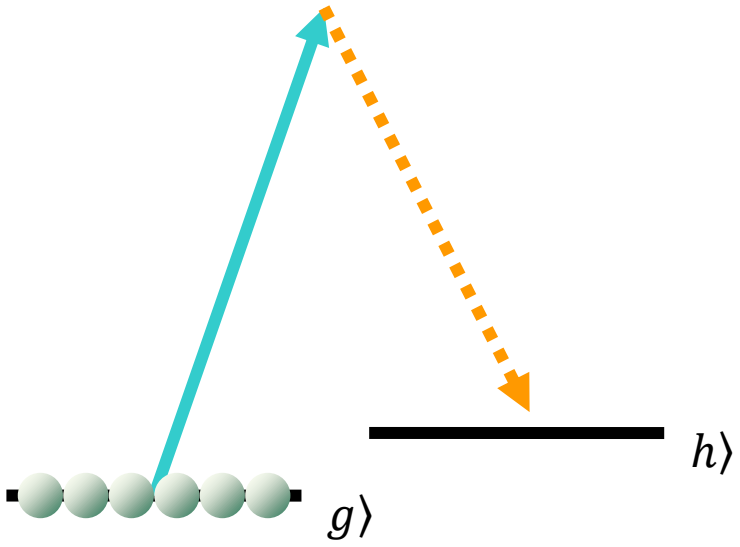


**two-mode squeezed state**
creation via off-resonant
**Raman scattering**

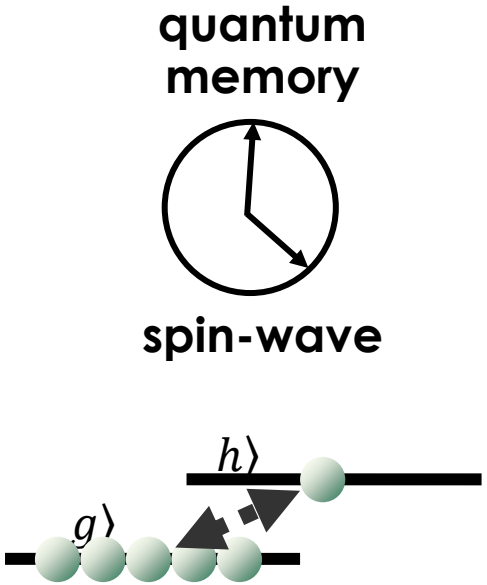


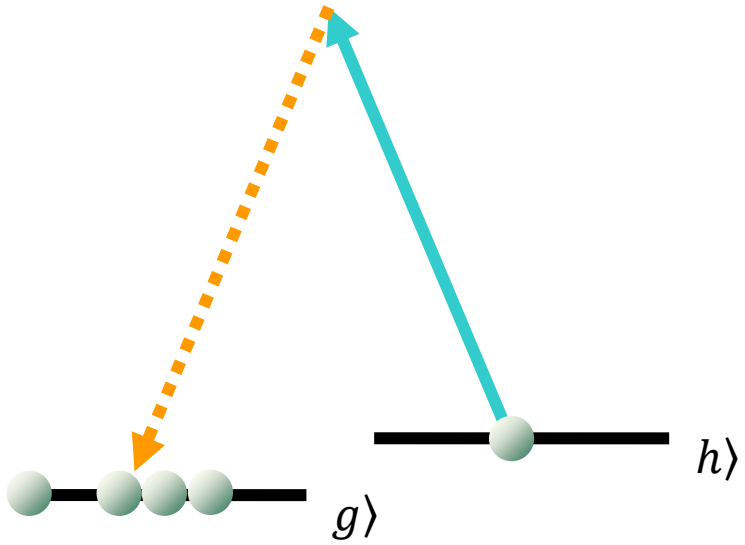


**readout stage** after storage time
results in **anihilation of spin-wave**

$$\frac{1}{\sqrt{N}}\left(e^{i\mathbf{K}\cdot\mathbf{r}_1}\left|\;\right\rangle + e^{i\mathbf{K}\cdot\mathbf{r}_2}\left|\;\right\rangle + e^{i\mathbf{K}\cdot\mathbf{r}_3}\left|\;\right\rangle + \ldots\right)$$

$|g\rangle$
$|h\rangle$

# Spin-wave storage and readout

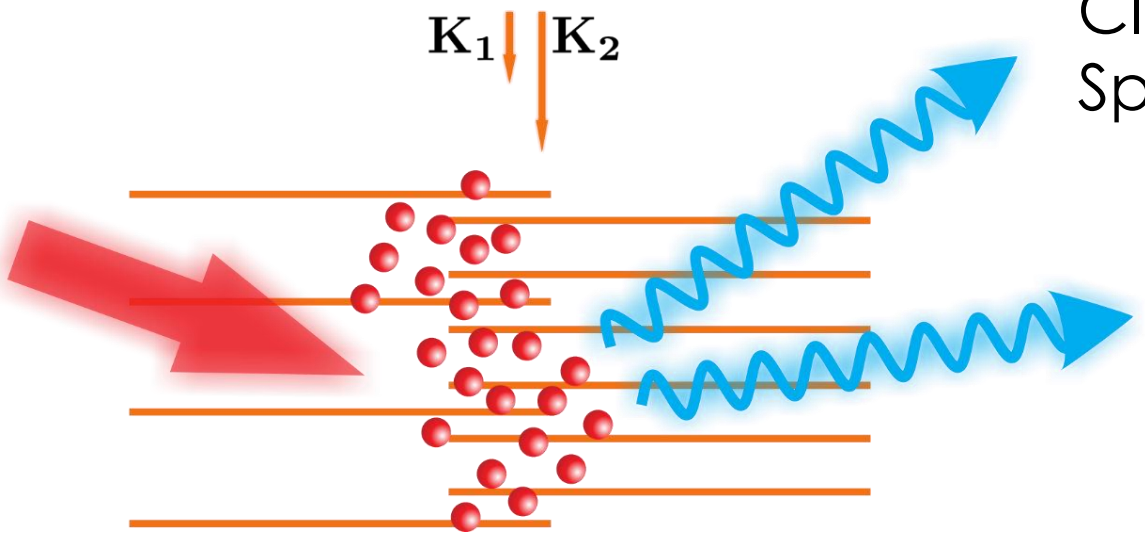


Classical analogue
Spatially-dependent atomic coherence

$$\hat{\rho}(\mathbf{r}) = \frac{1}{1+|\beta(\mathbf{r})|^2}\begin{pmatrix} 1 & \beta(\mathbf{r})e^{i\mathbf{K}\cdot\mathbf{r}} \\ \beta^*(\mathbf{r})e^{-i\mathbf{K}\cdot\mathbf{r}} & |\beta(\mathbf{r})|^2 \end{pmatrix}.$$

$$\tilde{\mathbf{P}} = n\mathrm{Tr}(\rho\hat{\mathbf{d}}),$$

$$2i\frac{\partial \mathbf{A}}{\partial z} = -\frac{\omega}{c\epsilon_0}\mathbf{P}.$$

$$\frac{1}{\sqrt{N}}\left(e^{i\mathbf{K}\cdot\mathbf{r}_1}\left|\ \right\rangle + e^{i\mathbf{K}\cdot\mathbf{r}_2}\left|\ \right\rangle + e^{i\mathbf{K}\cdot\mathbf{r}_3}\left|\ \right\rangle + \ldots\right)$$

$$\tau = \left(|\boldsymbol{k}|\sqrt{\frac{k_B T}{m}}\right)^{-1}$$

Result: directionial emission due to phase matching

# Collective excitations

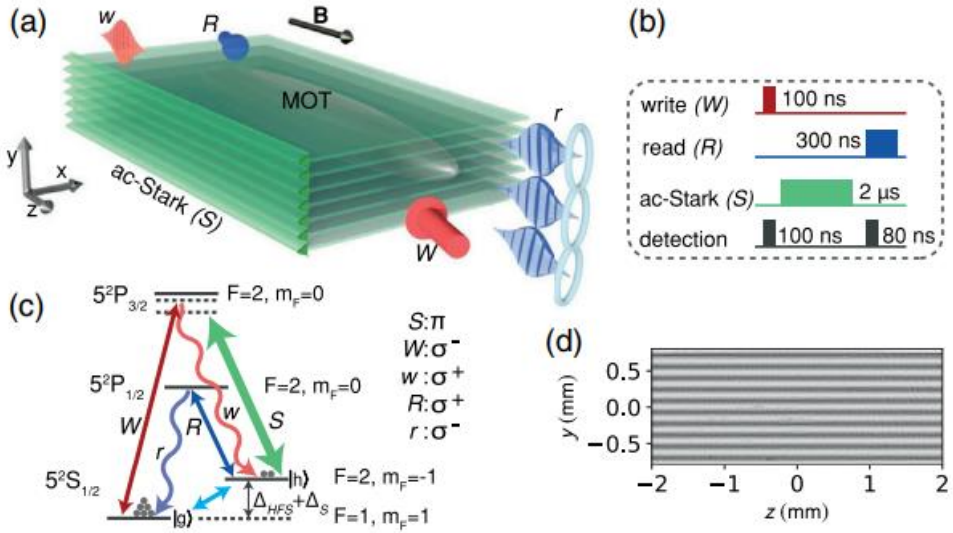


M. Parniak, et al. Phys. Rev. Lett. **122**, 063604

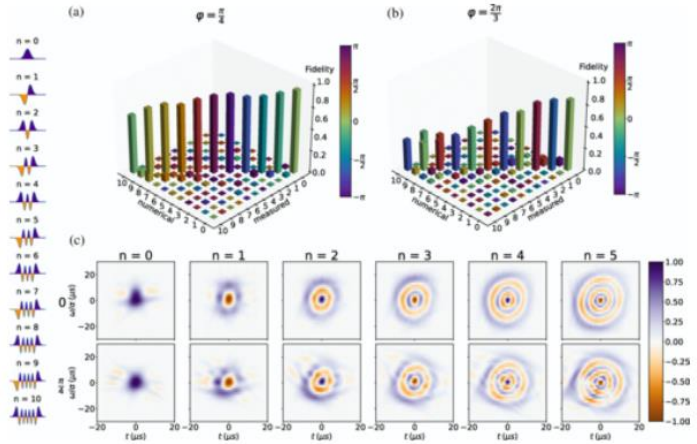

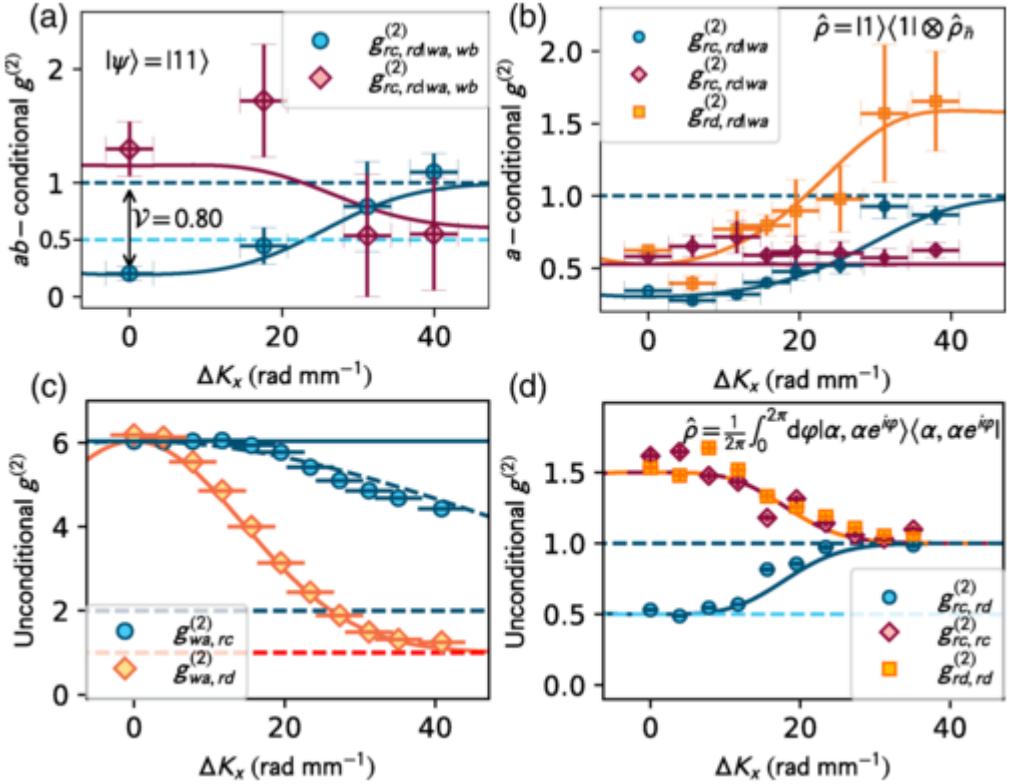


B. Niewelt et al. Phys. Rev. Lett. **130**, 240801

# Collective Rydberg qubits

- quantum information is distributed over many atoms
- direct readout in a well-defined spatial mode

$$|0\rangle = \frac{1}{\sqrt{N}} \sum_{j=1}^{N} e^{i(\boldsymbol{k}\cdot\boldsymbol{R}_j - \omega_r t)} |g_1, g_2, \ldots, r_j, \ldots, g_N\rangle$$

$$|1\rangle = \frac{1}{\sqrt{N}} \sum_{j=1}^{N} e^{i(\boldsymbol{k}\cdot\boldsymbol{R}_j - \omega_{r'} t)} |g_1, g_2, \ldots, r'_j, \ldots, g_N\rangle$$

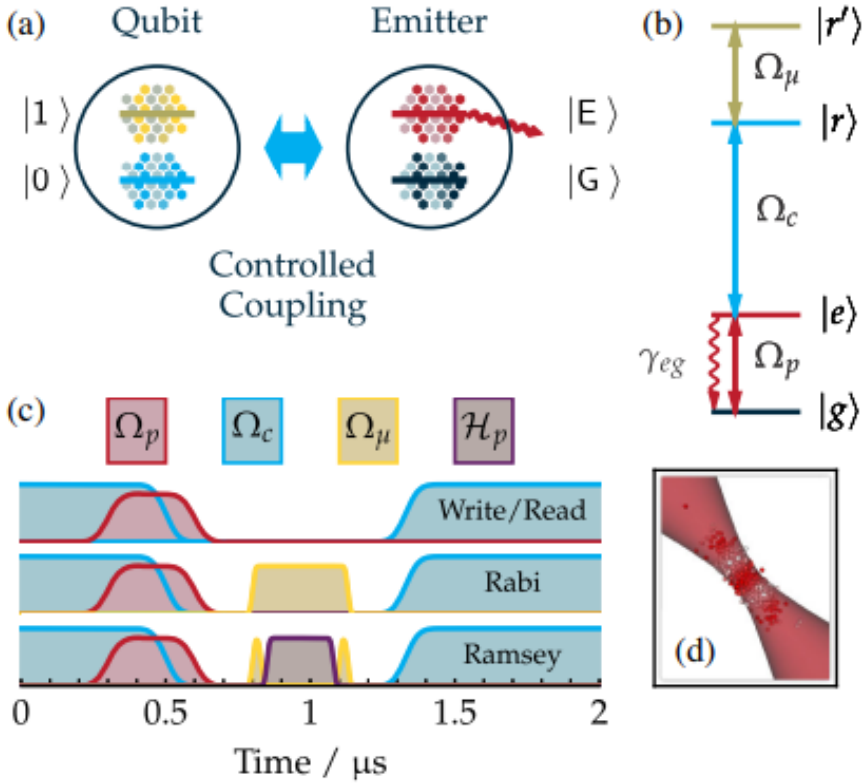


Collectively Encoded Rydberg Qubit
Nicholas L. R. Spong, et al., Phys. Rev. Lett. **127**, 063604

# Collective Rydberg qubits

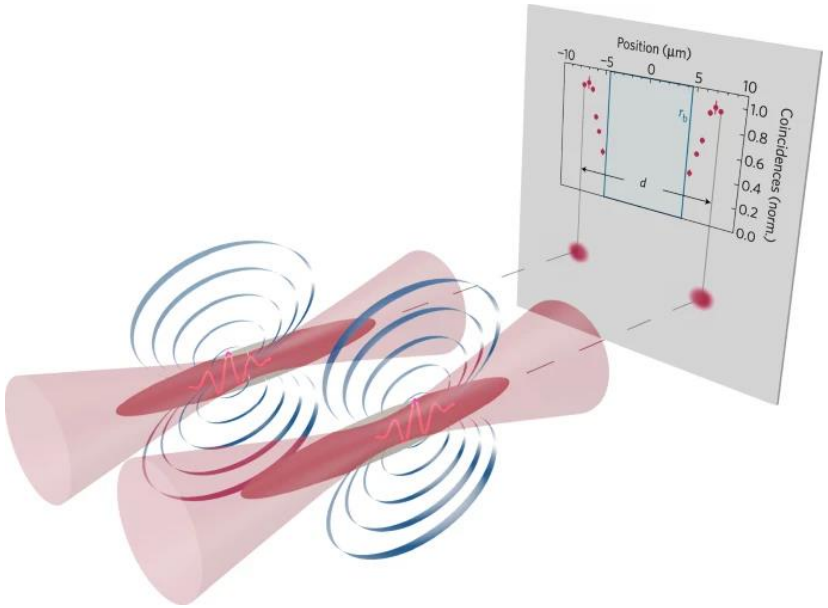


H. Busche, et al., Nature Physics 13, 655-658 (2017)

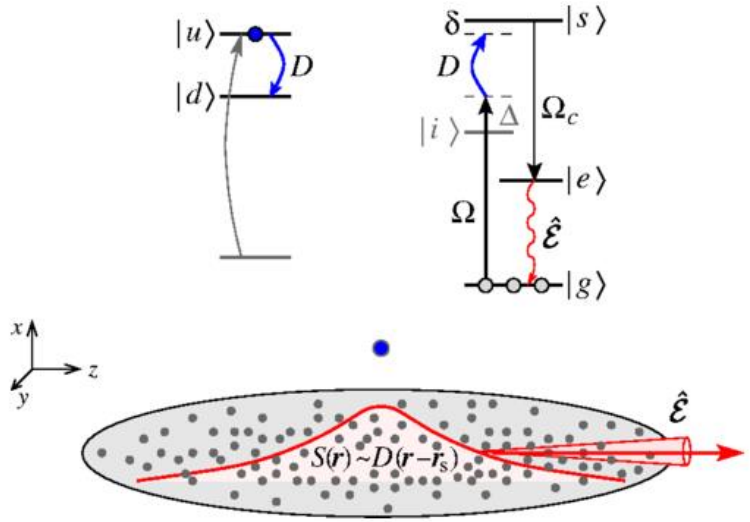


D. Petrosyan and K. Mølmer, Phys. Rev. Lett. 121, 123605 (2021)

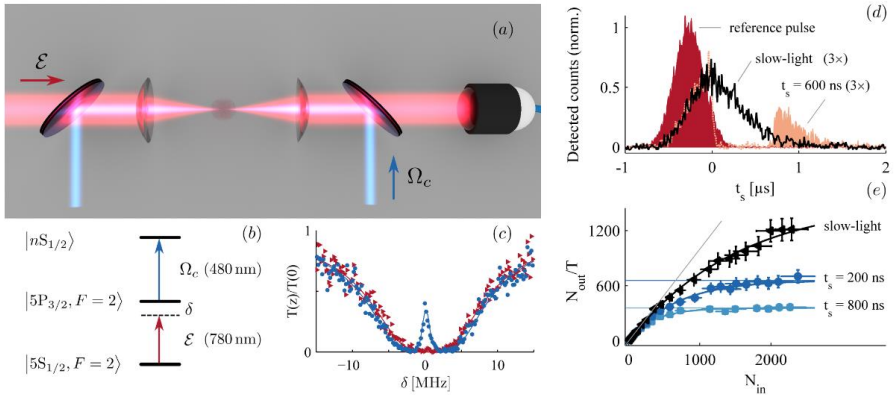


E. Distante et al., Phys. Rev. Lett. 117, 113001 (2016)

# EIT preparation and retrieval

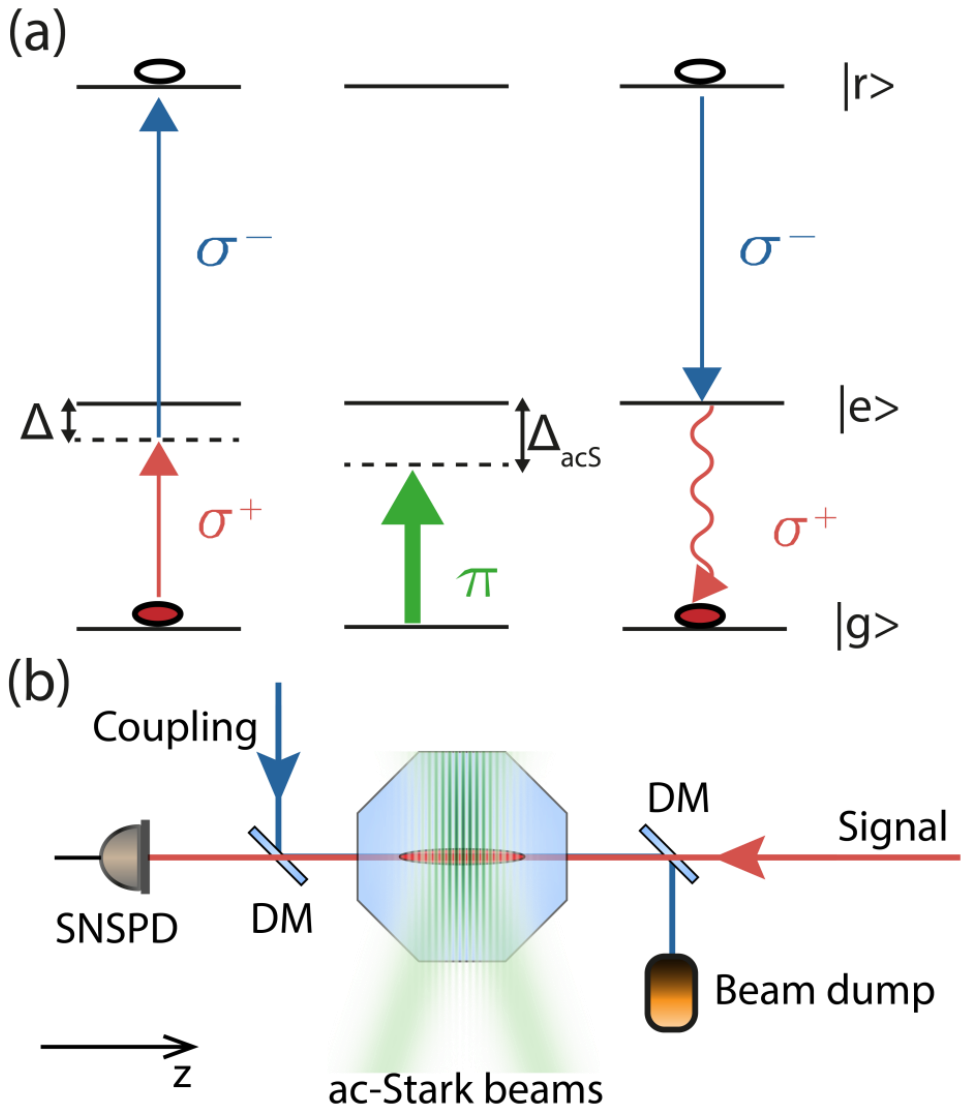


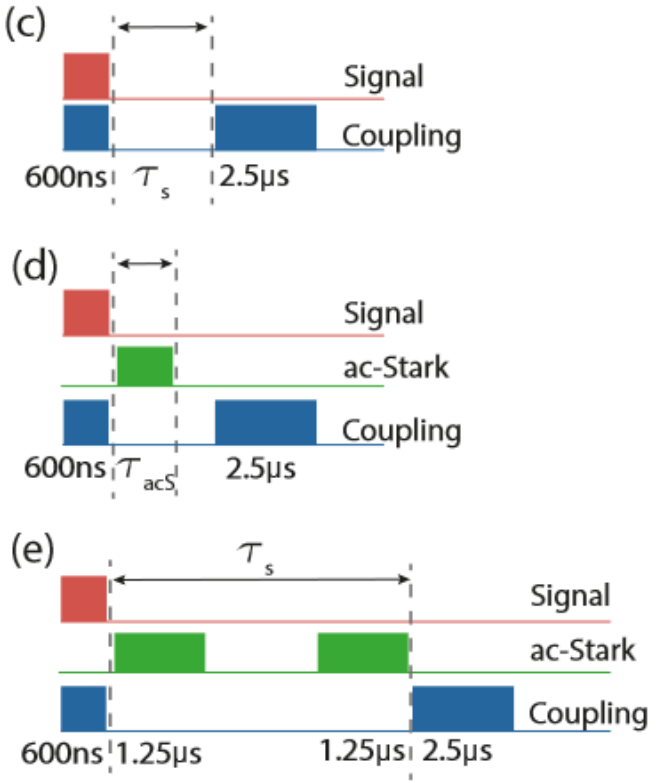


S. Kurzyna, B. Niewelt, W. Wasilewski, M. Mazelanik, M. Parniak
arXiv:2402:06513, Quantum 8, 1431 (2024)

Non-zero excitation wavevector ->
lifetime reduced to only 1 µs

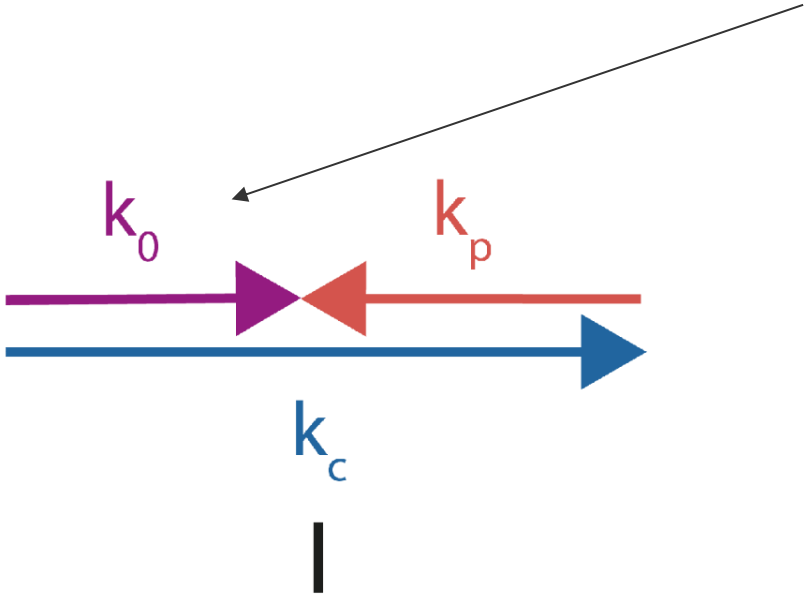


$$\tau = \left( |\boldsymbol{k}| \sqrt{\frac{k_B T}{m}} \right)^{-1}$$

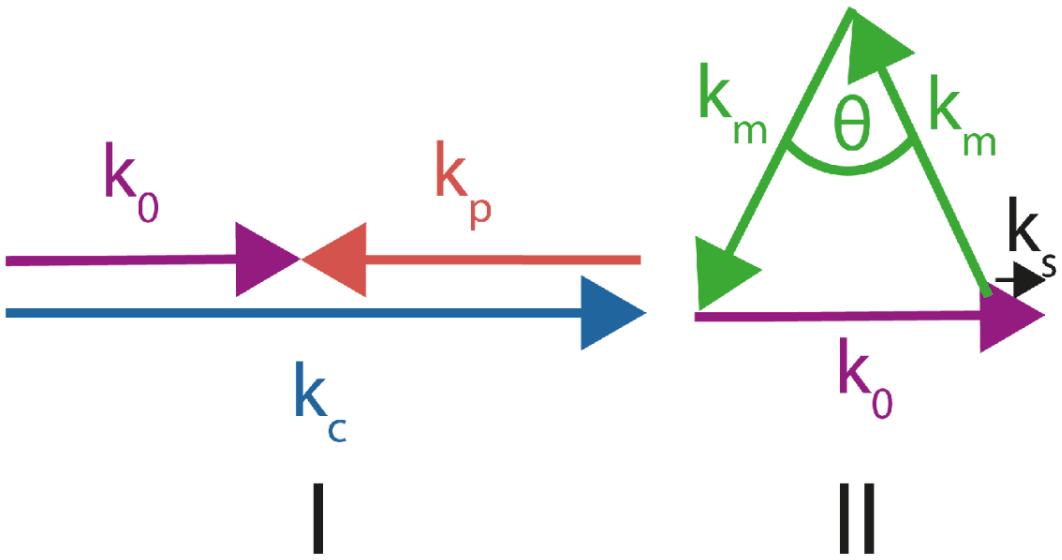
k0
kp
kc
I
km
θ
km
ks
k0
II

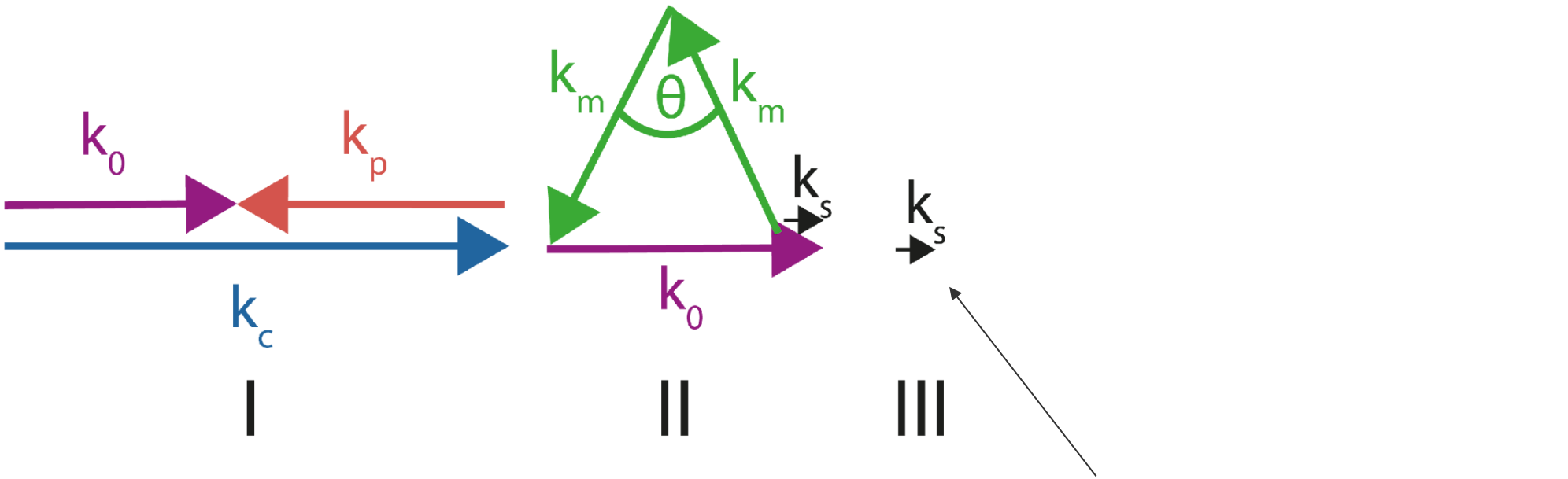


Thermal decay is halted

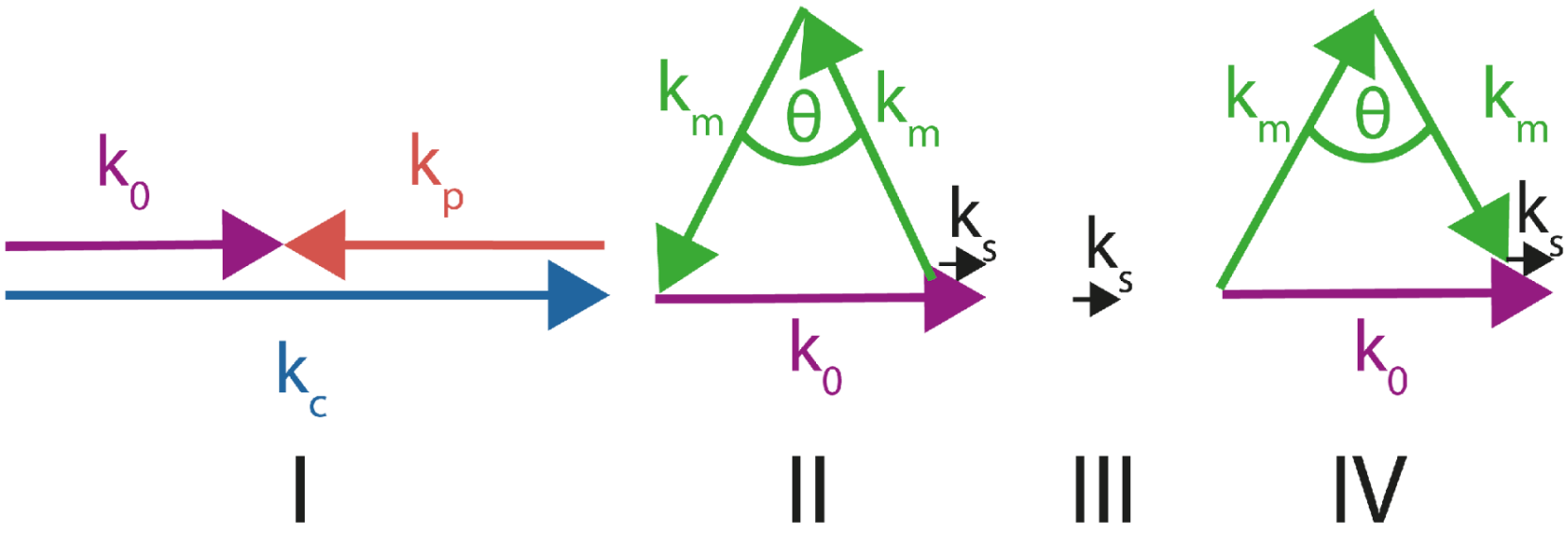
k0
kp
kc
km
θ
km
ks
k0
ks
km
θ
km
ks
k0
I
II
III
IV

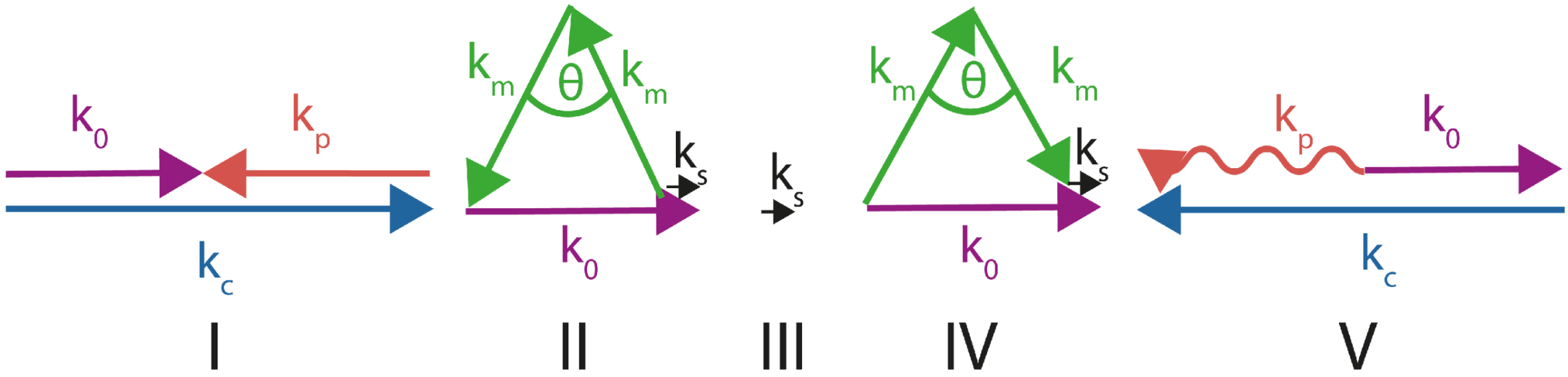
k0
kp
kc
I
km
θ
km
ks
k0
II
ks
III
km
θ
km
ks
k0
IV
kp
k0
kc
V

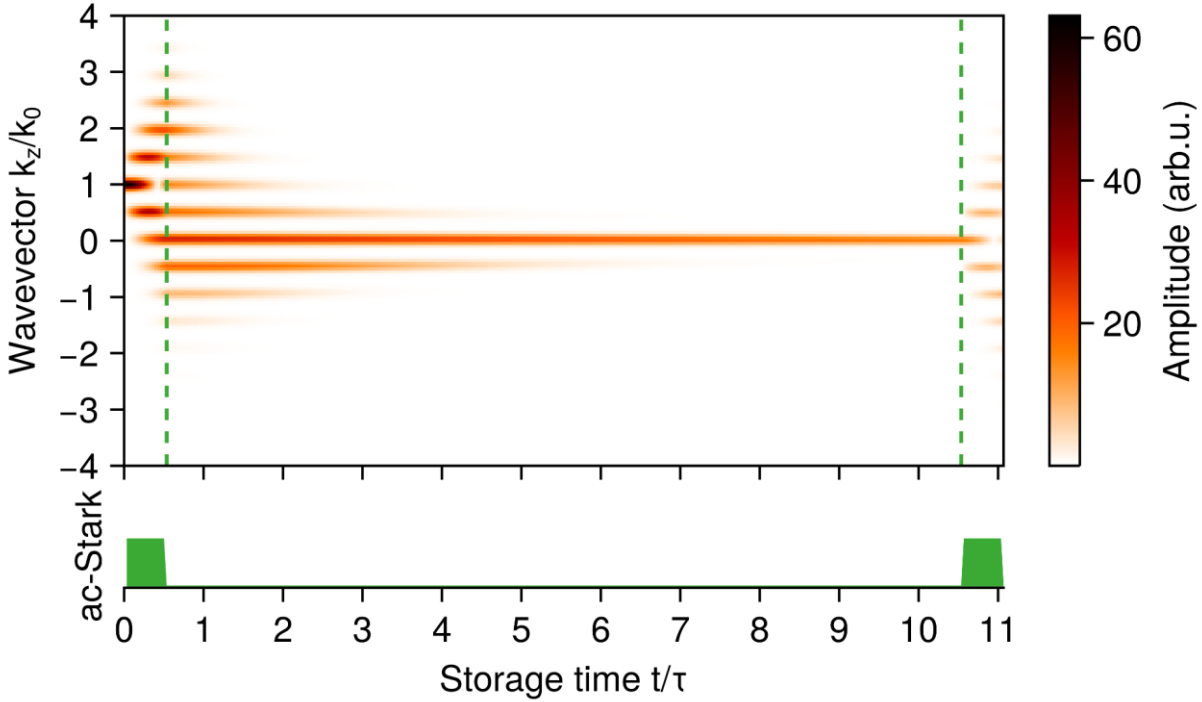


Efficiency is limited due to additional diffraction orders ~5.4%, yet this still gives large improvement for longer storage times

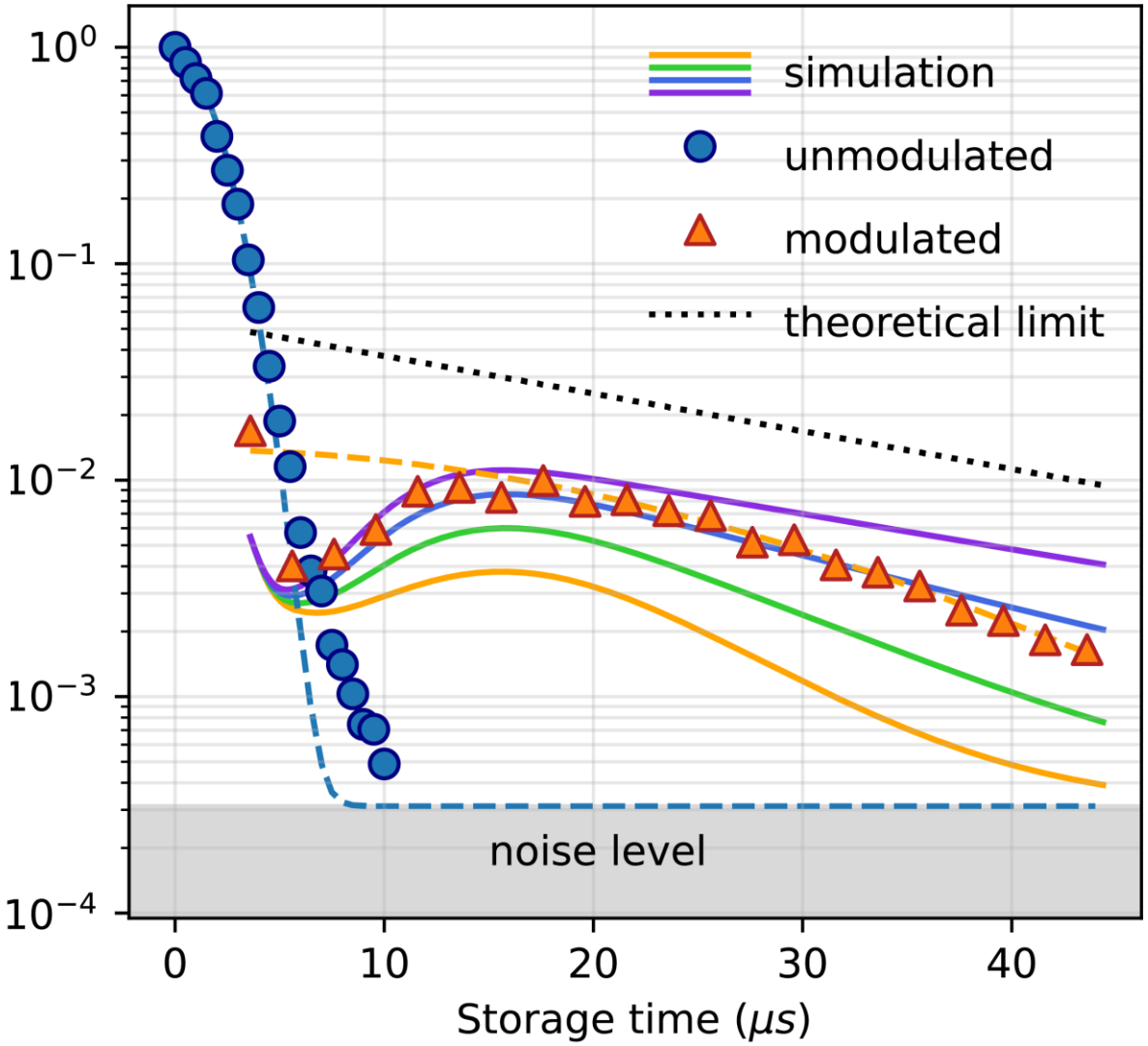


S. Kurzyna, B. Niewelt, W. Wasilewski, M. Mazelanik, M. Parniak
Quantum 8, 1431 (2024)

# State-selective modulation

Solution: two-Photon Rabi oscillation/Raman transition between hyperfine states with simultaneous momentum transfer

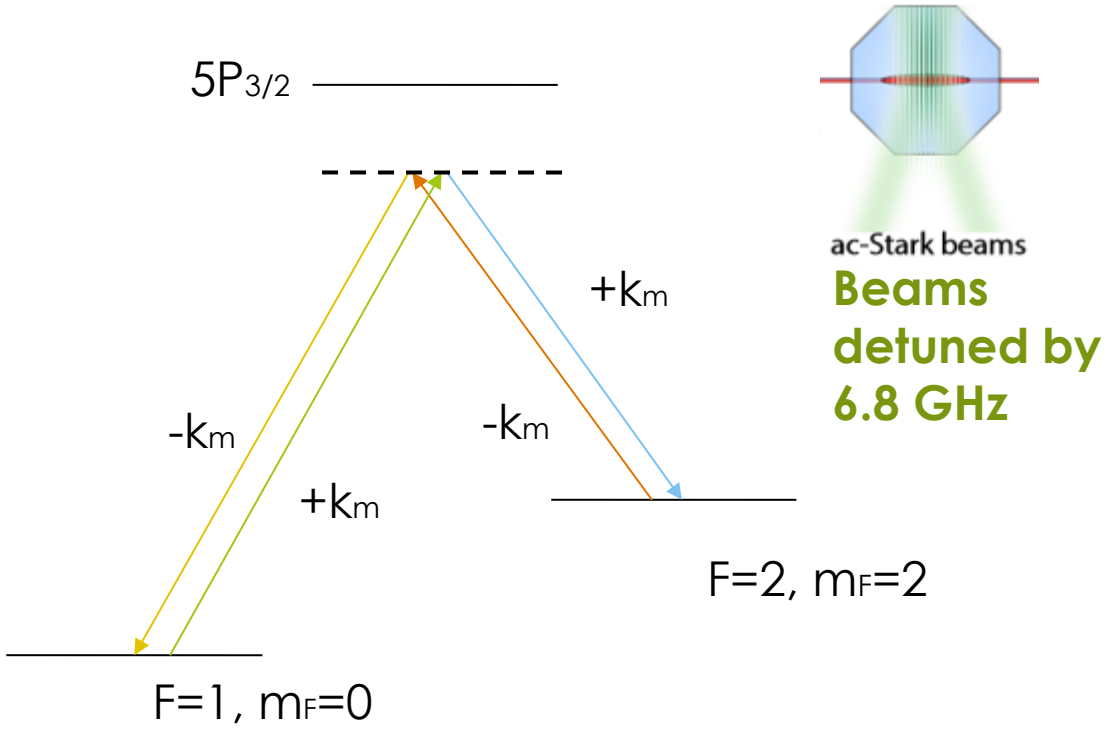





**Beams detuned by 6.8 GHz**

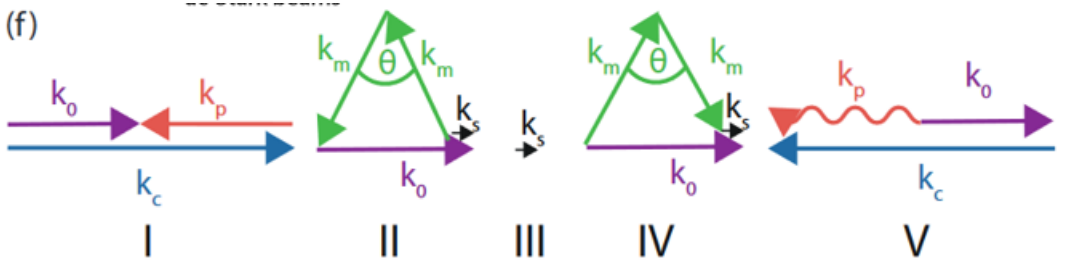


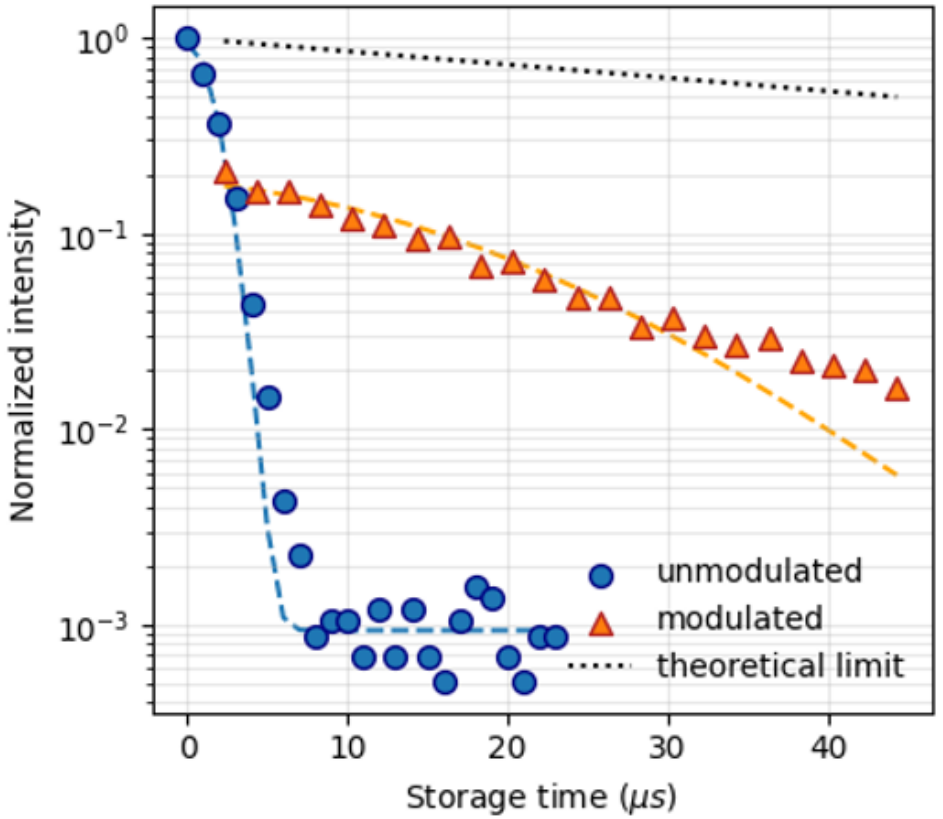

# Possible also in hot atoms

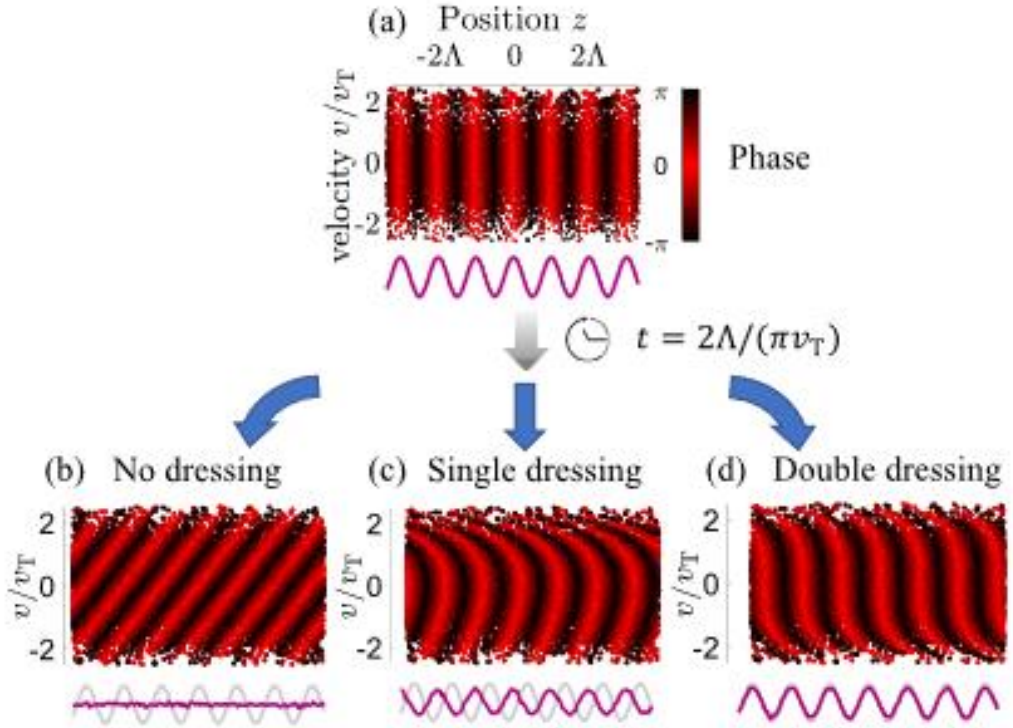


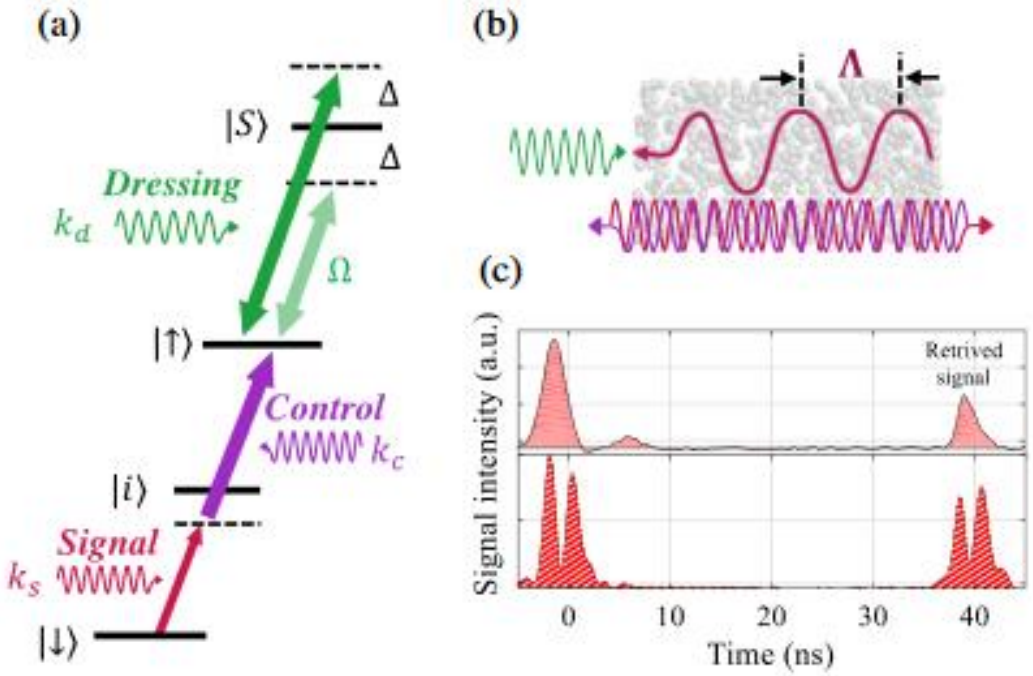


R. Finkelstein et al., Phys. Rev X 11, 011008 (2021)

# Rydberg Rabi oscillations

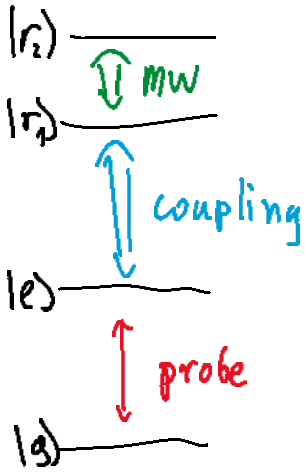


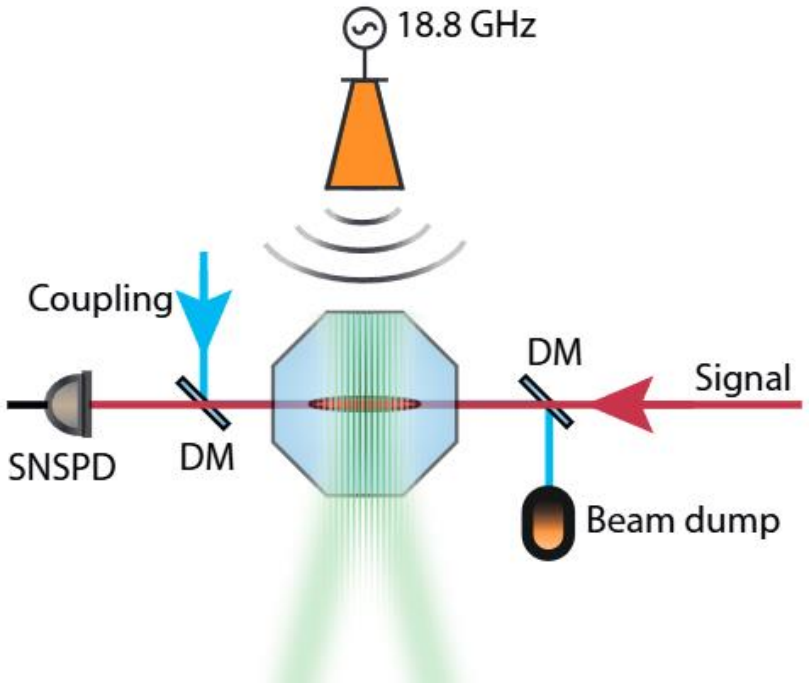


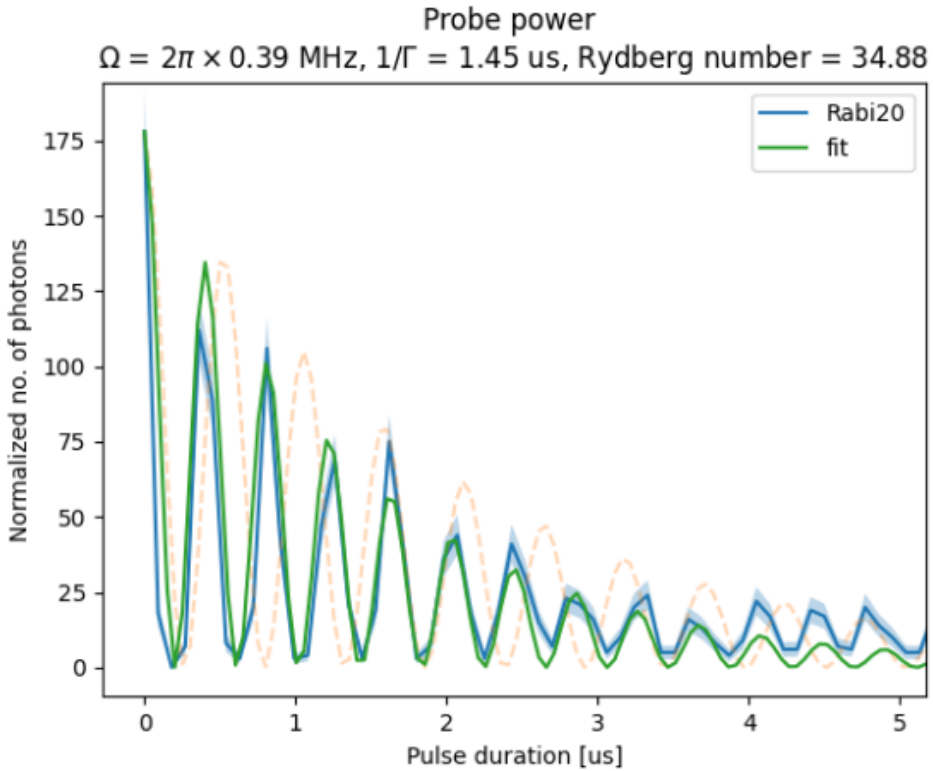


work in progress...

# Rydberg Rabi oscillations – qubit analysis picture

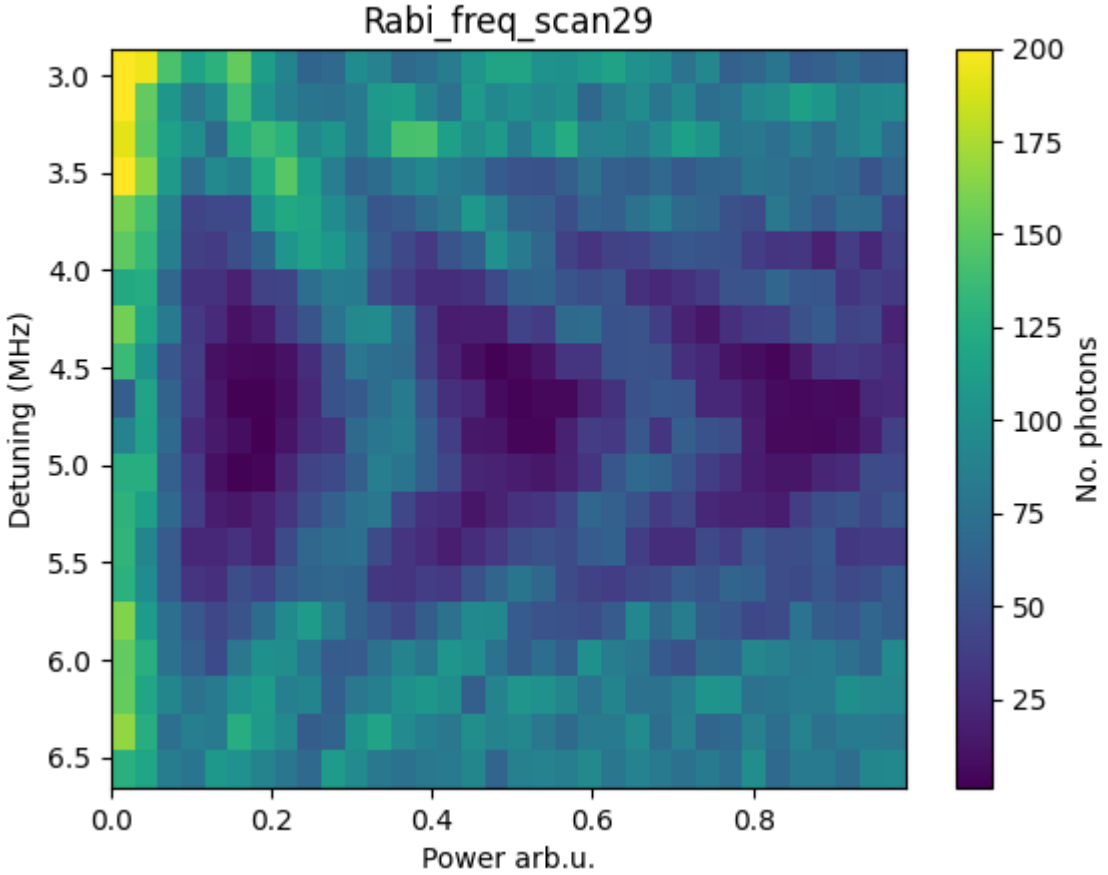


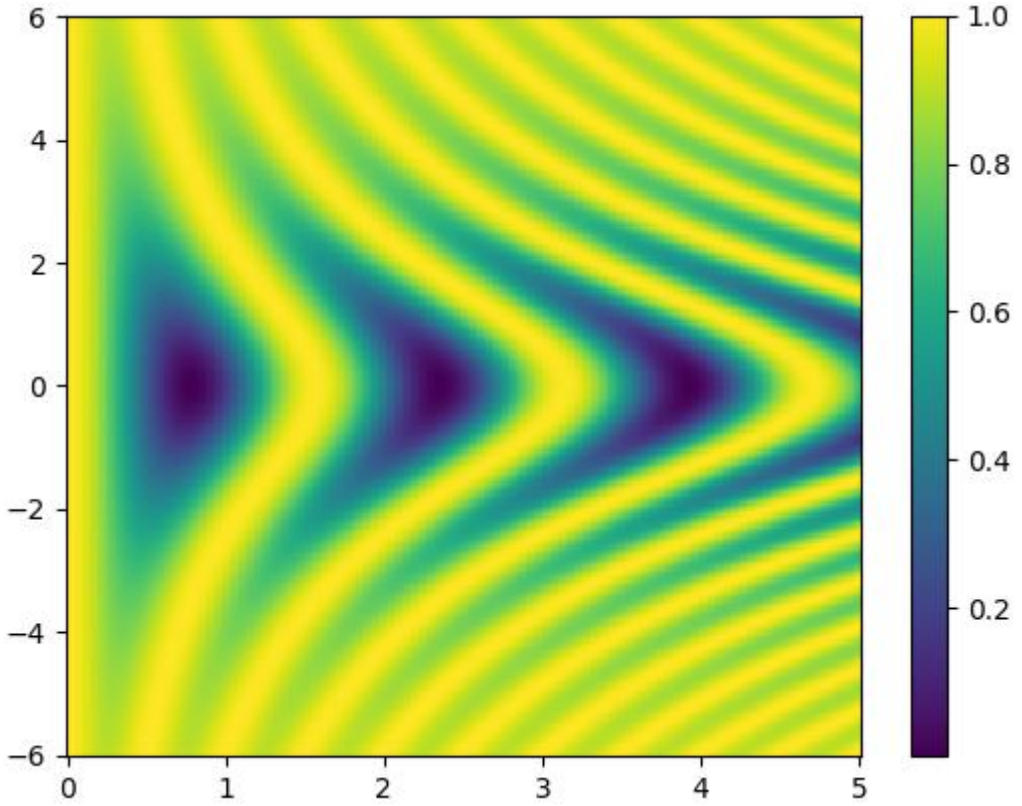

# Ramsey fringes

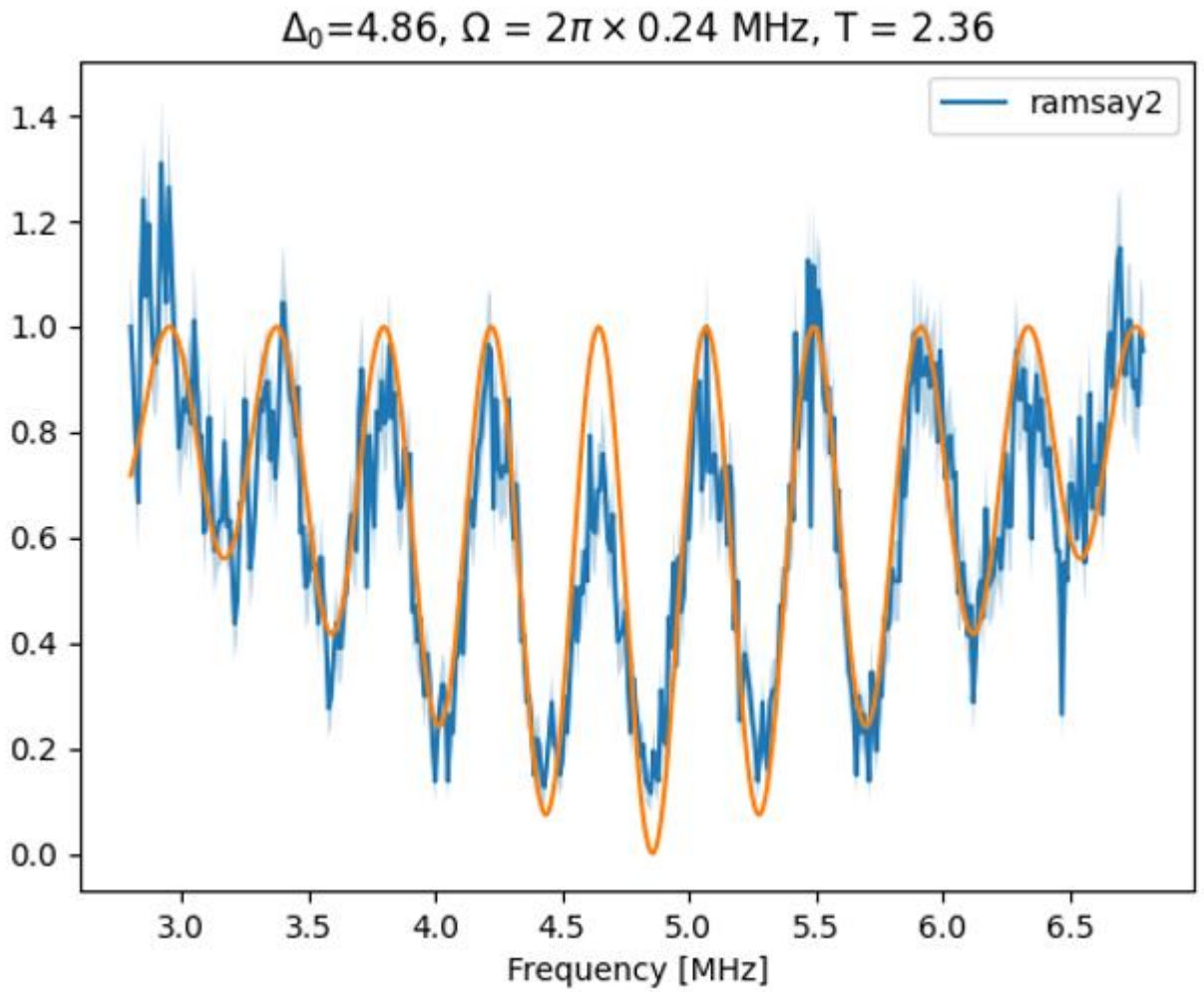


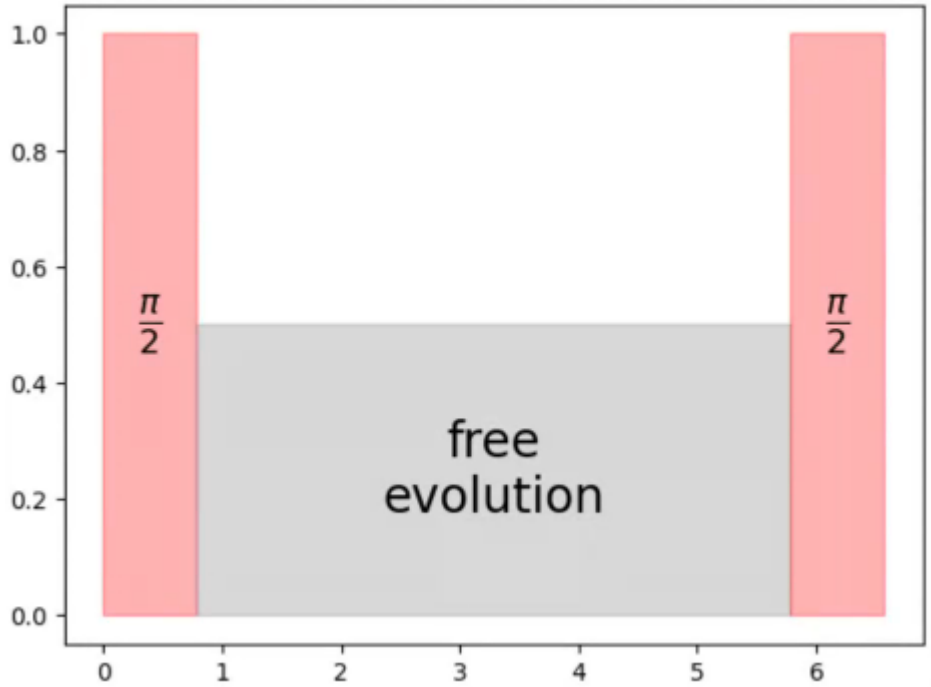

# E-field metrology

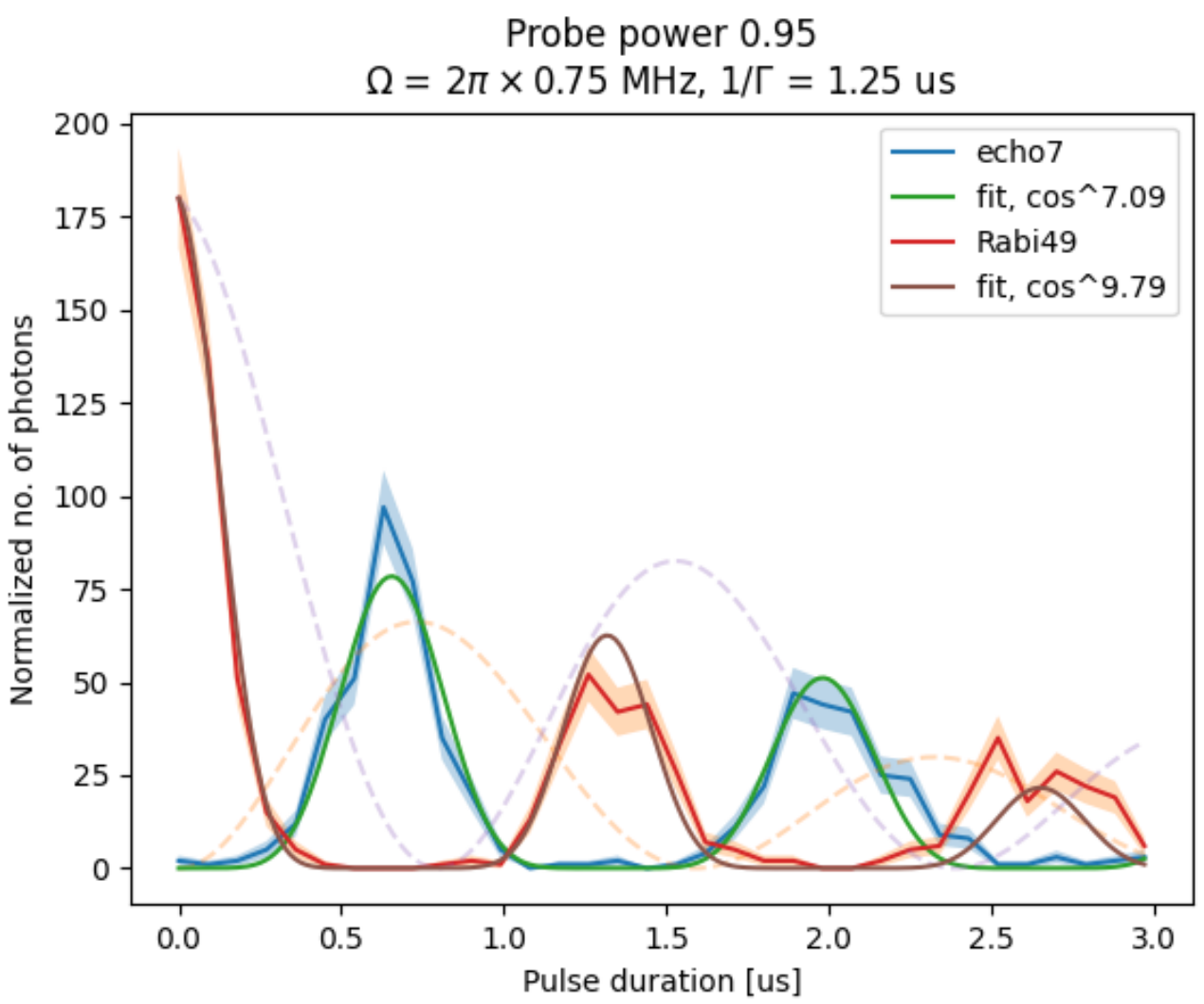


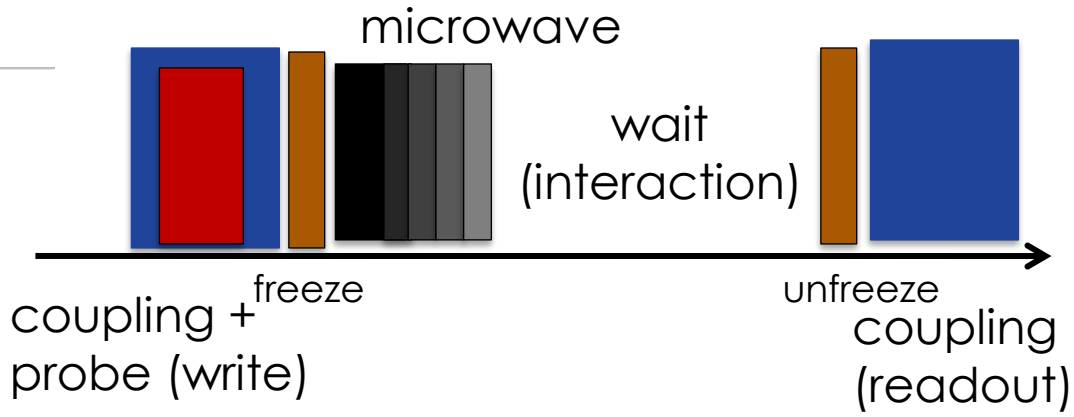


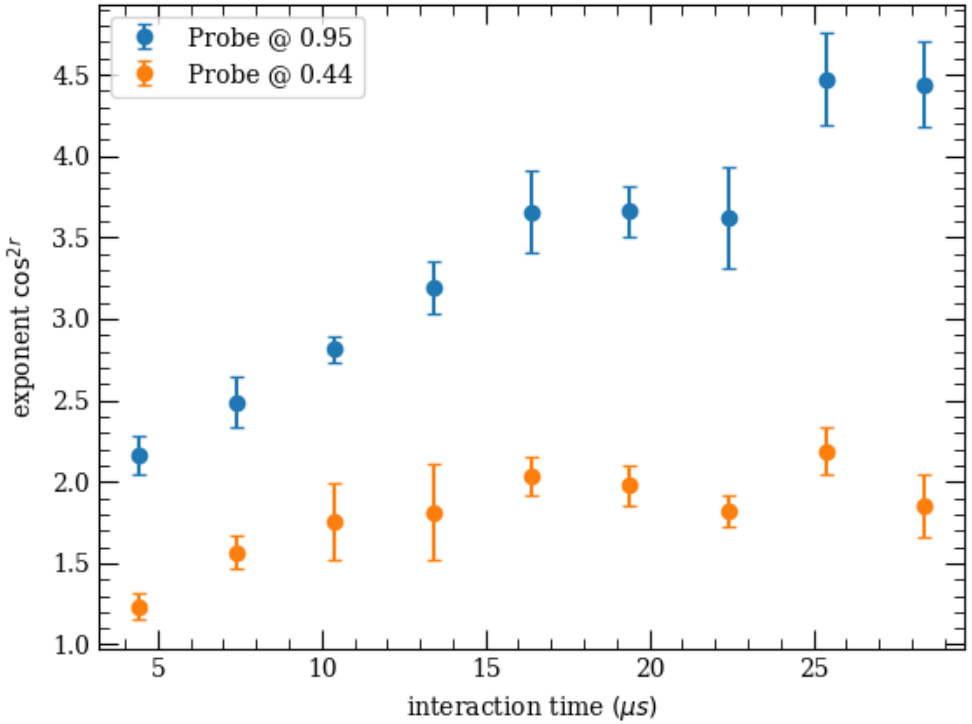

# Ramsey super-fringes

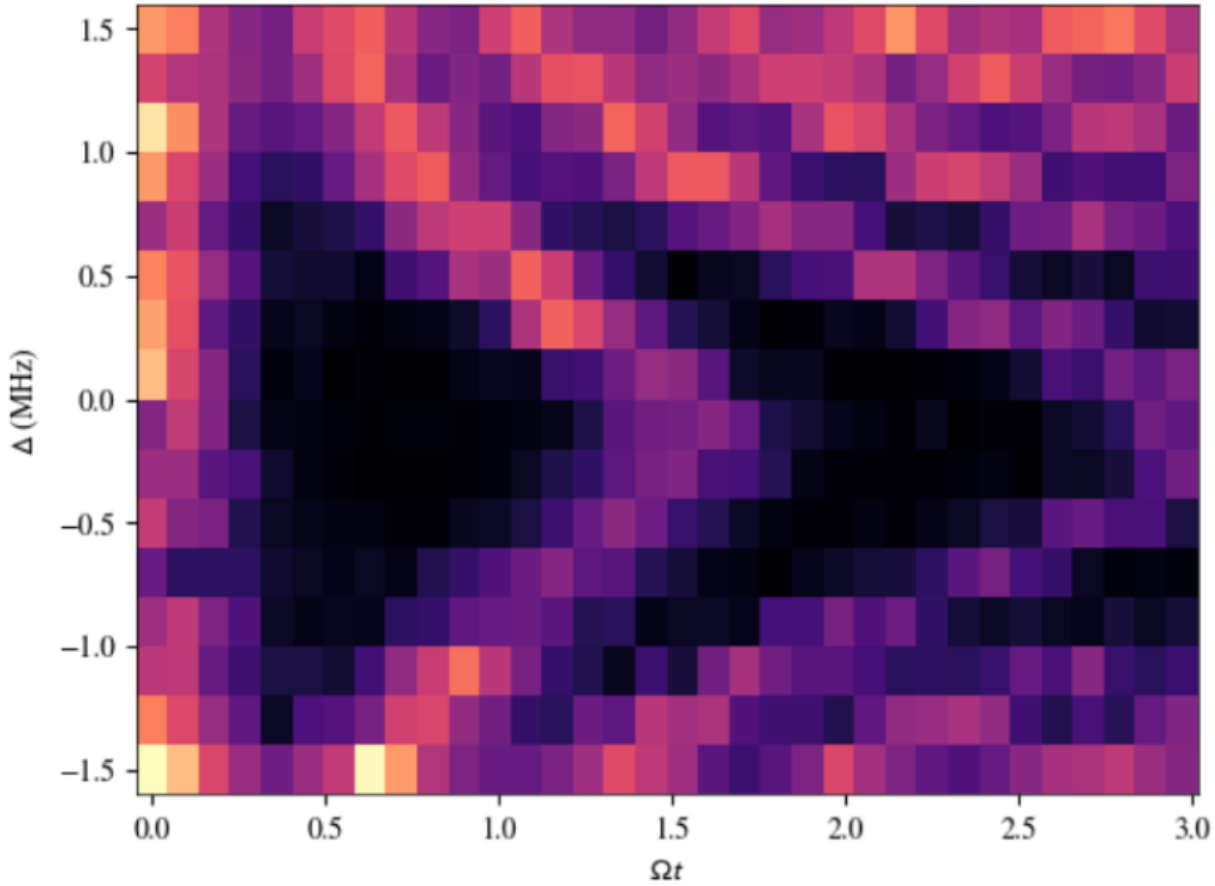

# Many-body decoherence

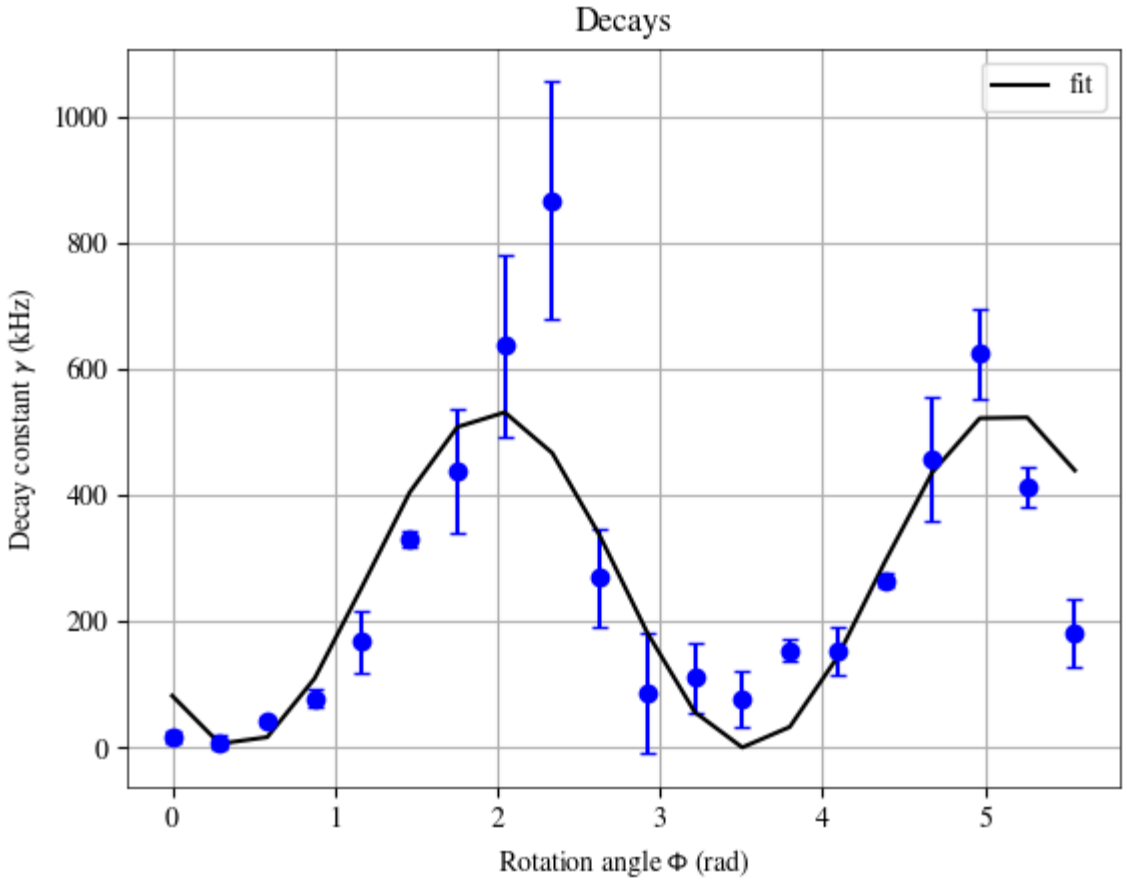


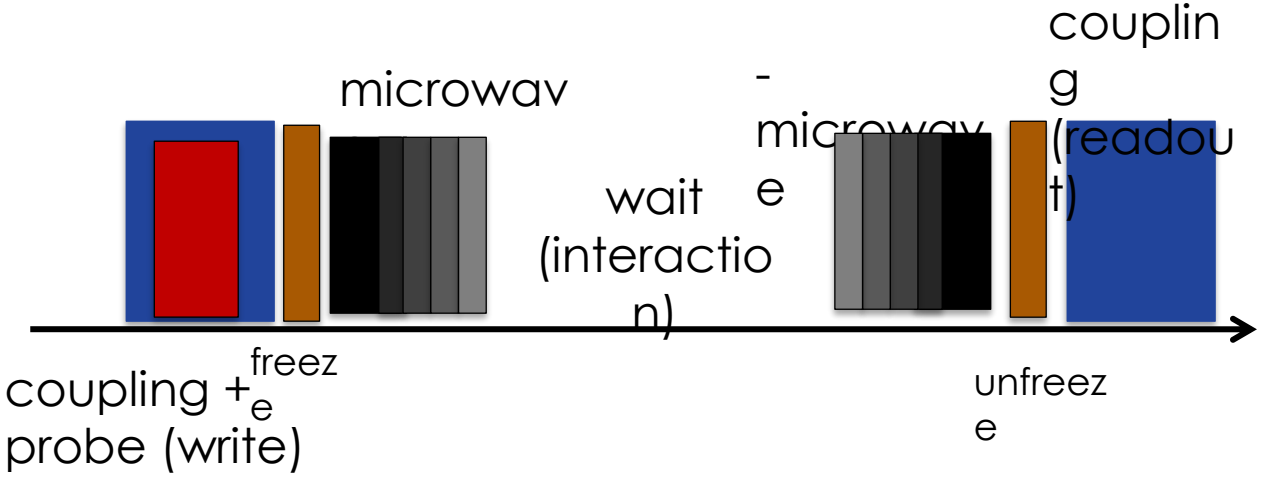


$$\hat{H} = \sum_q V(q) \sum_{\kappa,k} \hat{d}_\kappa \hat{p}_k \hat{d}^\dagger_{\kappa+q} \hat{p}^\dagger_{k-q} \quad \Rightarrow \quad \hat{L} = \hat{p}\hat{d}$$

The interaction (V(r)~1/r^3) scrambles the phase of the spin-waves -> scattering into different **k**-modes, but only modes with specific **k** (**k**=0) are coupled to light!
In result we get losses (modes with **k**=0):

$$\hat{d}' \to \hat{d}\exp\left(-\frac{\gamma\tau}{2}\hat{p}^\dagger\hat{p}\right) \quad \hat{p}' \to \hat{p}\exp\left(-\frac{\gamma\tau}{2}\hat{d}^\dagger\hat{d}\right)$$

# „Microscopic" picture

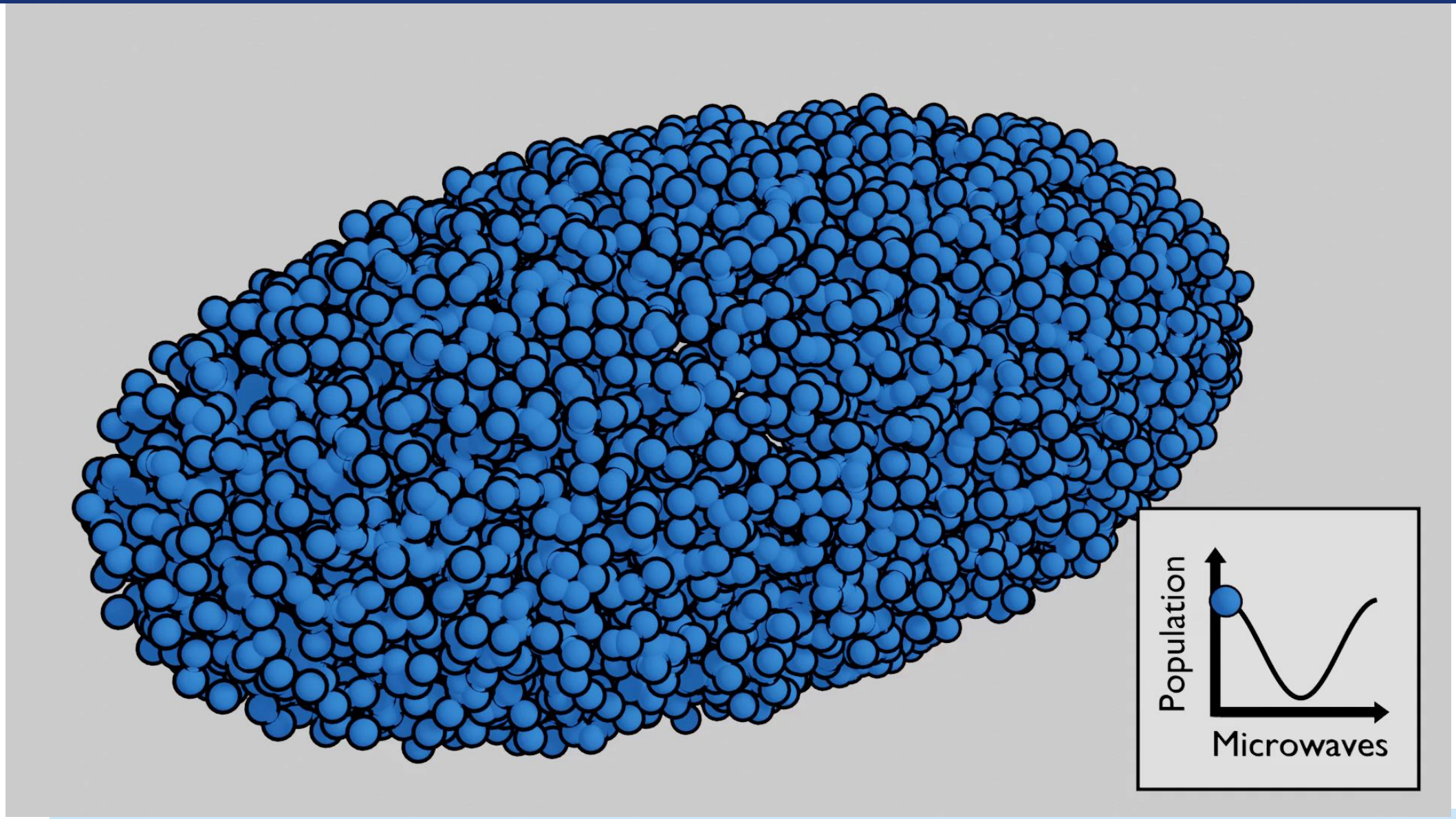

# Quantum metrology context

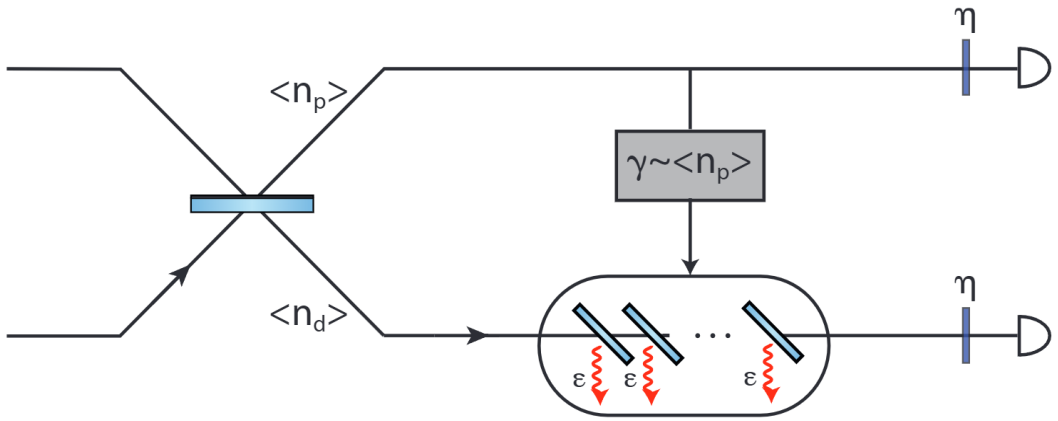


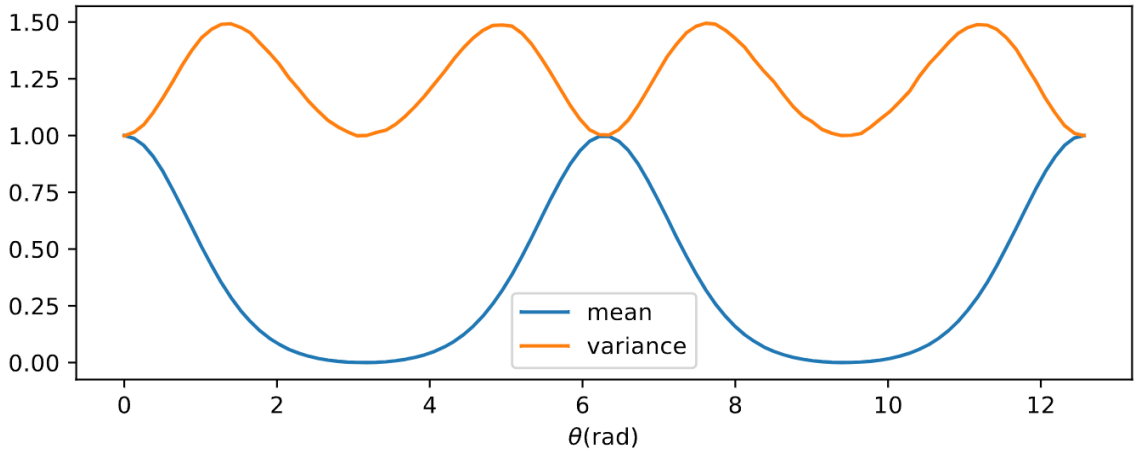


$$\begin{cases} \hat{d}' \to \hat{d}\exp\left(-\frac{\gamma\tau}{2}\hat{p}^\dagger\hat{p}\right) + \hat{v}_1\sqrt{1-\exp\left(-\gamma\tau\hat{p}^\dagger\hat{p}\right)} \\ \hat{p}' \to \hat{p}\exp\left(-\frac{\gamma\tau}{2}\hat{d}^\dagger\hat{d}\right) + \hat{v}_2\sqrt{1-\exp\left(-\gamma\tau\hat{d}^\dagger\hat{d}\right)} \end{cases}$$

$$\begin{cases} \hat{d}'' \to \sqrt{\eta}\hat{d}' + \sqrt{1-\eta}\hat{c}_1, \\ \hat{p}'' \to \sqrt{\eta}\hat{p}' + \sqrt{1-\eta}\hat{c}_2 \end{cases}$$

For η=1 we get sharper peaks but we pay for that with increased variance!
So where is the gain?

$$p(n) = \sum_{k=0}^{\infty} \frac{|p|^{2k}\left(|\delta|^2 e^{-2\gamma k}\right)^n e^{-|\delta|^2 e^{-2\gamma k} - |p|^2}}{k!n!}$$

work in progress...

# Losses at the input vs losses at the output

Losses at the output (after interaction)

Losses at the input (before interaction)

η=1

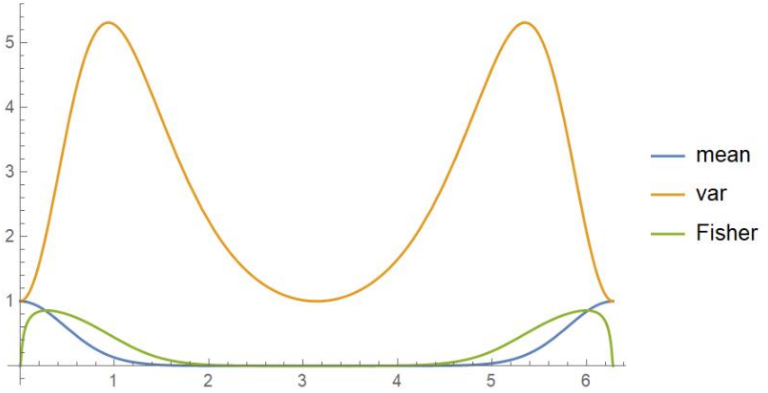


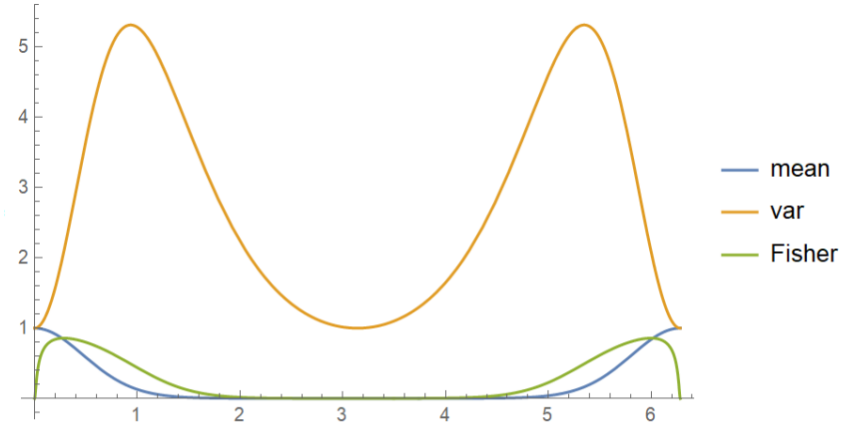


η=0.02

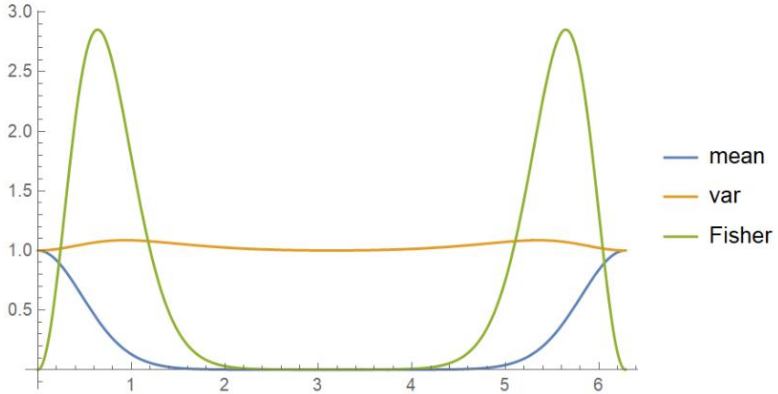


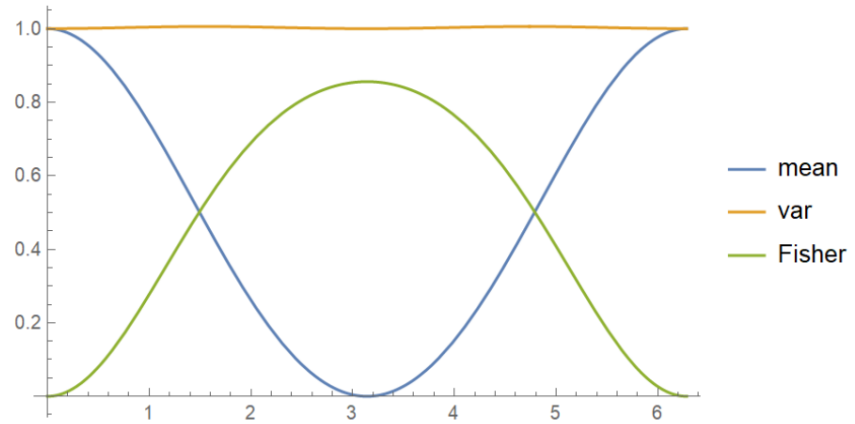


Fisher and mean divided by η

work in progress...

$$d\mathcal{F} = \left(\frac{\partial p_{n_d}(k,\theta)}{\partial \theta}\right)^2 \frac{1}{p_{n_d}(k,\theta)} \qquad \mathcal{F} = \sum_{k=0}^{\infty} d\mathcal{F}$$

# With losses there is an advantage!

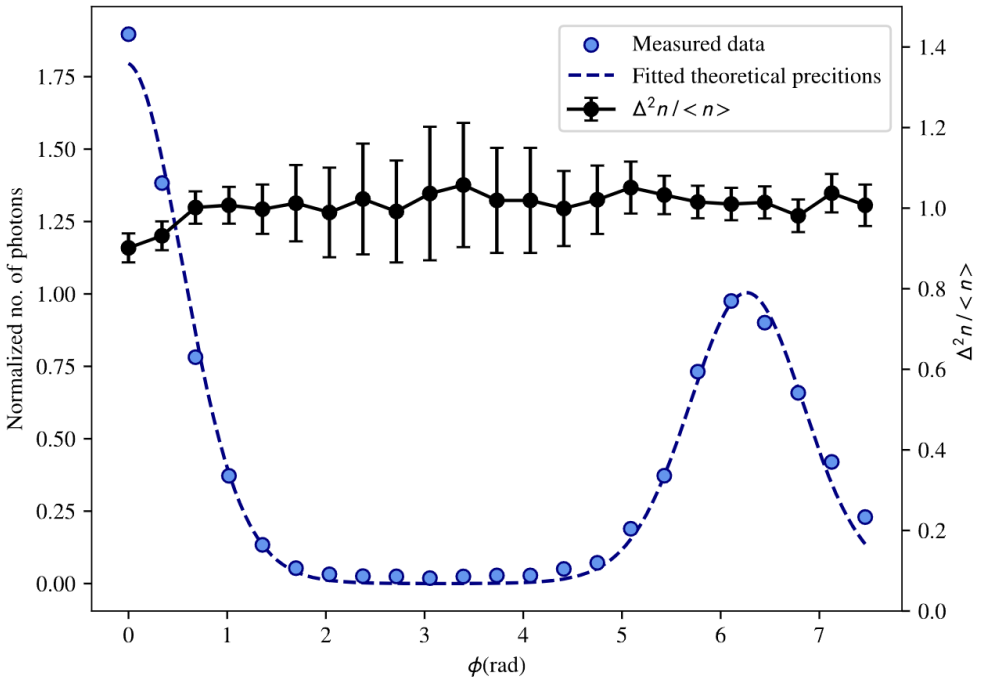


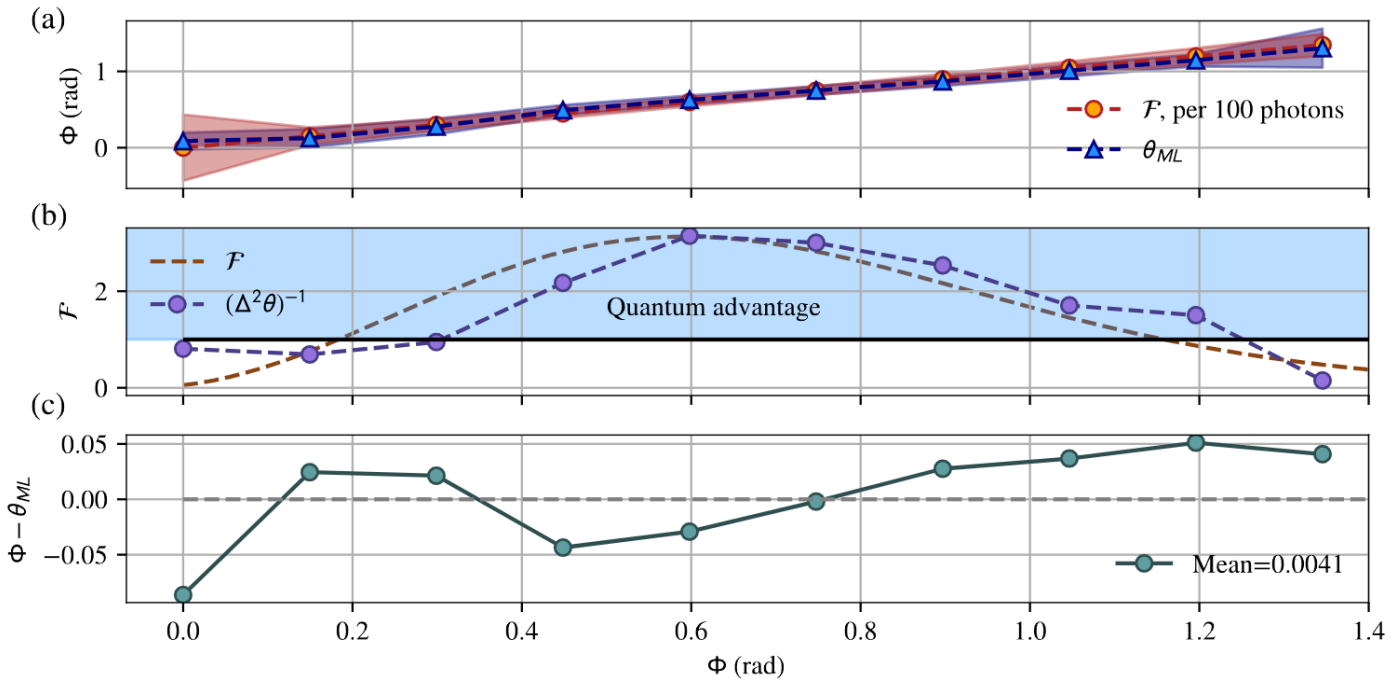


work in progress...

# Outlook: 3d Rydberg polaritons

Blockade regime

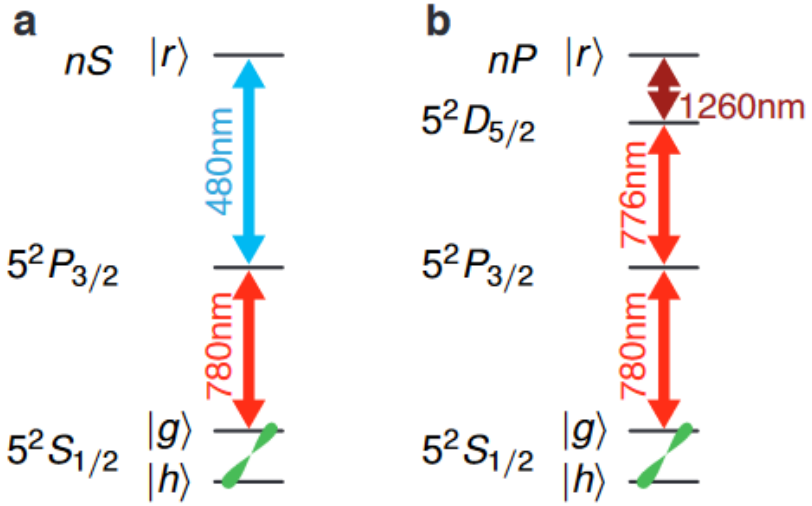


$$\frac{\partial EE}{\partial R} = C_D\left(\frac{\partial^2 EE}{\partial \rho^2} + \frac{1}{\rho}\frac{\partial EE}{\partial \rho}\right) - \left(C_{VR}V(r,\rho) - C_{Vr}\frac{\partial^2 V(r,\rho)}{\partial r^2}\right)EE + \\ + C_r\frac{\partial^2 EE}{\partial r^2} + C_{Vr}\left(\frac{\partial^2 EEV(r,\rho)}{\partial r^2} - 2\frac{\partial(EE\frac{\partial V(r,\rho)}{\partial r})}{\partial r}\right).$$

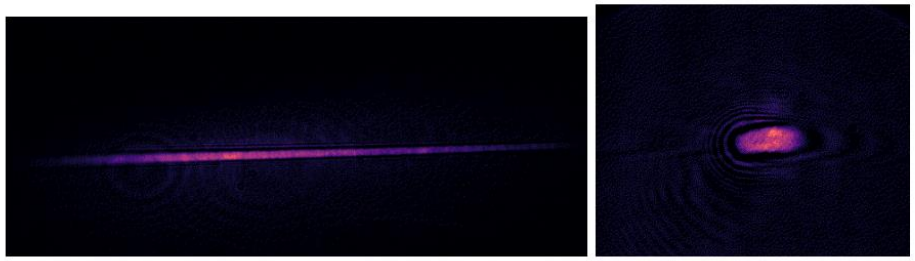

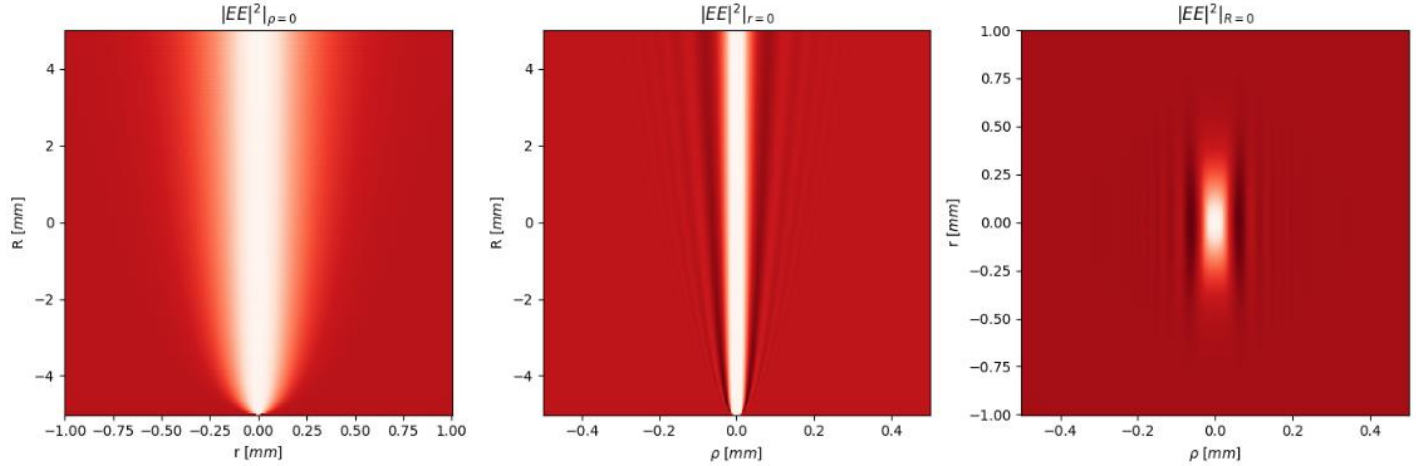

# Outlook: 3d Rydberg polaritons

Attractive potential regime

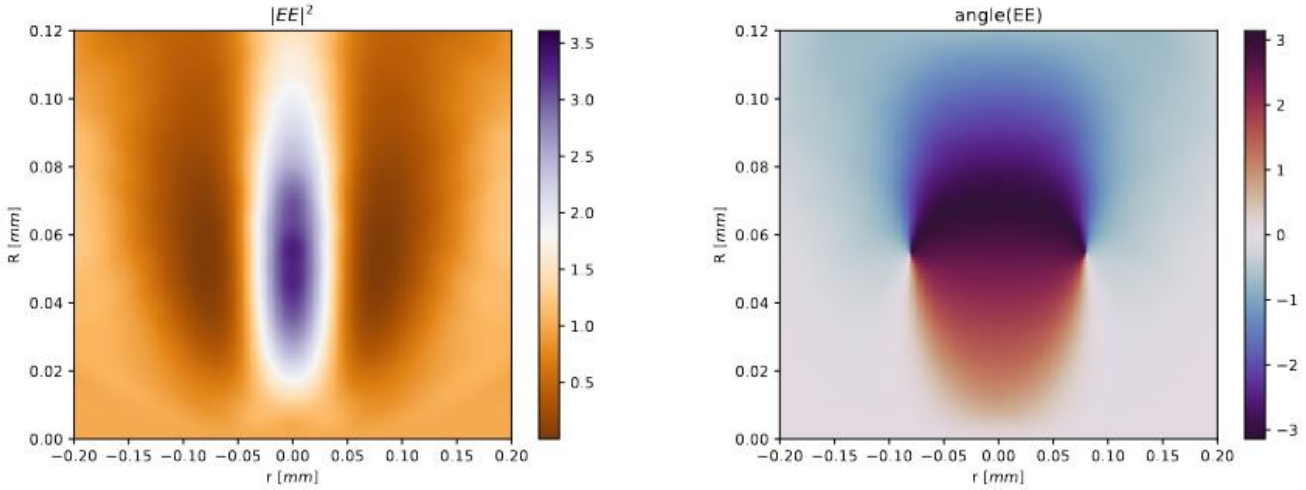


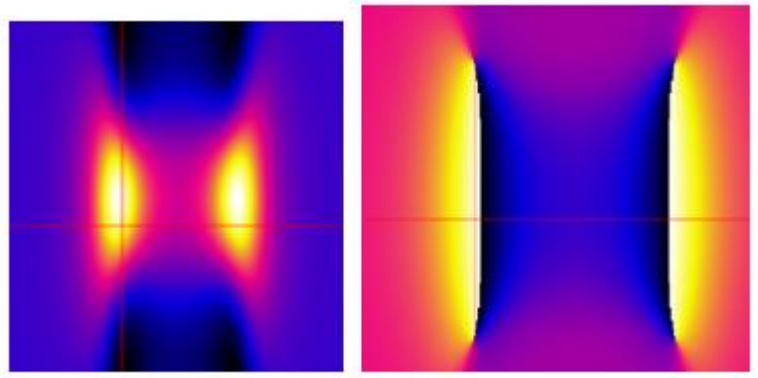

1d version of vortices – see below

3d version of vortices

**Quantum vortices of strongly interacting photons**

LEE DRORI, BANKIM CHANDRA DAS, TOMER DANINO ZOHAR, GAL WINER, EILON POEM, ALEXANDER PODDUBNY, AND OFER FIRSTENBERG

Authors Info & Affiliations

*SCIENCE* · 13 Jul 2023 · Vol 381, Issue 6654 · pp. 193-198 · DOI: 10.1126/science.adh5315

# Tomography

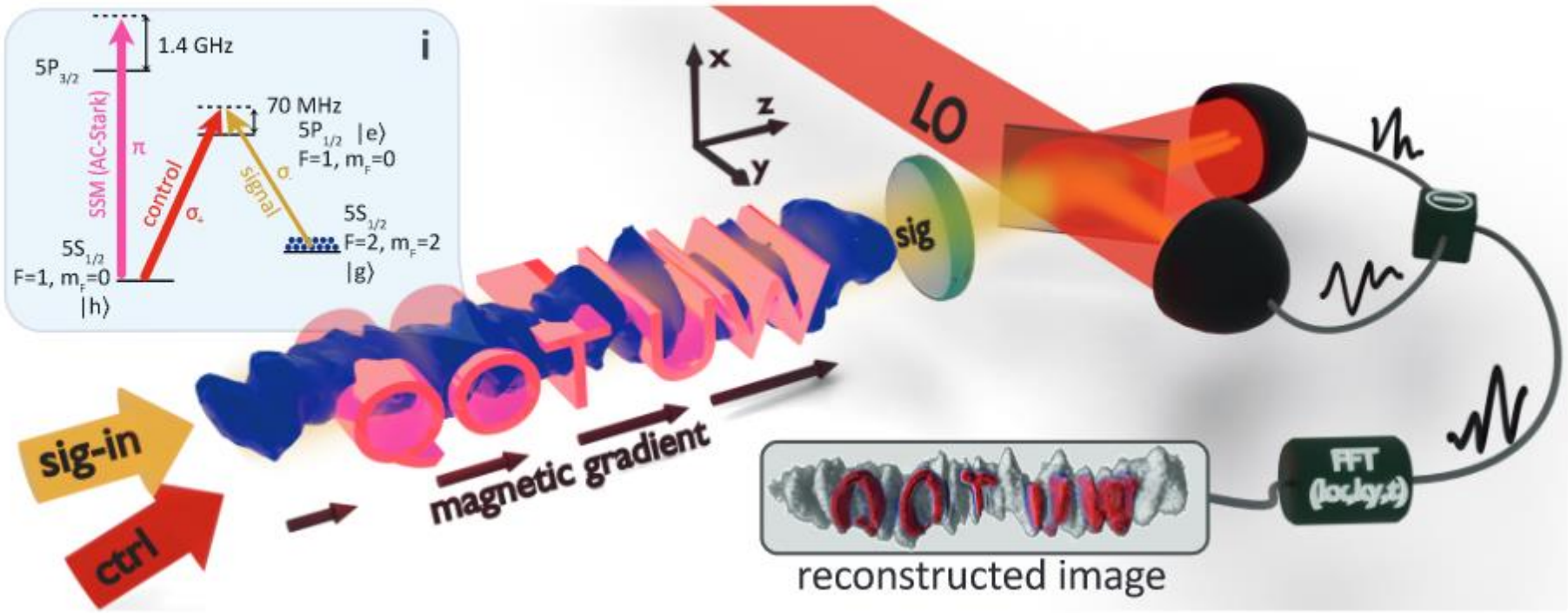


Communications Physics 6, 165 (2023)

# Tomography (1D -> 3D)

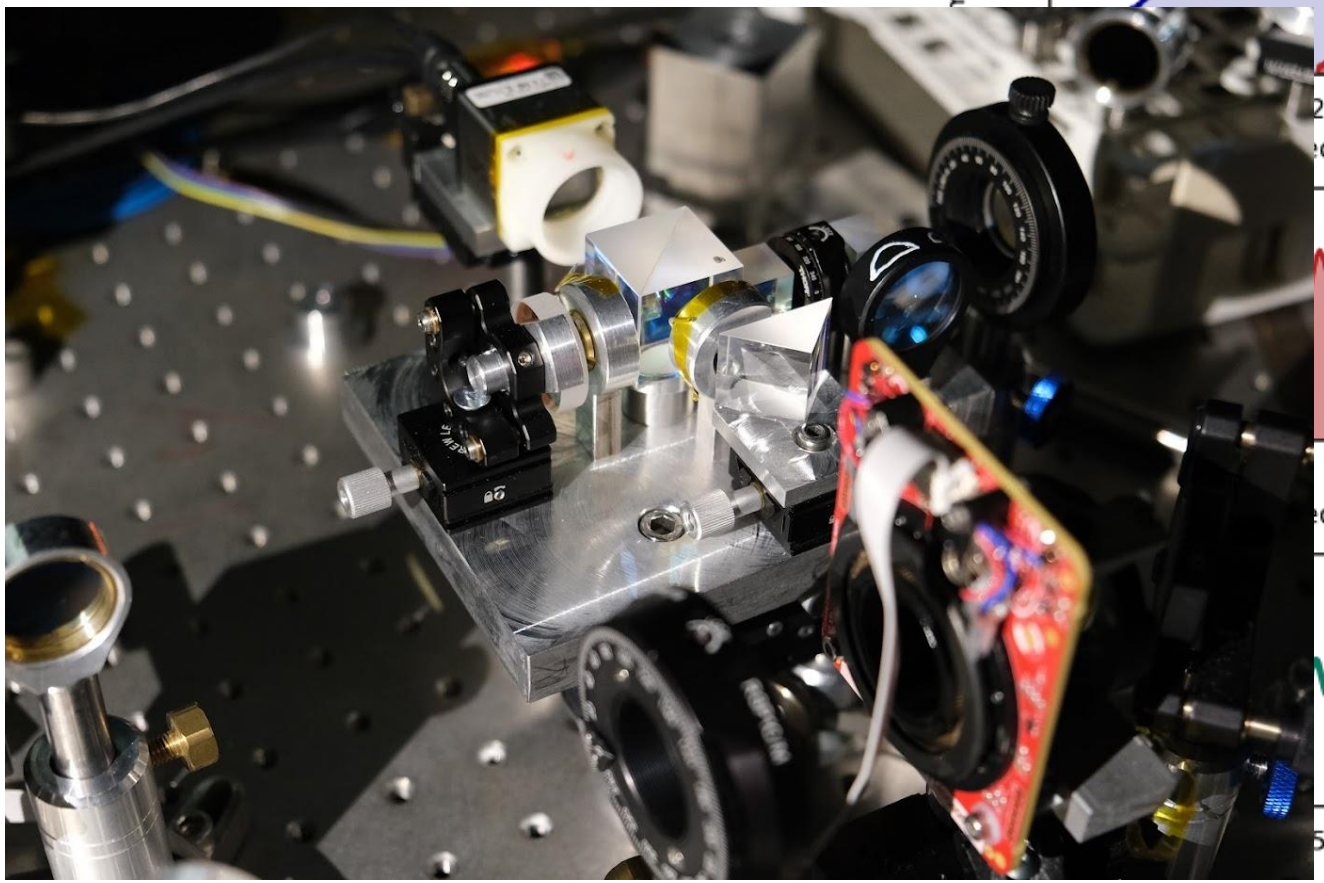

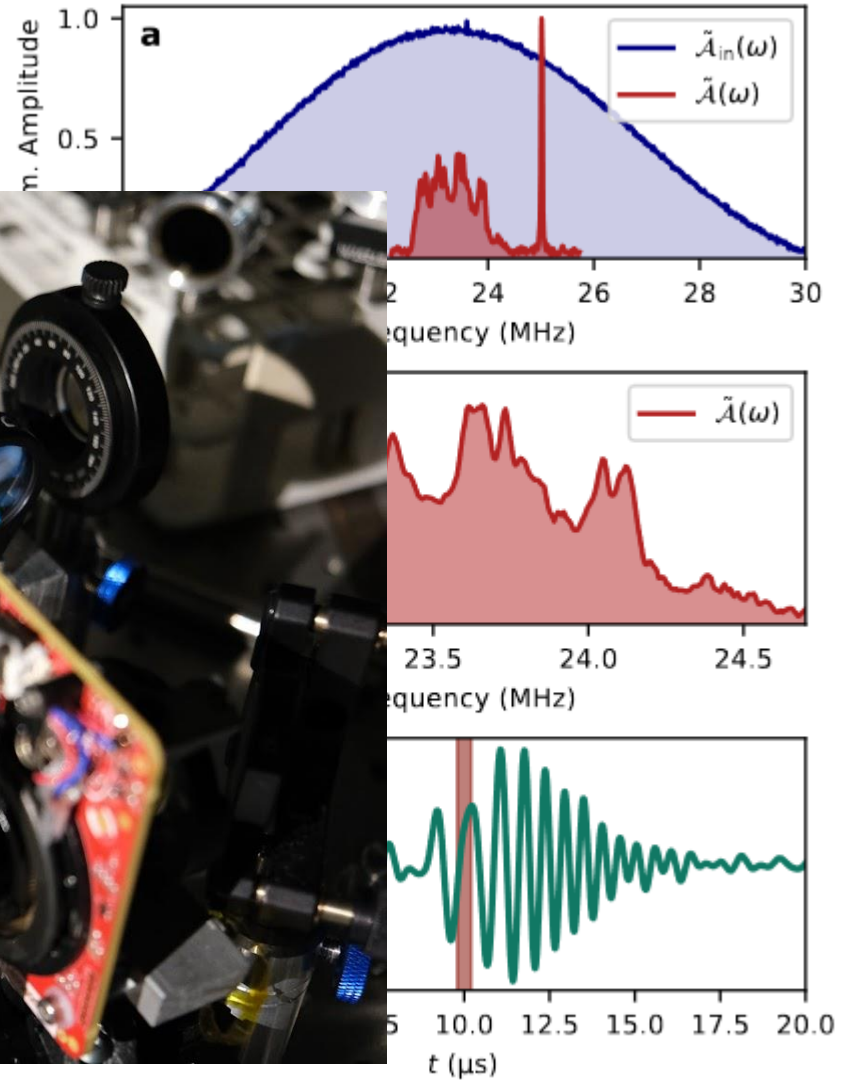


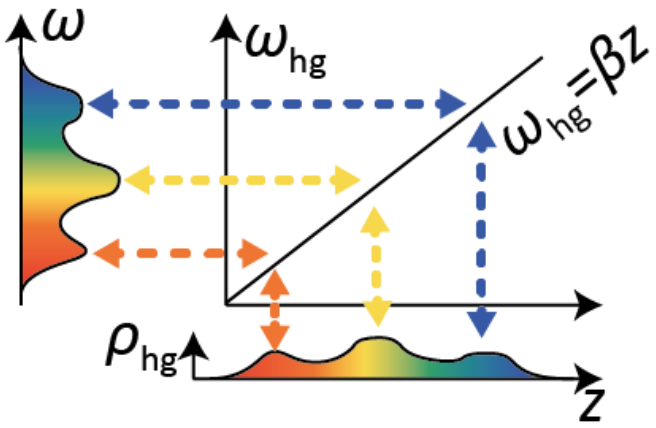

# Tomography (3D)

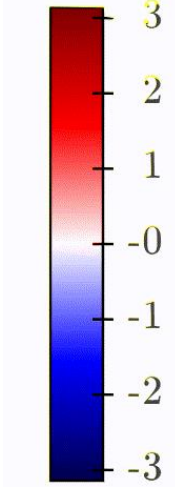


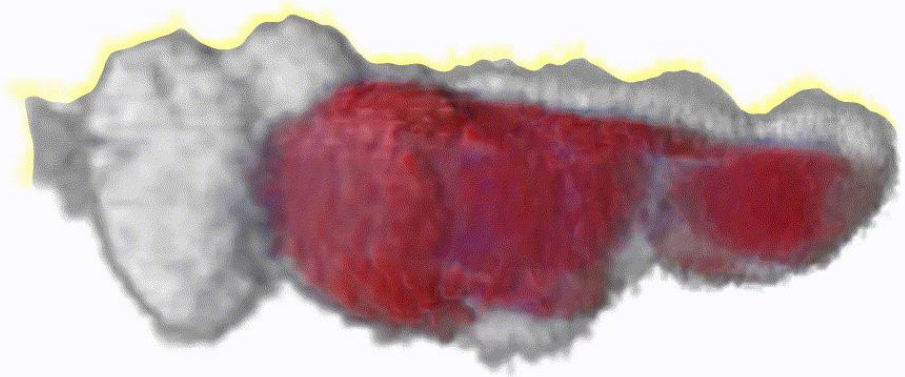

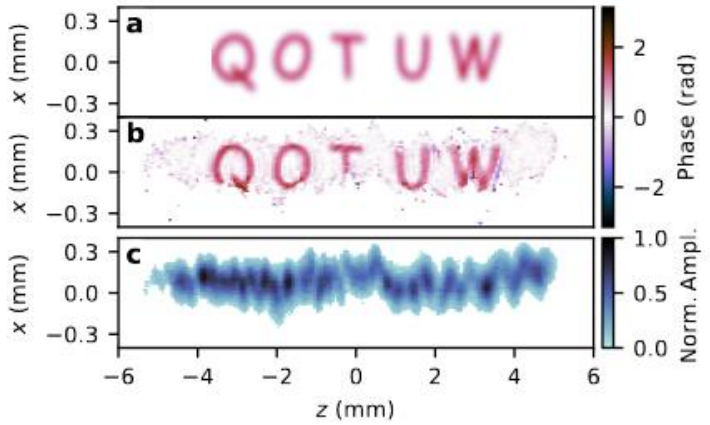


Communications Physics 6, 165 (2023)

# Rydberg blockade tomography